

DISSERTATION

FEASIBILITY OF TREATING CHLORINATED SOLVENTS STORED IN LOW  
PERMEABILITY ZONES IN SANDY AQUIFERS

Submitted by

Azadeh Bolhari

Department of Civil and Environmental Engineering

In partial fulfillment of the requirements

For the Degree of Doctor of Philosophy

Colorado State University

Fort Collins, Colorado

Summer 2012

Doctoral Committee:

Advisor: Thomas C. Sale

Domenico A. Bau  
Charles D. Shackelford  
Thomas Borch

Copyright by Azadeh Bolhari 2012

All Rights Reserved

## ABSTRACT

### FEASIBILITY OF TREATING CHLORINATED SOLVENTS STORED IN LOW PERMEABILITY ZONES IN SANDY AQUIFERS

Over the past thirty years, the primary objective for managing subsurface releases of chlorinated solvents has been restoration of groundwater, soils and soil gas to strict health-based cleanup standards. Unfortunately, attaining desired levels of cleanup has proven to be difficult at many sites. One of the primary constraints has been a failure to holistically consider all of the compartments that need to be addressed, including chlorinated solvents in low permeability zones. The premise of this thesis is that slow release of chlorinated solvents stored in low permeability zones can be a primary factor constraining the success of remedial actions. This thesis explores the feasibility of treating chlorinated solvents stored in low permeability zones through three activities: a modeling study addressing evolution of a chlorinated solvent release, a laboratory study involving treatment of contaminants using an alkaline persulfate solution, and laboratory testing of three innovative treatment technologies.

The hypothesis of the modeling study was that subsurface releases of chlorinated solvents evolve through time from a problem of dense non-aqueous phase liquids (DNAPLs) in transmissive zones, to a problem of dissolved and sorbed phases in low permeability zones. This hypothesis was tested using analytical solutions for a two-layer

system involving a horizontal transmissive layer situated above a low permeability layer and a DNAPL-like perchloroethene source at the contact between the two layers. The source was active with a constant strength for 1,000 days. Subsequently, the source was shut off and contaminant distribution through the domain of interest was evaluated for an additional 2,000 days. All calculations were carried out using Mathcad<sup>TM</sup> 14.

Given the model inputs, the DNAPL source was fully depleted at 1,000 days. At 1,000 days, given no retardation, 32% of the DNAPL source mass had been driven into the low permeability zone. The complement, 68%, was present in the transmissive zone. Given the same conditions along with a retardation factor of 10 in the low permeability layer, 58% of the released contaminant was present in the low permeability layer after 1,000 days and the complement (42%,) was present in the transmissive layer. Through an additional 2,000 days, after depletion of the DNAPL, the fraction of the contaminant mass in the low permeability zone increased to 34% and 61%, respectively, for no retardation and retardation factor of 10. This is explained through higher affinity of the contaminant to get sorbed to soil particles rather than the aqueous phase, when sorption is considered. Given that remedies for DNAPL in transmissive zones and contaminants in low permeability zones can be quite different, the observed evolution of the release leads to the conclusion that an understanding of the age of a release, along with the distribution of all phases in transmissive and low permeability zones, can be an important part of selecting appropriate site remedies.

Through the additional 2,000 days after the DNAPL source was depleted, the plume in the transmissive zone expanded while the contaminant mass in the low permeability layer remained in proximity to the original (DNAPL) source. Persistence of

contaminants in the low permeability zone in proximity to the original source, leads to the observation that much of the contaminant in low permeability zones may be limited to a subset of the plume indicated by dissolved phase contaminants in the transmissive zone. This observation provides an important guide for characterization and treatment of contaminants in low permeability zones.

The hypothesis of the alkaline persulfate laboratory study was that flushing an alkaline persulfate solution (a chemical oxidant) through a transmissive zone provides a means of significantly reducing future releases of contaminants from low permeability zones. A conceptual model and a laboratory-scale sand tank experiment were employed. The experiment involved a continuous transmissive sand layer with interbedded layers of kaolin-bentonite clay. The tank was flushed with water spiked with 100 mg/L fluorescein and 67 mg/L bromide for 92 days. During this period contaminants are attenuated by the clay layers. Fluorescein is the targeted contaminant and bromide is a conservative tracer. After 92 days, the tank was flushed with water without fluorescein and bromide for 38 days. This illustrates how release of contaminant stored in low permeability zones effects downgradient water quality. Next, fluorescein was treated by flushing the tank with 40,000 mg/L alkaline persulfate solution at pH 11 for eight days. The concentration and pH of persulfate were resolved through batch flask studies. Lastly, the tank was flushed with water with no additives for 69 days to evaluate post-treatment rebound of contaminant levels in the transmissive zones.

Data from the alkaline persulfate tank study included photographic images, fluorescein and bromide tank effluent concentrations, as well as spectrometer-based point measurements of fluorescein concentrations in the sand and clay layers. At the end of the

post-treatment phase, a three orders of magnitude decrease was observed in the normalized effluent concentrations, i.e., from less than 1 to 0.001. This result is consistent with the point measurements obtained using the spectrometer. Overall, results from the tank experiment suggest flushing the tank with an alkaline persulfate solution was effective in depleting fluorescein in both the transmissive and low permeability zones.

Results from the tank study may not be representative of performance under common field conditions. Constraints at field sites could include effective delivery of the high-density alkaline solution to a desired target, high soil oxidant demands in natural porous media that limit treatment of the targeted compounds, and uncertainties regarding treatment of compounds that are more recalcitrant than fluorescein. In addition, secondary water quality issues might arise from the use of a high pH and high total dissolved solids (TDS) alkaline persulfate solution.

The hypothesis of laboratory testing of innovative treatment technologies was that carbon sequestration, sonication, and calcium polysulfide (CPS) were promising technologies for treatment of chlorinated solvents in low permeability zones. Carbon sequestration involves emplacement of solid phase carbon in transmissive zones with the benefits of (1) adsorbing contaminants and (2) creating a redox poise that favors reductive dechlorination, and/or (3) providing a favorable substrate for microbes that facilitates *in situ* treatment. Column studies were performed to investigate deliverability of three carbon types (activated carbon, carbon black and charcoal) in a porous medium. In addition, vial studies were conducted to determine if conditions favoring reductive dechlorination were imposed. Delivery of carbon in sand columns resulted in clogging

the influent pores precluding effective delivery. Furthermore, no evidence was developed to indicate that carbon could impose redox conditions that would drive reductive dechlorination of TCE.

Sonication involves applying ultrasound energy to transmissive zones to degrade contaminants in low permeability zones. Sonication was evaluated through a series of vial studies involving trichloroethylene (TCE) solutions as the target contaminant. Initial vial studies indicated losses of TCE and increased chloride level with sonication. Unfortunately, these results were not reproducible. Also, the feasibility of driving TCE depletion at consequential distances from a sonication source appeared to be low.

Calcium polysulfide (CPS) studies focused on emplacement of reactive metal sulfides that could degrade chlorinated solvents. To evaluate this approach a series of vial studies was conducted using a range of CPS concentrations. Subsequently, a column study was conducted to examine the deliverability of CPS in porous media. Results obtained from laboratory experiments show that CPS can be delivered to soils without adverse plugging and that CPS imposed a redox condition of -500 mV (Ag-AgCl) and drove about 30%-40% reductions in TCE concentrations. Of the three experiment approaches investigated, CPS showed the greatest promise.

In summary, this dissertation provides original contributions regarding treating chlorinated solvents in low permeability zones. First, chlorinated solvent releases evolve through time. Understanding the age of a release, along with the distribution of the contaminant phases in transmissive and low permeability zones, is critical in selecting remedial measures. Second, with caveats, alkaline persulfate can deplete contaminants in low permeability zones sufficiently to preclude future releases. Lastly, preliminary

studies indicate that CPS may be a promising approach to treating contaminant in low permeability zones via emplacement of reactive metal sulfides.

## ACKNOWLEDGEMENTS

I would like to thank my respected committee members Dr. Thomas Sale, Dr. Domenico Bau, Dr. Charles Shakelford, and Dr. Thomas Borch. It has been a pleasure for me to have come to know and work with Dr. Sale during my doctoral studies at Colorado State University. He has been a professional and academic mentor to me and has shared his expertise with me, and has provided me with the support and encouragement I needed to go through my research. A big thank you goes to Dr. David Dandy, for his assistance and guidance with the modeling chapter. I sincerely appreciate Mitch Olson, Gary Dick and Julio Zimbron for their frequent assistance with my lab work. I also need to acknowledge our project sponsors, DuPont, GE, University Consortium for Field Focus Groundwater Contamination, and the staff and students at Center of Contaminant Hydrology.

On a more personal level, I would like to thank my dear parents, Dr. Jafar Bolhari and Soheila Monirijavid, who raised me with the love of learning and have provided me with passion, encouragement and best advices in every step of my life. I would like to thank my husband, Dr. Yaser Madani, for his heartwarming recommendations, support and patience during my PhD program. Additionally, I need to also mention the names of my amazing brothers, Amir and Ali, and my fabulous sister, Maryam, who have also motivated me by looking up to me as their oldest sibling. At the end, I have to mention the name of my utmost love, my nine-month-old son, Matin, who has been patiently cooperating with me in the whole process. I would like him to know that he has brought me a great sense of vivacity and delight that has encouraged me to work even harder.

FOR MATIN

# TABLE OF CONTENTS

	<u>Page</u>
<b>Chapter 1</b> .....	<b>1</b>
<b>INTRODUCTION</b> .....	<b>1</b>
1.1 Problem Statement.....	1
1.2 Research Hypotheses .....	5
1.3 Content and Organization .....	11
REFERENCES .....	12
<b>Chapter 2</b> .....	<b>14</b>
<b>EVOLUTION OF A CHLORINATED SOLVENT RELEASE IN A TWO LAYER SYSTEM THROUGH TIME</b> .....	<b>14</b>
SYNOPSIS.....	14
2.1 Introduction.....	15
2.2 Modeling.....	20
2.2.1 Assumptions.....	21
2.2.2 Computational Approach.....	24
2.3 Results.....	30
2.3.1 Temporal partitioning between transmissive and low permeability zones .....	30
2.3.1.1 Scenario 1: without adsorption.....	30
2.3.1.2 Scenario 2: with adsorption.....	32
2.3.2 Spatial variation in mass in low permeability zones.....	34
2.3.2.1 Scenario 1: without adsorption.....	34
2.3.2.2 Scenario 2: with adsorption.....	36
2.4 Conclusions.....	37
2.5 Acknowledgements.....	39
REFERENCES .....	40
<b>Chapter 3</b> .....	<b>45</b>
<b>CONCEPTUAL MODEL AND LABORATORY STUDIES ADDRESSING EFFECTS OF ALKALINE PERSULFATE FLUSHING ON CONTAMINANTS STORED IN LOW PERMEABILITY ZONES</b> .....	<b>45</b>
SYNOPSIS.....	45
3.1 Introduction.....	46
3.2 Material and Methods .....	51
3.3 Results and discussion .....	56
3.3.1 Photographic Images.....	57
3.3.2 Effluent Water Quality Data .....	60
3.3.3 Fiber Optic Spectrometer Data .....	62
3.3.4 Additional Considerations .....	65
3.4 Conclusions.....	66
Acknowledgments.....	67

REFERENCES .....	68
<b>Chapter 4 .....</b>	<b>70</b>
<b>POTENTIAL OF THREE INNOVATIVE APPROACHES FOR TREATING TRICHLOROETHENE IN LOW PERMEABILITY ZONES.....</b>	<b>70</b>
SYNOPSIS.....	70
4.1 Introduction.....	71
4.2 Carbon sequestration.....	74
4.2.1 Overview.....	74
4.2.1.1 Carbon Black.....	75
4.2.1.2 Activated carbon.....	76
4.2.1.3 Charcoal.....	78
4.2.2 Carbon laboratory studies.....	81
4.2.2.1 Methods.....	81
4.2.2.2 Results.....	83
4.2.3 Summary of carbon sequestration approach.....	85
4.3 Sonication.....	85
4.3.1 Overview.....	85
4.3.2 Sonication laboratory studies.....	90
4.3.2.1 Methods.....	90
4.3.2.2 Results.....	90
4.3.3 Summary for sonication.....	91
4.4 Calcium polysulfide (CPS).....	92
4.4.1 Overview.....	92
4.4.2 Calcium polysulfide laboratory studies.....	93
4.4.2.1 Short term proof of concept.....	93
4.4.2.1.1 Methods.....	93
4.4.2.1.2 Results.....	94
4.4.2.2 TCE degradation through CPS only.....	96
4.4.2.2.1 Methods.....	97
4.4.2.2.2 Results.....	97
4.4.2.3 TCE degradation through FeCl <sub>2</sub> activated CPS.....	100
4.4.2.3.1 Methods.....	100
4.4.2.3.2 Results.....	101
4.4.2.4 Deliverability of CPS.....	103
4.4.2.4.1 Methods.....	103
4.4.2.4.2 Results.....	104
4.4.3 Summary of CPS approach.....	104
4.5 Conclusion.....	104
REFERENCES .....	106
<b>Chapter 5 .....</b>	<b>111</b>
<b>SUMMARY OF RESULTS AND RECOMENDATIONS FOR FUTURE WORK</b>	<b>111</b>
<b>LIST OF ABBREVIATIONS .....</b>	<b>118</b>

## LIST OF TABLES

Table 1- Input parameters of the model.....	23
Table 2- Physical properties of porous media.....	52
Table 3- Influences of cavitation and aquasonolysis and their respective effects (After confidential Center for Contaminant Hydrology document written for GE).....	89
Table 4- Chloride and TCE results of the preliminary CPS experiment .....	95

## LIST OF FIGURES

Figure 1- Emerging focus of chlorinated solvent remediation efforts (after Sale et al. 2008a). .....	1
Figure 2- Fluorescein dye flushing through transmissive zones in a sand tank (Doner 2008). .....	2
Figure 3- Release of contaminants from low permeability zones after removal of fluorescein from the influent flushing solution (Doner 2008). .....	3
Figure 4- Anticipated water quality responses in a downgradient well to remediation technologies A, B and C addressing contaminants in low permeability zones. ....	6
Figure 5- The two-layer scenario conceptual model: A) Active source, B) Depleted source (after Sale et al. 2008). .....	18
Figure 6- Contaminant phases in transmissive and low permeability zones. Arrows: potential mass transfer between compartments. Dashed arrows: irreversible fluxes (after Sale and Newell 2011). .....	19
Figure 7- Predicted concentration contours in 1000 days from Sale et al. (2008): panels A and B, and hybrid method: panels C and D. ....	26
Figure 8- Transition distance calculated for $\Delta x=0.1$ m and $N_x=200$ . .....	27
Figure 9- PCE DNAPL and total aqueous PCE mass in transmissive ( $R=1$ ) and low permeability ( $R'=1$ ) layers over time. ....	31
Figure 10- Predicted PCE DNAPL and total aqueous PCE mass in transmissive ( $R=1$ ) and low permeability ( $R'=1$ ) layers over time. ....	31
Figure 11- The effect of elevating $R'$ from 1 to 10 on total PCE mass in transmissive ( $R=1$ ) and low permeability layers. ....	33
Figure 12- The effect of elevating $R'$ from 1 to 10 on predicted total aqueous and sorbed PCE mass in transmissive( $R=1$ ) and low permeability layers. ....	33
Figure 13- Spatial distribution of PCE mass in transects of the low permeability layer ( $R=1$ ). .....	35
Figure 14- Spatial distribution of PCE mass in transects of the low permeability layer ( $R=10$ ). .....	36
Figure 15 - Anticipated water quality responses in a downgradient well to technologies addressing contaminants in low permeability zones. ....	49
Figure 16- Dimensions of the sand tank embedded with clay layers .....	51
Figure 17- Experiment timeline .....	52
Figure 18- Soil-water calibration standards. ....	56
Figure 19- Images of the sand tanks at critical times in the experiment. ....	58
Figure 20- Normalized fluorescein and bromide effluent concentrations versus time (o fluorescein, x bromide) .....	61
Figure 21- Profiles of fluorescein concentration through the upper clay and adjacent sand layer. The point 0,0 is at the lower left hand corner of the tank. Horizontal position increasing to the right and vertical position increase upward. Transect A-A` lies along a line with a vertical position of 59 cm. Transect B-B` lies along a line with a horizontal position of 51cm. Transect C-C` lies along a line with a (vertical position of 71 cm. Gray shading indicates the position of the clay. Arrows indicate directions of diffusion-driven fluorescein transport in the clay. ....	64
Figure 22- Acrylic cylindrical columns used for the carbon experiment .....	81

Figure 23- a) Carbon deliverability column experiment, b) Carbon types redox poise vial study.....	83
Figure 24- Clogged columns after carbon delivery .....	84
Figure 25- pH and Eh data of carbon types vs. time.....	84
Figure 26- TCE and chloride concentration from sonication triplicate vials (one standard deviation bars are depicted on the graphs).....	91
Figure 27- From left to right: two saturated TCE solution controls, three iron sulfide vials, DIW and tap water controls in anaerobic chamber .....	94
Figure 28- PH and Eh (silver-silver chloride) of iron sulfide vials in anaerobic chamber	95
Figure 29- Titration of calcium polysulfide: pH data Eh data (mV of silver-silver chloride) .....	98
Figure 30- TCE (on left) and chloride (on right) concentration in CPS vials with time. .	99
Figure 31- TCE concentration with time: A) CPS (149 ppm) +FeCl <sub>2</sub> (44 ppm), B) CPS (893 ppm) +FeCl <sub>2</sub> (248 ppm) and C) CPS (3575 ppm) +FeCl <sub>2</sub> (992 ppm) .....	102
Figure 32- Deliverability of CPS solution column study .....	103

# Chapter 1

## INTRODUCTION

### 1.1 Problem Statement

After more than three decades of attention, managing subsurface releases of chlorinated solvents remains a major technical challenge (USEPA 2003, NRC 2005; Sale et al. 2008). Following Sale et al. (2008), prevailing thinking has evolved from the simple perspective of managing chlorinated solvent in groundwater in transmissive zones to a far more complex perspective of managing chlorinated solvents as nonaqueous, aqueous, sorbed, and vapor phases, in transmissive and low permeability zones, which occur in source zones and plumes. Figure 1 documents the emergence of key aspects of the problem with time.

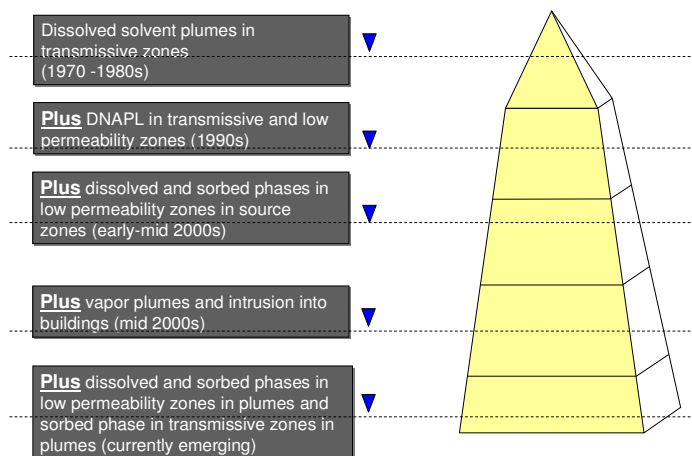
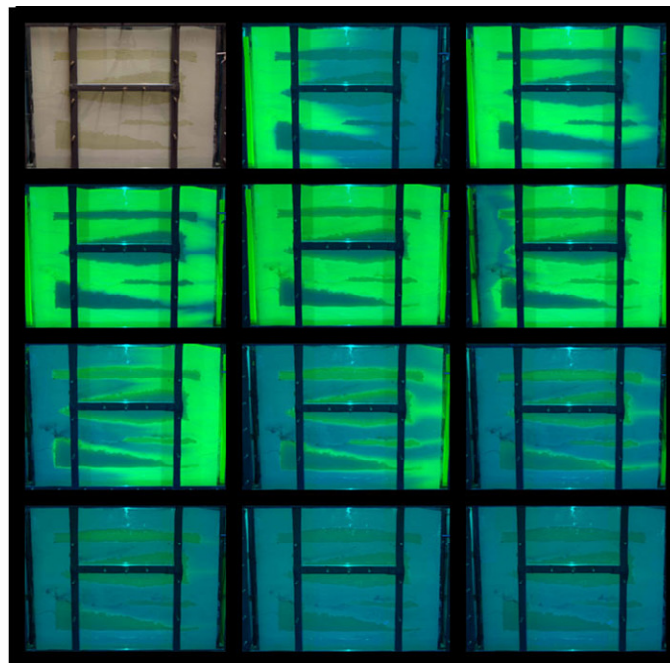


Figure 1- Emerging focus of chlorinated solvent remediation efforts (after Sale et al. 2008a).

Over the past thirty years the primary objective for managing subsurface chlorinated solvents releases has been restoration of groundwater, soils and soil gas to strict health-based numerical standards. One of the primary constraints to achieving this objective has been a failure to holistically consider all of the compartments that need to be addressed.

The problem is introduced by considering the evolution of a chlorinated solvent release. Most chlorinated solvent releases begin as a subsurface discharge in the form of a dense nonaqueous phase liquid (DNAPL). Initially, DNAPL moves through transmissive zones and becomes perched above low permeability capillary barriers (Feenstra et al. 1996). With time, DNAPL constituents partition into aqueous and vapor phases in transmissive zones. Aqueous phase chlorinated solvents initially move through transmissive zones via advection. This is illustrated in Figure 2, where fluorescein dye in water is pumped through a tank containing sand with interbeds of clay.



**Figure 2- Fluorescein dye flushing through transmissive zones in a sand tank (Doner 2008).**

At first, there is little or no contamination in the low permeability clay layers. With extended time, dissolved phase contaminants migrate into low permeability zones by diffusion and/or slow advection (Sudicky et al. 1985; Chapman and Parker 2005; Sale et al. 2008b; Liu et al. 2007). Ultimately, through natural processes and/or remediation, contaminants in the transmissive zones are depleted. This reduces aqueous concentrations in transmissive zones and drives the release of contaminants from low permeability zones via back diffusion and slow advection. The release process is illustrated by the trails of water containing fluorescein dye emanating from the clay layers in a sand tank study in Figure 3.

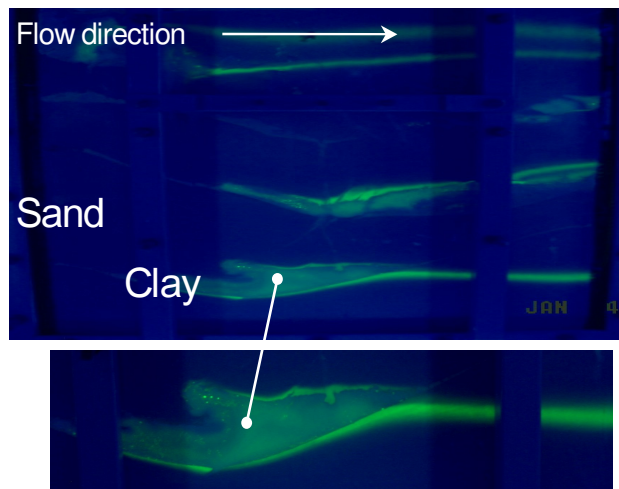


**Figure 3- Release of contaminants from low permeability zones after removal of fluorescein from the influent flushing solution (Doner 2008).**

Contaminants move out of low permeability zones far more slowly than they move into them (Feenstra et al. 1996). A primary implication of slow release is the potential for dilute plumes to be sustained for decades or even centuries after their original source has been depleted (Chapman and Parker 2005; Sale et al. 2008b). While the low conductivity layers provided a sink mechanism for migration of contaminants at

early-time, the layers became a source at late-time. Furthermore, contaminant sorption, as well as contaminant degradation in low permeability zones, is a critical factor governing the significance of contaminants in low permeability zones (Sale et al. 2008b).

Early recognition of contaminant storage and release in low permeability zones is found in Foster and Crease (1974). Foster and Crease (1974) observed slow transport of nitrate from overlying agricultural lands through fractured chalk to the water table. In 1975, Foster suggested that diffusion might be playing a key role; he further suggested that extensive investigation of diffusion during fracture flow should be considered. This was followed by a rich body of literature. Per Sale et al. (2008b) "The topic of diffusive transport in heterogeneous granular porous media has received broad attention, with key references including: Foster (1975), Freeze and Cherry (1979), Rao et al. (1980), Sudicky (1983), Sudicky et al. (1985), Goltz and Roberts (1987), Wilson (1997), Carrera et al. (1998), Liu and Ball (2002), Chapman and Parker (2005), and Liu et al. (2007)". Wilson (1997), Liu and Ball (2002), and Chapman and Parker (2005) specifically recognize that back diffusion can impact the timing and magnitude of the downgradient water quality improvements associated with upgradient reductions in contaminant loading." Consistent with this literature, McGuire et al. (2006) reviews 59 chlorinated solvent sites where remediation had targeted DNAPL source zones. Unfortunately none of these projects observe restoration of groundwater to risk-based maximum contaminant levels (MCLs). The hypothesis of this document is that the slow release of contaminants stored in low permeability zones is a primary factor constraining the success of the noted remedial actions.

Today the growing realization is that contaminants in low permeability zones are consequential in source zone and plume. Reflecting this, the U.S. Department of Defense (DoD) committed \$4 million dollars to fund related research in 2009. The paradigm of the past three decades, that depletion of contaminant in source zones would solve the problem in plumes, is fading. It is being replaced by a new paradigm centered on the theme that, in the case of older releases of persistent organic contaminants, it is possible that much of the released material no longer resides in the vicinity of the original release (the source zone), and instead resides as largely immobile phases in low permeability zones in plumes.

The emerging question is what can be done about contaminants in low permeability zones? Liu and Ball (2002) observe the effects of removing a chlorinated solvent source above a clay aquitard. Based on cores and modeling, persistent concentration of chlorinated solvents in groundwater are attributed to slow release of chlorinated solvents from an aquitard. Similarly, Chapman and Parker (2005) describe a scenario in which release of contaminants from low permeability zones sustains concentrations of chlorinated solvents in groundwater after isolation of the contaminants in the original release area. Thomson et al. (2008) describe treatment of a creosote impacted aquifer impacted using chemical oxidants. Four years after treatment, contaminant levels in groundwater rebounded to pretreatment levels.

## **1.2 Research Hypotheses**

The following text elucidates an overall hypothesis for this dissertation and specific hypotheses for three supporting activities.

## The Overall Hypothesis

Building on the aforementioned observations, Figure 4 presents the overall hypothesis for this research following Freeze and McWhorter 1997. The scenario considered is a monitoring well in a heterogeneous sandy aquifer downgradient of a chlorinated solvent release. The graph presents the concentration of an aqueous phase chlorinated solvent in the well as a function of time. Following the release at time  $t_0$ , concentrations of the contaminant increase at the well (located downgradient of the source) through  $t_1$ . When the upgradient source is removed the contaminant concentration at the well asymptotically approaches  $C_0$  at  $t_1$ , resulting in slower rates of contaminant attenuation by the low permeability zone.

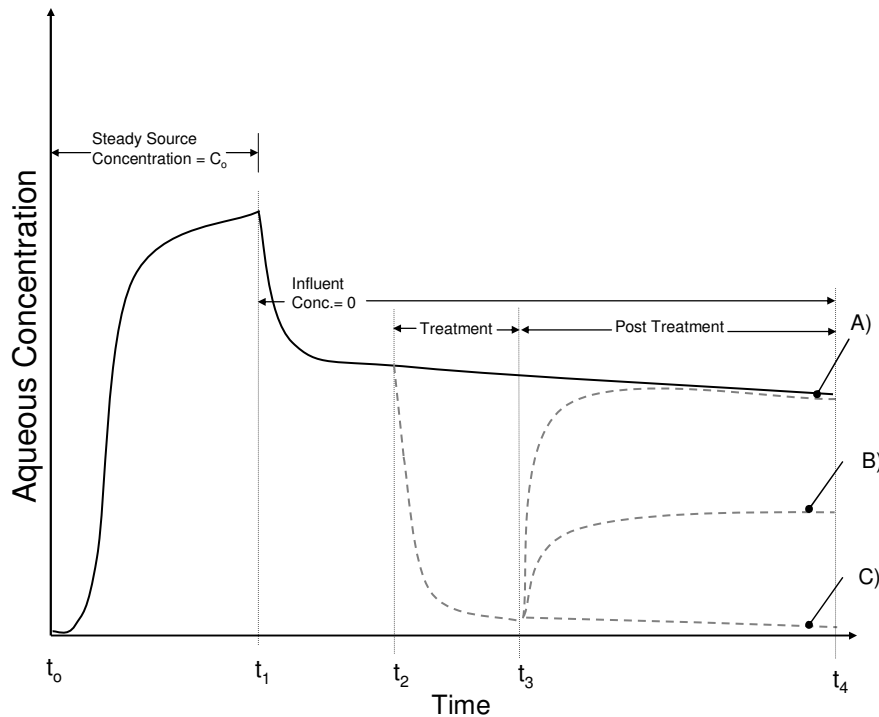


**Figure 4- Anticipated water quality responses in a downgradient well to remediation technologies A, B and C addressing contaminants in low permeability zones.**

At time  $t_1$  the effect of eliminating contaminant discharge from the original release area (the source) propagates to the well. During the period  $t_1$  to  $t_2$ , concentrations

of chlorinated solvents decrease at the well. In the absence of an upgradient source, aqueous phase concentrations at the well are sustained by ever slowing rates of contaminant release from low permeability zones. During the period  $t_2$  to  $t_3$  a treatment is employed that depletes concentrations of aqueous phase contaminant in the transmissive portion of the aquifer. Subsequently three hypothetical water quality responses at the monitoring well are contemplated, including:

- A. Concentrations at the well return to levels that would have been observed in the absence of treatment. This behavior would be attributed to remedy that had no effect on contaminant release from low permeability zones.
- B. Concentrations at the well are reduced to a level below what would have been observed in the absence of treatment but above risk-based numerical standards. This behavior would be attributed to a partial reduction in the rates of contaminant release from low permeability zones.
- C. Concentrations at the well are reduced to levels below what would have been observed in the absence of treatment and below risk-based numerical standards. This behavior is considered to be a sufficient depletion of contaminant from the low permeability zones.

### **Activity Specific Hypotheses**

The overall objective of this dissertation was to resolve if and when it is technically feasible to treat contaminants stored in low permeability zones. The following identifies three supporting hypotheses and provides a brief introduction to the associated research activities.

## **Activity 1- Modeling release evolution**

Activity 1 is predicated on the hypothesis that, subsurface releases of chlorinated solvents through time evolve from a problem of DNAPL in transmissive zones to one of dissolved and sorbed phases in low permeability zones. This hypothesis is tested using analytical solutions for a two-layer system described in Sale et al. (2008b) to track the distribution of DNAPL, aqueous, and sorbed constituents in the transmissive layer and aqueous, and sorbed constituents in the low permeability layer, as a function of time. This work is presented in Chapter 2 of this dissertation.

More specifically, the physical setting considered was a two-layer system consisting of a semi-infinite transmissive zone and a semi-infinite low permeability zone. A transmissive layer was situated above the low permeability layer. Point concentrations of sorbed and aqueous phase were calculated at points across the domain of interest. Source input parameters were based on producing a source equivalent to a thin 1 m long horizontal pool of perchloroethene (PCE) located in the transmissive layer, immediately above the low permeability layer. The source was on with a constant strength for 1,000 days. Subsequently, the source was shut off and contaminant distribution through the domain of interest was evaluated for an additional 2,000 days. All calculations were carried out using Mathcad<sup>TM</sup> 14. This work shows that chlorinated solvent releases evolve through time in terms of contaminant phases and distribution in transmissive and low permeability zones. Furthermore results show that contaminants in low permeability zones, which may require treatment, can be limited to a subset of the overall dissolved phase plume.

### **Activity 2- Alkaline activated persulfate**

The hypothesis for Activity 2 is that flushing an alkaline activated persulfate solution through transmissive zones can deplete contaminants in low permeability zones sufficiently to achieve Type C behavior as illustrated in Figure 4. This hypothesis is tested via a 208 day sand tank experiment in which fluorescein is used as a surrogate contaminant for a chlorinated solvent. This activity is described in Chapter 3 of this dissertation.

In more detail, the experiment involved transmissive sand with interbedded low permeability clay layers. Fluorescein and bromide were employed as reactive and conservative contaminants, respectively. Excitation of fluorescein using ultraviolet light provided a unique opportunity to observe and quantify treatment of a contaminant in transmissive and low permeability zones. Data from the experiment include photographic images, fluorescein and bromide tank effluent concentrations, and spectrometer-based point measurements of fluorescein concentrations in the sand and clay layers. Primary developments include insights regarding governing processes and a dataset that can be used to develop and test mathematical models that address treatment of contaminants in low permeability zones.

### **Activity 3- Exploration of innovative solutions**

The hypothesis for Activity 3 is that novel applications of carbon sequestration, sonication, and calcium polysulfide (CPS) are promising technologies for treatment of contaminants in low permeability zones. This hypothesis explored a review of work by

others, as well as bench-scale laboratory proof-of-concept experiments. This activity is presented in Chapter 4.

In more detail:

- a. The vision for carbon sequestration was to emplace solid phase carbon in transmissive zones as a means of 1) adsorbing contaminants, 2) creating a redox poise that favors reductive dechlorination, and/or 3) providing a favorable substrate for microbes that facilitate *in situ* treatment. Column studies were performed to investigate deliverability of three carbon types in porous media, and also vial studies were conducted to determine if conditions favoring reductive dechlorination were imposed by the carbon.
- b. The vision for sonication was to reduce future releases of contaminants from low permeability zones by applying ultrasound energy to the transmissive zone. The anticipated result was that sonication would reduce aqueous concentration in transmissive zones and low permeability zones and/or provide preferential displacement of contaminants out of low permeability zones. This was evaluated through a series of vial studies involving trichloroethylene (TCE) solutions as the target contaminant.
- c. The vision for CPS was to form reactive sulfide precipitants on the solid media in transmissive zones that could degrade chlorinated solvents. To evaluate this approach a series of vial studies were undertaken using a range of CPS concentrations. Subsequently, a column study was conducted to examine the deliverability of CPS in porous media.

### **1.3 Content and Organization**

This dissertation is organized into three chapters written in journal manuscript format, each addressing the hypotheses presented above. Chapter 2 was published in Hydrology Days 2012 conference. Chapter 3 was submitted to Groundwater Monitoring and Remediation in June of 2012. Regrettably, the results in Chapter 4 were negative for two of three promising technologies. Further evaluation of CPS is ongoing at Colorado State University. As such, results from Chapter 4 have not been published. In contrast, the results from Chapter 4 have provided a valuable basis for ongoing studies regarding further testing of promising technologies for treatment of contaminants in low-permeability zones.

Furthermore, Chapters 2, 3 and 4 have been presented in 2008 and 2009 at the Annual Progress Meetings of the University Consortium for Field-Focused Groundwater Contamination Research in Ontario, Canada; and also in 2007, 2009 and 2010 at the American Geophysical Union Hydrology Days in Fort Collins, Colorado. More recently, Chapter 2 was presented at the 2011 Fall American Geophysical Union meeting in San Francisco, the 2011 SERDP/ESTCP Partner meeting in Washington D.C., and also Hydrology Days 2012 in Fort Collins. The final Chapter of this thesis, Chapter 5, provides a summary of results from all of the studies and recommendations for additional work.

## REFERENCES

- Carrera, J., Sanchez-Villa, X., Benet, I., Medina, A., Galarza G., Guimera, I., 1998. On matrix diffusion: solutions methods and qualitative effects, *Hydrogeology Journal* 6 (1), 178–190.
- Chapman, S.W., B.L. Parker, 2005. Plume Persistence Due to Aquitard Back Diffusion Following Dense Nonaqueous Phase Liquid Removal or Isolation, *Water Resource Research* 41 (12), W12411.
- Doner, L.A., 2008. Tools to resolve water quality benefits of upgradient contaminant flux reduction. MS thesis, Colorado State University, Fort Collins, COLORADO.
- Feenstra, S., Cherry, J.A., Parker, B.L., 1996. Conceptual Models for the Behavior of Dense Nonaqueous Phase Liquids (DNAPLs) in the Subsurface, Chapter 2 in Dense Chlorinated Solvents and Other DNAPLs in Groundwater, J.F Pankow and J.A. Cherry, Editors. Waterloo Press, pp. 53-88.
- Foster, S. S. D., 1975. The chalk groundwater tritium anomaly—a possible explanation, *Journal of Hydrology* 25, 159–165.
- Foster, S. S. D., Crease, R. I., 1974. Nitrate pollution of chalk groundwater in east Yorkshire – A hydrogeological appraisal, *Journal of Institution of Water Engineers and Scientists* 28, 178-194.
- Freeze, R.A., Cherry, J.A., 1979. Groundwater. Prentice-Hall Publishing Company, Englewood Cliffs, NJ
- Freeze, R. A., McWhorter, D. B., 1997. A framework for assessing risk reduction due to DNAPL mass removal from low permeability soils. *Journal of Ground Water*, 35, 1, 111-123.
- Goltz, M.N., Roberts, P.V., 1987. Using the method of moments to analyze three-dimensional diffusion-limited solute transport from temporal and spatial perspectives. *Water Resour. Res.* 23, 1575–1585.
- Liu, G., Ball, W. P., 2002. Back diffusion of chlorinated solvent contamination from a natural aquitard to a remediated aquifer under well-controlled field conditions: predictions and measurements, *Journal of Ground Water* 40, pp. 175–184.
- Liu, G., Zheng, C., Gorelick, S., 2007. Evaluation of the applicability of the dual-domain mass transfer model in porous media containing connected high- conductivity channels, *Water Resource Research* 43, p. W12407.

- McGuire, T.M., McDade, J.M., Newell, C.J., 2006. Performance of DNAPL source depletion technologies at 59 chlorinated solvent-impacted sites. *Ground Water Monit Remediat* 26, 73–84.
- National Research Council (NRC), 2005. Contaminants in the Subsurface: Source Zone Assessment and Remediation. National Academies Press, Washington, D.C.
- Rao, P.S.C., Rolston, D.E., Jessup, R.E., Davidson, J.M., 1980. Solute transport in aggregated porous media: theoretical and experimental evaluation, *Journal of Soil Science of America* 44, 1139–1146.
- Sale, T. C., Newell, C., Stroo, H., Hinchee, R., Johnson, P., 2008a. Frequently asked questions regarding management of chlorinated solvents in soils and groundwater, Environmental Security Technology Certification Program (ESTCP), ER-0530. is at: <http://www.estcp.org/Technology/upload/ER-0530-FAQ.pdf>.
- Sale, T. C., Zimbron, J., Dandy, D., 2008b. Effects of reduced contaminant loading on downgradient water quality in an idealized two-layer granular porous media, *Journal of Contaminant Hydrology* 102, 72-85.
- Sudicky, E.A., 1983. An convection–diffusion theory of contaminant transport for stratified porous media, Ph.D. dissertation, 203 pp., University of Waterloo, Waterloo, Canada, 6 May.
- Sudicky, E.A., Gillham, R.W., Frind, E.O., 1985. Experimental investigation of solute transport in stratified porous media 1. The nonreactive case, *Water Resources Research* 21, 1035–1041.
- U.S. Environmental Protection Agency (EPA), 2003. *The DNAPL Remediation Challenge: Is There a Case for Source Depletion?* EPA/600/R-03/143
- Wilson, J.L., 1997. Removal of aqueous phase dissolved contamination: non-chemically enhanced pump and treat. In: C.H. Ward *et al.*, Editors, *Subsurface Remediation Handbook*, Ann Arbor Press, Chelsea, MI, pp. 271–285.

## Chapter 2

# EVOLUTION OF A CHLORINATED SOLVENT RELEASE IN A TWO LAYER SYSTEM THROUGH TIME<sup>1</sup>

### SYNOPSIS

This paper explores the hypothesis that chlorinated solvent releases evolve temporally and spatially. A two-layer system was considered, involving a transmissive layer (e.g., sand) situated above a low permeability layer (e.g., silt). A DNAPL-like source was present in the transmissive layer at the upgradient edge of the model domain at the contact between the two layers. A constant source was active for 1,000 days. Subsequently the source was shut off and the problem was studied for an additional 2,000 days. Total contaminant mass in transmissive and low permeability layers, along with total mass in selected profiles of the soil were evaluated. Calculations take into account the effect of retardation.

At 1,000 days, given no retardation, 32% of the DNAPL source mass has been driven into the low permeability zone. The complement (68%) is present in the transmissive zone. Given the same conditions and a retardation factor of 10 in the low permeability layer, 58% of the released contaminant is present in the low permeability layer after 1,000 days and the complement (42%) is present in the transmissive layer. Through an additional 2,000 days, after depletion of the DNAPL, the fraction of the contaminant mass in the low permeability zone increases to 34% and 61% for no

---

<sup>1</sup> A. Bolhari and T. Sale, Department of Civil and Environmental Engineering, Colorado State University, Fort Collins, Colorado.

retardation and low permeability zone retardation factor of 10, respectively. Given that remedies for DNAPL in transmissive zones and contaminants in low permeability zones can be quite different, the observed evolution of the release leads to the conclusion that an understanding of the age of a release, as well as the distribution of all phases in transmissive and low permeability zones, can be an important part of selecting appropriate site remedies.

Through the additional 2,000 days after the DNAPL source is depleted the plume in the transmissive zone expands while the contaminant mass in the low permeability layer remains in proximity to the original (DNAPL) source. Persistence of contaminants in the low permeability zone, in proximity to the original source, leads to the observation that much of the contaminant in low permeability zones may be limited to a subset of the plume indicated by dissolved phase contaminants in the transmissive zone. This observation provides an important guide for characterization and treatment of contaminants in low permeability zones.

## **2.1 Introduction**

At many sites, chlorinated solvents were historically released into subsurface setting in the form of dense non-aqueous phase liquids (DNAPLs). With time, DNAPL constituents partition into water, sorb to solids, and partition into soil gas. Following Feenstra et al. (1996) and Kueper and McWhorter (1991), DNAPLs preferentially move through the most transmissive portions of subsurface media and frequently come to rest above low permeability zones. Entry of DNAPL into low permeability zones is often precluded by insufficient capillary pressures (pool height) to displace the water from the pore spaces in low permeability zones. As such, DNAPL is most often found in the

transmissive portions of source zones. An important exception can be secondary permeability features in low permeability zones (e.g., root cast and slickensides) that have large opening and relatively lower entry pressures.

With time, DNAPL constituents partition into the aqueous phase and advection carries the dissolved phase downgradient through transmissive intervals creating dissolved phase plumes. Herein, transmissive zones are conceptually defined as intervals in which advection is a primary transport process (seepage velocities  $> 1$  m/year). In evaluating 88 sites, Newell et al., (1990) reports a median plume length of 1,000 ft for chlorinated ethenes. Concurrently, vapor phase plumes can form in unsaturated zones via direct evaporation of DNAPL in unsaturated zones or partitioning from aqueous phases.

A potential consequence of DNAPL dissolution and constituent advection is the formation of large concentration gradients at the contacts between transmissive and low permeability zones (Sudicky et al. 1986; Chapman and Parker 2005; Parker et al. 2008; and Sale et al. 2008). Herein, low permeability zones are conceptually defined as intervals in which advection is a weak process (seepage velocities  $< 1$  m/yr). With time large contaminant concentration gradients at contacts between transmissive and low permeability zones drive dissolve phase constituents into low permeability zones via diffusion. Processes that can enhance diffusive transport into low permeability zones (by increasing concentration gradients) include sorption (Parker et al. 1994) and degradation (Sale et al. 2008). Assuming insignificant advective transport, dissolved phase constituents will continue to move across contacts from transmissive to low permeability zones as long as the dissolved phase constituent concentrations are greater in the transmissive zone. Conversely, given concentrations in transmissive zones, at contacts,

that are less than concentrations in low permeability zones, diffusion can drive release of constituent from low permeability zones.

A number of researchers have recognized that contaminant stored in low permeability zones can sustain plumes with adverse contaminant concentrations long after mass flux from the original DNAPL source is depleted. Liu and Ball (2002) observed a slow release of chlorinated solvents from an aquitards after a source removal from an overlying sand unit. Chapman and Parker (2005) illustrated sustained releases from a low permeability unit to an overlying transmissive sand 6 years after the original DNAPL source zone was isolated from the plume using a physical barrier. Furthermore, Chapman and Parker (2005) employed high resolution numerical modeling methods to demonstrate that releases from low permeability zones can sustain adverse concentration in a transmissive zone for 100 years after source isolation. Sale et al. (2008) advanced an analytical solution for a two layer system consisting of a semi-infinite transmissive zone overlying a semi-infinite low permeability layer with a constant DNAPL like source in the transmissive zone. Figure 5 presents the conceptual frame work of the two layer model. Results presented in Sale et al. (2008) show that releases from low permeability zones is a function of position downgradient of the original source, retardation in the low permeability zone, and rates of degradation in the low permeability zone.

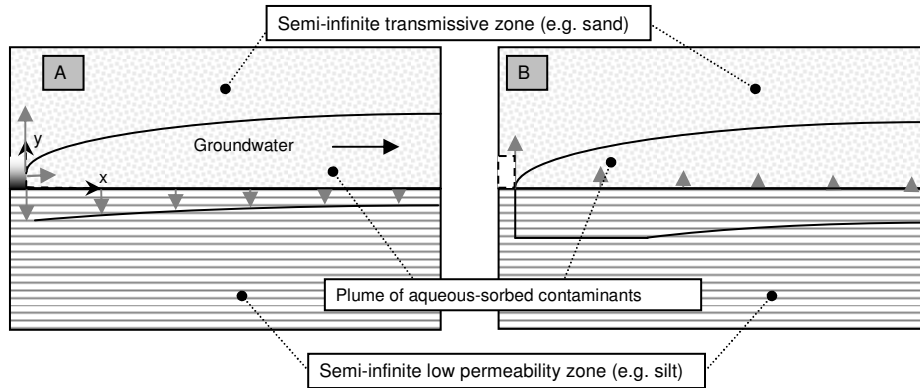


**Figure 5- The two-layer scenario conceptual model: A) Active source, B) Depleted source (after Sale et al. 2008).**

Analytical solutions of advective-dispersive equation have been widely applied to describe solute transport in porous media. Early studies such as Skopp and Warrick (1974) and Al-Niami and Rushton (1979) neglected the effect of retardation. Tang et al. (1981) studies single thin fracture whereas Sudicky and Frind (1982) considered system of parallel thin fractures. Others focused on transient one-dimensional (Cameron and Klute 1977) or steady three-dimensional transport (Sale and McWhorter 2001). All these studies considered relatively narrow aspects of a much larger problem.

Building on all of the above noted concepts, Sale and Newell (2011) developed the 14 Compartment Model (Figure 6) as a tool for identifying all of the potential combinations of contaminant phases in transmissive and low permeability zones, in source zones and plumes. Furthermore, the 14 Compartment model can be used to map contaminant fluxes between the compartments and anticipate the benefits of remedial measures.

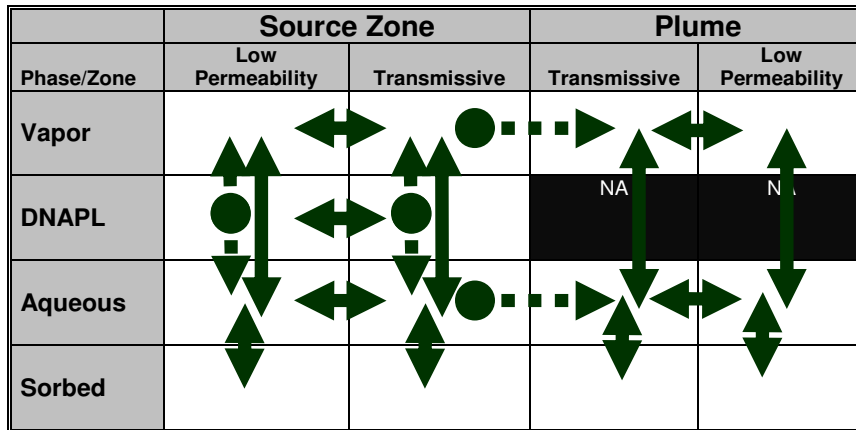


**Figure 6- Contaminant phases in transmissive and low permeability zones. Arrows: potential mass transfer between compartments. Dashed arrows: irreversible fluxes (after Sale and Newell 2011).**

The 14 Compartment model uses the NRC (2005) definition of a source zone - a zone in which a DNAPL was released that can include contaminants stored about the original DNAPL release. Conversely, by exclusion, the 14 Compartment Model definition of a plume is the contaminated zones in which DNAPL was never present.

The objective of this paper is to illustrate the evolution of a chlorinated solvent release through time per the concepts advanced in the 14 Compartment Model. More specifically, the objective is to resolve the distribution of contaminant mass in critical compartments as a function of time and position. Following Sale and Newell (2011), the distribution of contaminant mass in compartments is seen as a potentially critical aspect of selecting remedies and anticipating associated benefits. Furthermore, the distribution of contaminant mass in compartments is seen as a problem that varies in both time and space. As such, the position in the body of a chlorinated solvent release and the age of the release can play an important role in selecting appropriate remedies.

This paper employs the two-layer scenario and analytical solutions developed in Sale et al. (2008) to estimate contaminant mass present in selected compartments as a function of time, position, and retardation in the low permeability zones. Given the fact that the Sale et al. (2008) analytical model only addresses saturated media, vapor phase compartments are excluded from the analysis. An important constraint to using the Sale et al. (2008) Mathcad worksheet is that it only works for domains less than 100 m in transmissive zone. Beyond 100m the Sale et al. (2008) Mathcad worksheet runs into computational problems associated with calculating error function values for large arguments and raising  $e$  to large powers. A partial solution is found to this problem wherein a series approximation is used for those portions of the domain where the Sale et al. (2008) Mathcad worksheet fails. The combined series - Sale et al. (2008) Mathcad worksheet approach is referred to as the hybrid solution. Unfortunately, the hybrid approach also has a limited domain of application. In the end, the manuscript relies solely on the low permeability layer solution from Sale et al. (2008) which can be applied to large domains. Contaminant mass in transmissive zones is estimated as the difference between the mass released from the source and the mass in the low permeability zone. To date, ongoing efforts at Colorado State University to find practical computational approaches for the Sale et al. (2008) transmissive zone solution have been unsuccessful.

## **2.2 Modeling**

Analytical solutions described in Sale et al. (2008) were used to estimate the distribution of DNAPL, aqueous and sorbed phase in transmissive and low permeability zones as a function of time. These solutions were employed to address two main questions or concerns: 1) temporal partitioning of the contaminant between transmissive

and low permeability zones and 2) spatial variation in mass in low permeability zones. These questions are explored in two scenarios. The first scenario assumes no retardation in either layer. The second scenario includes a retardation factor of 10 for the low permeability zone. All calculations were carried out using Mathcad<sup>TM</sup> 14. The following describes modeling assumptions, computational approach, and model limitations.

### **2.2.1 Assumptions**

The physical setting of the two-dimensional (2-D) two-layer system considered in this modeling effort was previously introduced in Figure 5. The transmissive layer is situated above the low permeability layer. A DNAPL like source exists at the contact of the two layers. Primary assumptions are as follows:

- 1) Transmissive and low permeability layers are uniform, homogeneous, isotropic, and infinite in  $y \rightarrow \infty$  (transmissive layer) and  $y' \rightarrow \infty$  (low permeability layer; note  $y'$  increases with depth below the contact),
- 2) One-dimensional (1-D) advective transport in the transmissive layer parallel to the boundary of the layers is accompanied by transverse diffusion and dispersion,
- 3) Longitudinal dispersion is not considered in the transmissive layer,
- 4) 1-D transverse diffusion transport exists in low permeability layer,
- 5) Retardation of contaminants in both the transmissive and low permeability layers (described by  $R$  and  $R'$  respectively) is based on instantaneous equilibrium between aqueous and sorbed phases
- 6) No degradation is considered in either layer,

In more detail, initial and boundary conditions include:

$$c(x, y, 0) = 0 \quad (y \geq 0) \quad (1a)$$

$$c'(x, y, 0) = 0 \quad (-\infty < y \leq 0) \quad (1b)$$

$$c(x, y \rightarrow \infty, t) = 0 \quad (2a)$$

$$c'(x, y \rightarrow -\infty, t) = 0 \quad (2b)$$

$$c(x, 0, t) = c'(x, 0, t) \quad (3a)$$

$$nD_t \frac{\partial c}{\partial y}(x, 0, t) = n'D^* \frac{\partial c'}{\partial y}(x, 0, t) \quad (3b)$$

where,  $c(x,y,t)$ ,  $n$  and  $D_t$  are solute concentration, porosity and effective transverse diffusion coefficient of the transmissive layer and  $c'(x,y,t)$ ,  $n'$  and  $D^*$  are solute concentration, porosity and effective transverse diffusion coefficient of the low permeability layer, respectively.

The source occurs in the transmissive layer at  $x=0$ . It is modeled as:

$$c(0, y, t) = c_0 e^{-by} [1 - H(t - t^*)] \quad (y \geq 0) \quad (4)$$

where  $c_0$  is the aqueous concentration at  $x=0$ ,  $y=0$  and  $b$  is the source distribution constant, Furthermore,  $t^*$  is the persistence time of the source and  $H$  is the Heaviside step function, such that:

$$H(t - t^*) = \begin{cases} 0 & \text{if } t \leq t^* \\ 1 & \text{if } t > t^* \end{cases} \quad (5)$$

Input values used in the model are presented in Table 1. Table 1 values are based on common conditions found in alluvial setting.

**Table 1- Input parameters of the model**

Parameter	Values	Units
Average linear groundwater velocity, $v$	0.27	m/day
Porosity of the transmissive layer, $n$	0.25	dimensionless
Porosity of the low permeability layer, $n'$	0.4	dimensionless
Hydraulic conductivity of the transmissive layer, $k$	$1.4 \times 10^{-4}$	m/s
Hydraulic conductivity of the low permeability layer, $k'$	$1.7 \times 10^{-6}$	m/s
Aqueous solubility of PCE, $c_0$	240	mg/L
Retardation factor of the transmissive layer, $R$	1	dimensionless
<sup>1</sup> Retardation factor of the low permeability layer, $R'$	1 and 10	dimensionless
Effective transverse diffusion or dispersion coefficient of the transmissive layer, $D_t$	$4.5 \times 10^{-9}$	$m^2/s$
Effective transverse diffusion coefficient of the low permeability layer, $D^*$	$5.5 \times 10^{-7}$ 10	$m^2/s$

<sup>1</sup>Retardation factor of the low permeability layer is 1 for scenario 1 and 10 for scenario 2.

In this study the source is on for 1000 days ( $t'$ ) and then shut completely off allowing clean water to flush through the media for an additional period of 2000 days. The aqueous concentration associated with the source decays exponentially with increasing distance above the interface of two layers in the transmissive layer (see Figure 5). The source term  $b$  and  $c_0$  values used in this study are based on a thin 1 m long horizontal pool of PCE located upgradient of the point  $x=0$  and  $y=0$ .

In Table 1 the effective transverse diffusion coefficients of PCE in transmissive and low permeability layers ( $D_t$  and  $D^*$ ) are respectively estimated as:

$$D_t = v\alpha_t + D_e \quad (6a)$$

$$D^* = n'^{\frac{1}{3}} D_{aq} \quad (6b)$$

where,  $D_e$ , the effective molecular diffusion coefficient of PCE in transmissive layer is calculated from:

$$D_e = n^{\frac{1}{3}} D_{aq} \quad (6c)$$

In the above equations,  $\alpha_t = 0.0013 \text{ m}$  is the coefficient of transverse hydrodynamic dispersion and  $D_{aq} = 7.5 \times 10^{-10} \text{ m}^2/\text{s}$  is the aqueous diffusion coefficient of PCE.

### 2.2.2 Computational Approach

Contaminant concentrations in the transmissive and low permeability layer at a desired location and time are calculated from Equations (7)-(10), per Sale et al. (2008):

$$c_{trans.}(x, y, t) = c_0 \left( \frac{1}{2} e^{\frac{b^2 x}{\phi^2}} \left[ e^{by} \operatorname{erfc} \left( \frac{b}{\phi} \sqrt{x} + \frac{\phi y}{2\sqrt{x}} \right) + e^{-by} + e^{-by} \operatorname{erf} \left( \frac{-b}{\phi} \sqrt{x} + \frac{\phi y}{2\sqrt{x}} \right) \right] \right. \\ \left. + \frac{-\phi \gamma}{\pi} e^{by} \sqrt{t - \frac{x}{v_c}} \int_0^x \frac{e^{\frac{b^2 \xi}{\phi^2}}}{\sqrt{x - \xi}} \left( \frac{\operatorname{erfc} \left( \frac{b}{\phi} \sqrt{\xi} + \frac{\phi y}{2\sqrt{\xi}} \right)}{\gamma^2 (x - \xi) + \phi^2 \left( t - \frac{x}{v_c} \right)} \right) d\xi \right) \quad (7)$$

where,  $\phi$ ,  $\gamma$  and  $v_c$  are defined as:

$$\phi = \sqrt{\frac{v}{D_t}} \quad (8a)$$

$$\gamma = \frac{n' \sqrt{R' D^*}}{n D_t} \quad (8b)$$

$$v_c = \frac{v}{R} \quad (8c)$$

and  $R$  and  $R'$  are retardation factors of the transmissive and low permeability layer, respectively.

$$c_{lowk}(x, y, t) = c_0 \left( \frac{1}{\sqrt{\pi}} \int_0^x \frac{I_1(x, y, t, \xi)}{\sqrt{x-\xi}} \left[ \frac{1}{\sqrt{\pi\xi}} - \frac{b}{\phi} e^{\frac{b^2\xi}{\phi^2}} \operatorname{erfc}\left(\frac{b}{\phi}\sqrt{\xi}\right) \right] d\xi \right) \quad (9)$$

where,

$$I_1(x, y, t, \xi) = \operatorname{erfc}\left(\frac{y}{2\sqrt{t-\frac{x}{v_c}}}\sqrt{\frac{D^*}{R^*}}\right) - \gamma \frac{\operatorname{erfc}\left(\frac{\frac{\gamma y}{\sqrt{\frac{D^*}{R^*}}}}{2\left(t-\frac{x}{v_c}\right)\sqrt{\frac{\gamma^2}{t-\frac{x}{v_c}} + \frac{\phi^2}{x-\xi}}}\right)}{\sqrt{t-\frac{x}{v_c}}\sqrt{\frac{\gamma^2}{t-\frac{x}{v_c}} + \frac{\phi^2}{x-\xi}}} \exp\left[\frac{\frac{\phi^2 y^2}{\left(\frac{D^*}{R^*}\right)}}{4\left(\gamma^2\left(x-\xi\right) + \phi^2\left(t-\frac{x}{v_c}\right)\right)}\right] \quad (10)$$

Concentration contours generated using a Sale et al. (2008) Mathcad worksheet is presented in Figure 7. Also shown in Figure 7 are concentration contours generated using a “hybrid method” that is described in the following text. Concentrations in Figure 7 are presented in mass of PCE per volume of water. Unfortunately, Sale et al. (2008) Mathcad worksheet for transmissive layer does not result in accurate values for larger plume lengths (greater than 100m). This is due to problems with calculating the differences between error function values with large arguments and raising e to large powers (see Equation 7). Consequently, the Sale et al. (2008) Mathcad worksheet for Equation (7) has a finite domain of application. The distance at which the Sale et al. (2008) Mathcad worksheet approach fails is referred to as the transition distance.

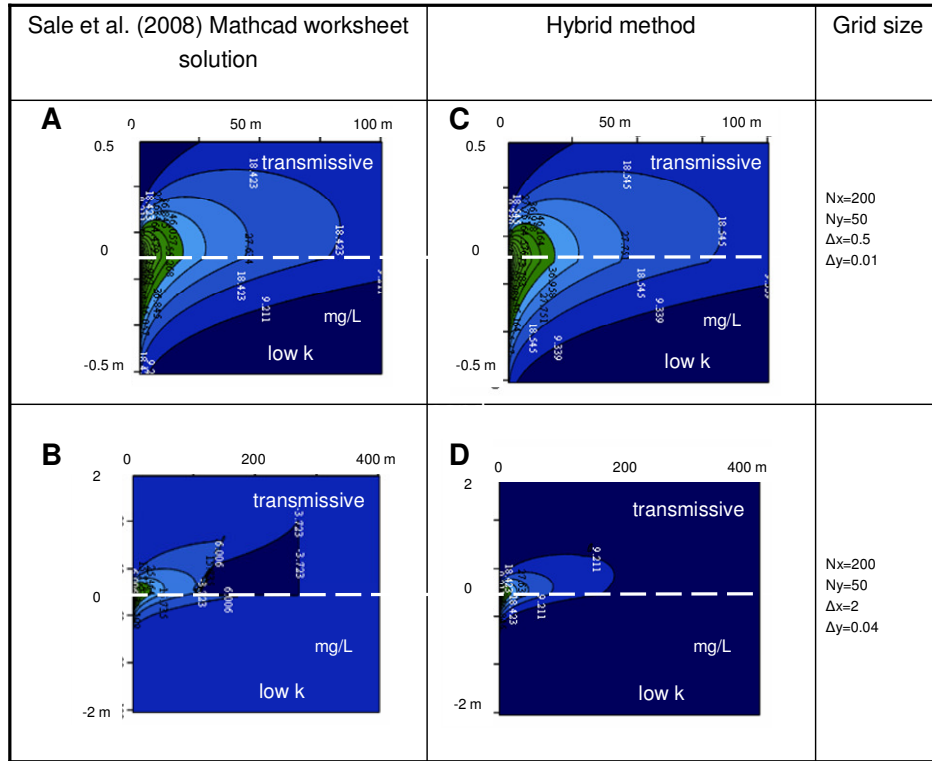


**Figure 7- Predicted concentration contours in 1000 days from Sale et al. (2008): panels A and B, and hybrid method: panels C and D.**

For larger distances an alternative computational strategy is required. For this

research, a series expansion was used to approximate  $e^{\frac{b^2x}{\phi^2}} \operatorname{erfc}\left(\frac{b}{\phi}\sqrt{x} + \frac{\phi y}{2\sqrt{x}}\right)$  and

$e^{\frac{b^2x}{\phi^2}} \left(1 + \operatorname{erf}\left(\frac{-b}{\phi}\sqrt{x} + \frac{\phi y}{2\sqrt{x}}\right)\right)$  in Equation (7). These series are summarized in Appendix

1 and Appendix 2. Unfortunately, series are incorrect at small distances. Realization of the limitation of both the Sale et al. (2008) Mathcad solution and the series approximation lead to a strategy of using each of the approaches in the domain where they are accurate. This approach is referred to as the hybrid approach. The hybrid approach involves using the Sale et al. (2008) Mathcad worksheet solution for distances less than the transition distance and series approximation for distances greater than the

transition distance. Using the hybrid approach, concentrations are evaluated over the domain of interest at  $N_x$  points in the x direction and  $N_y$  points in the y direction. The distances between the points are  $\Delta x$  and  $\Delta y$ . The Transition distance can be solved for by employing a Mathcad programming loop for a desired  $\Delta x$  and y (vertical distance from the interface of two layers in the transmissive layer). The loop reports the transition distance when the results from Equation (7) and its equivalent series approximation differ less than 0.2%. The red line in Figure 8 shows the Transition distance for a desired y in the transmissive layer when  $\Delta x=0.1$  m and  $N_x=200$ . The area above and below the red line, respectively indicates the domain where Sale et al. (2008) Mathcad worksheet solution and the series are applied.

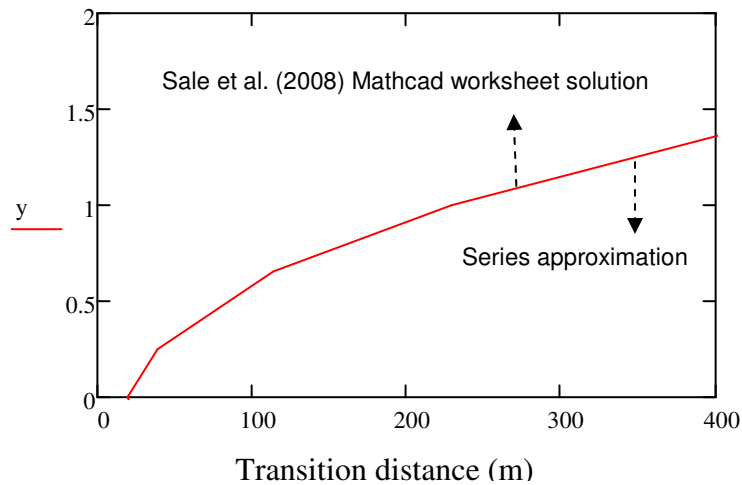


**Figure 8- Transition distance calculated for  $\Delta x=0.1$  m and  $N_x=200$ .**

Therefore,  $c_{low k}(x, y, t)$  and the modified  $c_{trans.}(x, y, t)$  can be employed to calculate contaminant concentrations in transmissive and low permeability layers in larger desired location and time by departing from Sale et al. (2008) solution to the series expansion. For instance, Figure 7 (panel B) reflects concentration contours generated

from Sale et al. (2008) versus the hybrid method (panel D) in 1000 days and the domain size of  $L_x = 400$  m and  $L_y = 4$  m. Panel C also illustrates the same scenario as panel A, but through the hybrid method.

One of the applications of the model is to predict total contaminant mass in transmissive and low permeability layers. Mathcad's numerical integral scheme was employed to calculate the total mass in the transmissive and low permeability layers as follows in Equation (11a-b).

$$M_{trans.}(\Delta x, \Delta y, t) = \int_0^{N_y \Delta y} \int_0^{N_x \Delta x} n R c_0 c_{trans.}(x, y, t) dx dy \quad (11a)$$

$$M_{low k}(\Delta x, \Delta y, t) = \int_0^{N_y \Delta y} \int_0^{N_x \Delta x} n' R' c_0 c_{low k}(x, y, t) dx dy \quad (11b)$$

Unfortunately, hardware and/or software limitations resulted in floating point error and cease of operations in the transmissive layer solution due to insufficient computer memory for distances larger than 689 m. This resulted in calculation failure following a prolonged attempt to run calculations (over 24 hours). Therefore, total PCE concentration in the low permeability layer at a desired time of  $t$  and a grid spacing of  $\Delta x$  and  $\Delta y$  is evaluated during the loading (Equation 11c) and back diffusion (Equation 11d) as follows:

$$M_{low k}(\Delta x, \Delta y, t) = \Delta x \Delta y n' \sum_{j=0}^{N_y} \sum_{i=0}^{N_x} (R' c_0 c_{low k}(i \Delta x, j \Delta y, t)) \quad (11c)$$

$$M_{low k\_back\ diffusion}(\Delta x, \Delta y, t', t) = \Delta x \Delta y n' \sum_{j=0}^{N_y} \sum_{i=0}^{N_x} (R' c_0 c_{low k}(i \Delta x, j \Delta y, t', t)) \quad (11d)$$

where,  $t'$  is the source persistence time,  $i$  and  $j$  are integer counter variables and  $c_{low k}(i \Delta x, j \Delta y, t)$  is calculated from Equation (9). To minimize errors associated with spatial discretization of the domain, fine discretization ( $N_x$  and  $N_y$  of up to 11000 and

5000, respectively) and a grid spacing as tight as  $\Delta x=0.1$  m and  $\Delta y=0.001$  m were used. These values were chosen iteratively with the goal of a mass balance error of less than 0.1% (see Appendix 3).

The total contaminant mass in the system as a function of time is defined by integrating the influent flux of contaminants at  $x=0$  over  $y$  and over time.

$$M_{source}(t) = \int_0^t \int_0^\infty v n c_0 e^{-by} dy dt \quad (12)$$

The contaminant mass in the transmissive layer is determined as the difference between total mass that entered the system at  $x=0$  (Equation 12) and the total contaminant mass in the low permeability layer (Equations 11c and 11d).

$$M_{transmissive}(\Delta x, \Delta y, t) = M_{source}(t) - M_{lowk}(\Delta x, \Delta y, t) \quad (13)$$

Another application of the model is to predict aqueous and sorbed mass through select vertical columns (transects) in the low permeability layer at select times. Mass in transects during the loading and back diffusion are calculated, respectively, as:

$$M_{transect}(\Delta x, \Delta y, t) = \Delta x \Delta y n' \sum_{j=0}^{N_y} (R' c_0 c_{lowk}(x, j\Delta y, t)) \quad (14)$$

$$M_{transect\_back\ diffusion}(\Delta x, \Delta y, t', t) = \Delta x \Delta y n' \sum_{j=0}^{N_y} (R' c_0 c_{lowk}(x, j\Delta y, t', t)) \quad (15)$$

where,  $M_{transect\_back\ diffusion}(\Delta x, \Delta y, t', t)$  is the total mass and  $c_{lowk}(x, j\Delta y, t', t)$  is the PCE aqueous concentration in the low permeability from back diffusion (after source is shut down).

One of the limitations of this method is that contaminant mass in the transmissive layer is determined indirectly through subtraction of the contaminant mass in the low permeability layer from the total contaminant mass introduced to the system. Another

limitation is that degradation of contaminants is not addressed in either transmissive or low permeability layers. Lastly, the analytical model only addresses saturated media excluding vapor phase compartments from the analysis.

## **2.3 Results**

### **2.3.1 Temporal partitioning between transmissive and low permeability zones**

#### *2.3.1.1 Scenario 1: without adsorption*

Figure 9 and Figure 10 illustrate the case where no adsorption occurs in the transmissive and low permeability layers (retardation coefficients of 1). The PCE DNAPL source is on for 1000 days and completely off for 2000 days. Contaminant mass is reported in kilograms per 1 meter width of the porous media over the entire domain impacted by the source. In Figure 9 accumulated PCE mass in the system,  $M_{\text{source}}(t)$ , increases with time following Equation (12). Mass in the low permeability layer is calculated from Equations (11c-d) and mass in the transmissive layer is obtained by difference following Equation (12).

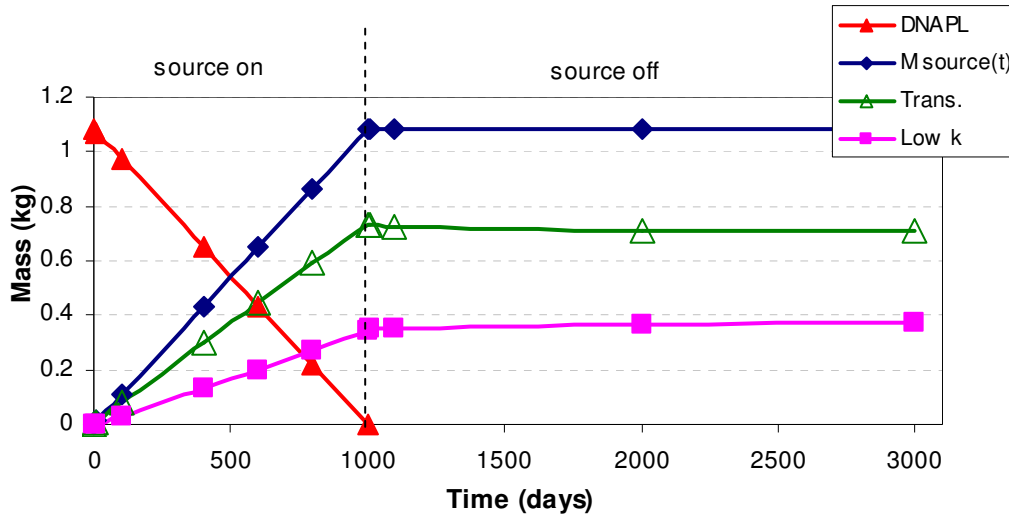


Figure 9- PCE DNAPL and total aqueous PCE mass in transmissive ( $R=1$ ) and low permeability ( $R'=1$ ) layers over time.

$R=1$   
 $L_x=1100$  m  
 $L_y=5$  m  
 $V_w=0.27$  m/d

Time (days)	DNAPL (kg)	Low k (kg)	Trans. (kg)
0	1.08	-	-
10	0.97	-	-
100	0.97	0.03	0.08
400	0.45	0.15	0.3
600	0.25	0.2	0.45
800	0.22	0.27	0.59
1000	-	0.37	0.59
1010	-	0.37	0.59
1100	-	0.37	0.59
2000	-	0.37	0.59
3000	-	0.37	0.71

Source on (0 to 1000 days)  
 Source off (1000 to 3000 days)

Figure 10- Predicted PCE DNAPL and total aqueous PCE mass in transmissive ( $R=1$ ) and low permeability ( $R'=1$ ) layers over time

In Figure 10, circles (bubbles) represent the total mass in transmissive and low permeability layers at different times. As DNAPL is depleted, contaminants move from the transmissive layer into the low permeability layer. At the end of the loading with no retardation in the low permeability zone, 32% of the released contaminant is present in the low permeability layer. Even after the source is shut down, contaminant mass in the transmissive layer is growing through inward diffusion from the low permeability layer.

#### *2.3.1.2 Scenario 2: with adsorption*

To take into account the effect of sorption, the retardation coefficient of the low permeability layer is elevated to 10 and Figure 11 and Figure 12 are generated following the same scenario as presented in Figure 9 and Figure 10. The low permeability layer's retardation factor is based on a bulk density of  $1590 \text{ kg/m}^3$ ,  $f_{oc} = 0.006$  and  $K_{oc} = 0.364 \text{ mL/g}$  for PCE.

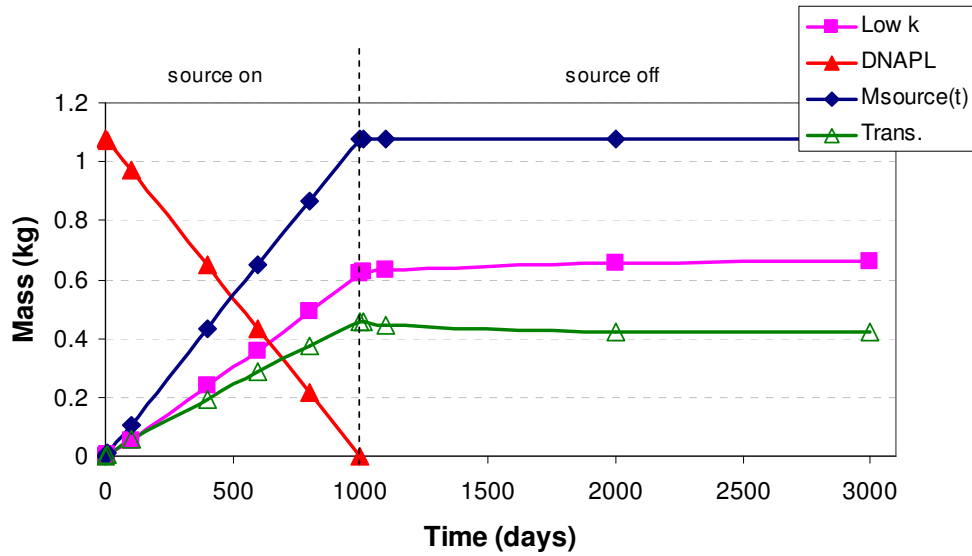


Figure 11- The effect of elevating  $R'$  from 1 to 10 on total PCE mass in transmissive ( $R=1$ ) and low permeability layers.

$R' = 10$   
 $L_x = 1100$  m  
 $L_y = 5$  m  
 $V_w = 0.27$  m/d

	Time (days)	DNAPL (kg)	Low k (kg)	Trans. (kg)
Source on	0	1.08 →	-	-
	10		-	-
	100		0.05 →	0.06 →
	400		Aq →  Sorbed	
	600			
	800	0.22 →	0.49 →	0.37 →
Source off	1000	-		0.46 →
	1010	-		
	1100	-		
	2000	-		
	3000	-	0.66 →	0.42 →

Figure 12- The effect of elevating  $R'$  from 1 to 10 on predicted total aqueous and sorbed PCE mass in transmissive ( $R=1$ ) and low permeability layers.

Masses are reported in kilograms per 1 meter width of the porous media. Total masses were calculated from Equations (11a) to (13). Figure 11 illustrates that in the end of loading given a retardation factor of 10 in the low permeability zone, 58% of the released contaminant is present in the low permeability layer versus 32% before. In Figure 12 blue wedges represent aqueous PCE mass and gray represents sorbed PCE mass in the low permeability layer. And, again an increase in PCE mass in low permeability layer is observed after source is off due to back diffusion.

### **2.3.2 Spatial variation in mass in low permeability zones**

#### *2.3.2.1 Scenario 1: without adsorption*

Figure 13 illustrates contaminant mass in the low permeability zone in terms of  $mg / (m^2$  of contact area of the plume and the low permeability layer) when no adsorption occurs in the transmissive and low permeability layers (retardation coefficients of 1). Masses are calculated from Equations (14-15). Areas of the circles are proportional to the total mass present at given position and time.

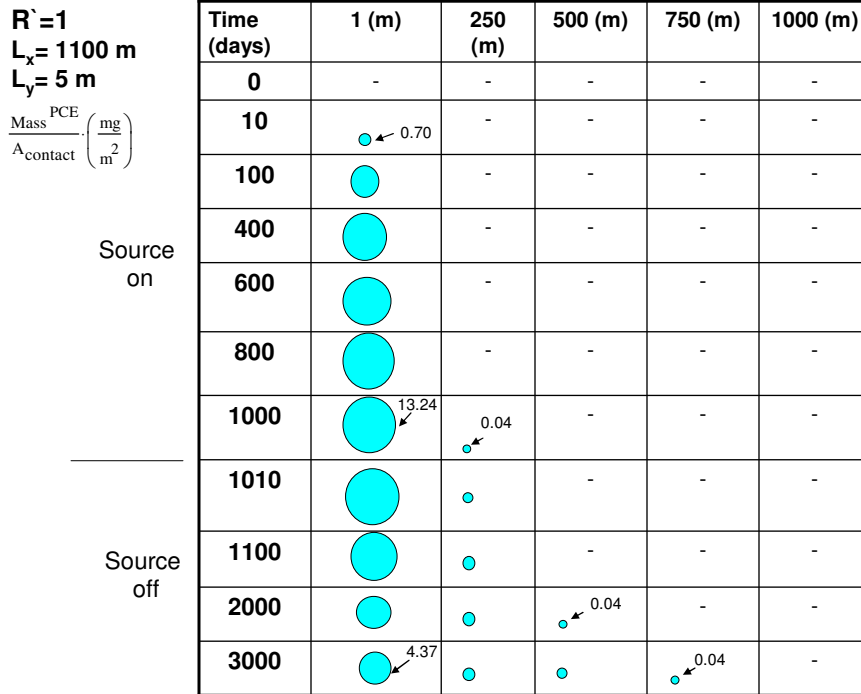


**Figure 13- Spatial distribution of PCE mass in transects of the low permeability layer ( $R = 1$ ).**

As DNAPL gets depleted, contaminants move from the transmissive layer into the low permeability layer. Figure 13 shows that first of all PCE mass is not uniformly distributed in the soil profile. Second of all, PCE mass is decreasing in source vicinity after the source has been exhausted. Third of all, PCE mass is increasing in the leading edge. Lastly, the domain with significant mass is observed to be located in proximity of the DNAPL release area in the plume. This reflects the fact that, for the scenarios considered, the domain located in proximity of the DNAPL areas has had contact with the highest contaminant concentrations for the longest period of time. Future work should focus on a more comprehensive analysis of spatial and temporal variations in contaminant storage in low permeability zones after source removal.

2.3.2.2 Scenario 2: with adsorption

Figure 14 depicts the same scenario as Figure 13 with the modification of retardation factor of the low permeability layer from 1 to 10.

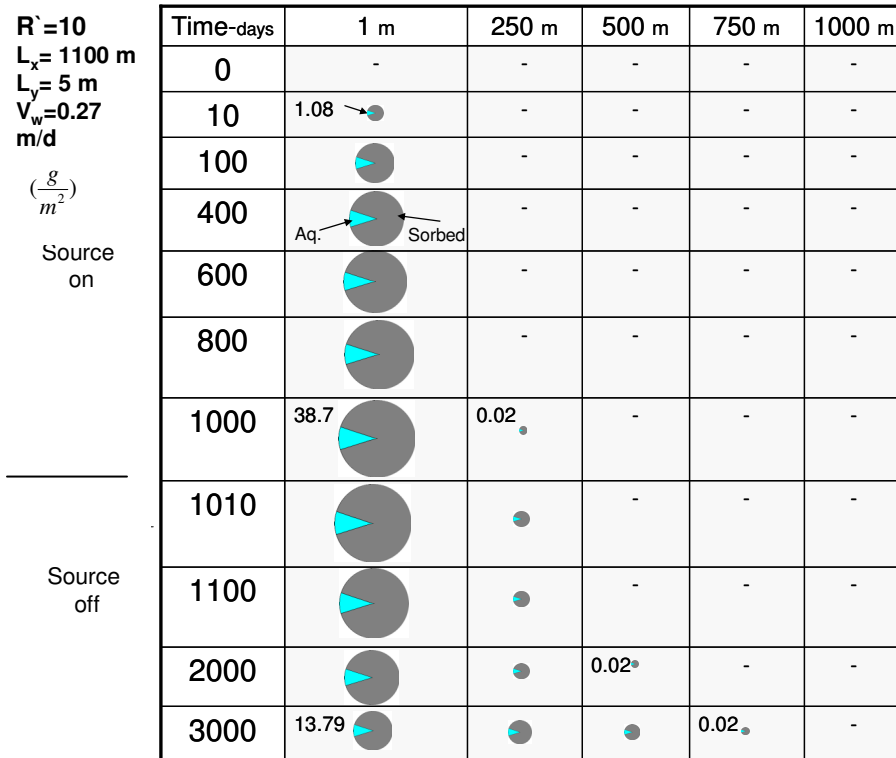


Figure 14- Spatial distribution of PCE mass in transects of the low permeability layer ( $R^* = 10$ ).

In this figure masses are also in grams per square meter of the contact area of the plume and the low permeability layer. Fraction of organic carbon of the low permeability layer, octanol-carbon partitioning coefficient of PCE, and bulk density of the low permeability layer are the same as Section 2.3.1.2. Comparison of Figure 14 with Figure 13 indicates almost 3 times less PCE mass accumulation in the aqueous phase of the low permeability layer when sorption is considered. A key element in Figure 14 is that the contaminants are not uniformly distributed in the low permeability layer. An interesting

aspect of this observation is that the need to treat contaminants in low permeability zones may be limited to a subset of the plume domain. Specifically, the majority of the mass in the low permeability layer remain in vicinity of the DNAPL source.

## **2.4 Conclusions**

The temporal and spatial evolution of a contaminant release in transmissive and low permeability zones has been examined using analytical solutions. The model addresses a two-layer system involving a transmissive layer (e.g., sand) situated above a low permeability layer (e.g., silt) with a DNAPL like source at the contact of the two layers. The model is based on advective flow through the transmissive layer, transverse diffusion across the transmissive layer, and transverse molecular diffusion in the low permeability layer. Initial efforts focused on conducted calculations using a hybrid method employing a Sale et al. (2008) Mathcad worksheet solution for small distances and series approximation for large distances. While the hybrid approach expanded the domain of accurate calculation it also failed at large domains. In the end, this analysis relies on using the Sale et al. (2008) solution for the low permeability layer (which is stable for all values of  $x$ ), an estimate of the total mass in the system from the source, and defining the contaminant mass in the transmissive layer as the difference between total mass in the system and total mass in the low permeability layer. Efforts to develop practical approaches for the transmissive layer solution at large domains are ongoing at Colorado State University.

Three important observations are developed from this study. First, the hypothesis that chlorinated solvent releases can evolve with time has been validated. Specially,

through time, the nature of the problem changed from DNAPL in the transmissive layer to that of aqueous and sorbed contaminants in the low permeability layer. Given that remedies for DNAPL in transmissive zones and contaminants in low permeability zones can be quite different, an understanding of the age of a release can be an important part of selecting appropriate site remedies and anticipating their performance.

The second major result of this work is that contaminant storage in low permeability zones varies spatially with time. Specially, observed contaminant distributions in the low permeability layer suggest that even at late stages much of the contaminant mass in low permeability zone remains in proximity to the DNAPL source. This leads to the observation that domain in which contaminants are present (at significant levels) in low permeability zones can be a subset of the entire plume domain. An ability to resolve treatment of contaminant in low permeability zones holds promise for more efficient remedies for chlorinated solvent releases.

Lastly, retardation in the low permeability layer controls contaminants mass stored in the low permeability layer at late time. In the case of  $R=1$  in the low permeability layer, 32% of the released contaminant mass is present in the low permeability layer after 1000 days. In contrast, given  $R=10$  in the low permeability layer, 58% of the released contaminant mass is present in the low permeability layer after 1000 days. Overall, the low permeability zone retardation factors appear to be an important factor in understanding the nature of the problem posed by late stage chlorinated solvent releases.

## **2.5 Acknowledgements**

To be greatly thanked are Dr. David Dandy and Dr. Domenico Bau, professors at Colorado State University, for their great support and guidelines on different aspects of the modeling. Funding of this research was in part provided by University Consortium for Field-Focused Groundwater Contamination.

## REFERENCES

- Al-Niami, A.N.S., Rushton, K.R., 1979. Dispersion in stratified porous media: analytical solutions. *Water Resources Research* 15, 1044-1048.
- Cameron, D.R., Klute, A., 1977. Convective-dispersive solute transport with a combined equilibrium and kinetic adsorption model. *Water Resources Research* 13, 183-188.
- Chapman, S.W., B.L. Parker, 2005. Plume persistence due to aquitard back diffusion following dense nonaqueous phase liquid removal or isolation, *Water Resource Research* 41 (12), W12411.
- Feenstra, S., Cherry, J.A., Parker, B.L., 1996. Conceptual Models for the Behavior of Dense Nonaqueous Phase Liquids (DNAPLs) in the Subsurface, Chapter 2 in Dense Chlorinated Solvents and Other DNAPLs in Groundwater, J.F Pankow and J.A. Cherry, Editors. Waterloo Press, pp. 53-88.
- Guyonnet, G., Neville, C., 2004. Dimensionless analysis of two analytical solutions for 3-D solute transport in groundwater. *Journal of Contaminant Hydrology* 75, 141-153.
- Kueper, B.H., McWhorter, D.B., 1991. The behavior of dense nonaqueous phase liquids in fractured clay and rock. *Journal of Ground Water* 29, 716-728.
- Liu, G., Ball, W.P., 2002. Back diffusion of chlorinated solvent contamination from a natural aquitard to a remediated aquifer under well-controlled field conditions: predictions and measurements, *Journal of Ground Water* 40, 175-184.
- National Research Council (NRC), 2005. *Contaminants in the Subsurface: Source Zone Assessment and Remediation*. National Academies Press, Washington, D.C.
- Newell, C.J., Hopkins, L.P., Bedient, P.B., 1990. A hydrogeologic database for ground water- modeling. *Ground Water* 28(5): 703-714.
- Parker, B.L., Chapman, S.W., Guilbeault, M.A., 2008. Plume resistance caused by back diffusion from thin clay layers in a sand aquifer following TCE source-zone hydraulic isolation, *Journal of Contaminant Hydrology* 102, 72-85.
- Parker B.L., Gillham R.W., Cherry J.A., 1994. Diffusive disappearance of immiscible-phase organic liquids in fractured geologic media. *Ground Water* 32: 805-820.

- Sale, T.C., McWhorter, D.B., 2001. Steady state mass transfer from single component dense nonaqueous phase liquids in uniform flow fields. *Water Resources Research* 37, 393-404.
- Sale, T. C., Newell, C., 2011. A Guide for Selecting Remedies for Subsurface Releases of Chlorinated Solvents, ESTCP Project ER-0530.
- Sale, T. C., Zimbron, J., Dandy, D., 2008. Effects of reduced contaminant loading on downgradient water quality in an idealized two-layer granular porous media, *Journal of Contaminant Hydrology* 102, 72-85.
- Skopp, J., Warrick, A.W., 1974. A two-phase model for the miscible displacement of reactive solutes in soils. *Soil Science Society of America Proceedings* 38, 545-550.
- Sudicky E.A., 1986. A natural gradient experiment on solute transport in a sand aquifer: Spatial variability of hydraulic conductivity and its role in the dispersion process. *Water Resources Research* 22, 2069-2082.
- Sudicky, E.A., Frind, E.O., 1982. Contaminant transport in fractured porous media: analytical solutions for a system of parallel fractures. *Water Resources Research* 18, 1634-1642.
- Tang, D.H., Frind, E.O., Sudicky, E.A., 1981. Contaminant transport in fractured porous media: analytical solution for a single fracture. *Water Resources Research* 17, 555-564.

**Appendix 1- Summarized equivalent series for:**  $e^{\frac{b^2 \cdot x}{\phi^2}} * \operatorname{erfc}\left(\frac{b}{\phi} * \sqrt{x} + \frac{\phi * y}{2\sqrt{x}}\right)$

$$\begin{aligned}
 & \frac{1}{\phi} \left[ \frac{e^{-\frac{\phi \cdot y}{2} \cdot \frac{b}{\phi} \cdot \sqrt{\frac{1}{x}}}}{\sqrt{\pi}} \dots \right. \\
 & + \frac{\left[ -2\left(\frac{b}{\phi}\right)^2 \left(\frac{\phi \cdot y}{2}\right)^2 + 2\frac{b}{\phi} \frac{\phi \cdot y}{2} + 1 \right] e^{-2\left(\frac{b}{\phi} \frac{\phi \cdot y}{2}\right)} \left(\frac{1}{x}\right)^{\frac{3}{2}}}{2\left(\frac{b}{\phi}\right)^2 \sqrt{\pi}} \dots \\
 & + \frac{\left[ 2\left(\frac{b}{\phi}\right)^4 \left(\frac{\phi \cdot y}{2}\right)^4 + 4\left(\frac{b}{\phi}\right)^3 \left(\frac{\phi \cdot y}{2}\right)^3 + 6\left(\frac{b}{\phi}\right)^2 \left(\frac{\phi \cdot y}{2}\right)^2 + 6\left(\frac{b}{\phi}\right) \left(\frac{\phi \cdot y}{2}\right) + 3 \right] e^{-2\left(\frac{b}{\phi} \frac{\phi \cdot y}{2}\right)} \left(\frac{1}{x}\right)^{\frac{5}{2}}}{4\left(\frac{b}{\phi}\right)^4 \sqrt{\pi}} \dots \\
 & - \frac{\left[ 4\left(\frac{b}{\phi}\right)^6 \left(\frac{\phi \cdot y}{2}\right)^6 + 12\left(\frac{b}{\phi}\right)^5 \left(\frac{\phi \cdot y}{2}\right)^5 + 30\left(\frac{b}{\phi}\right)^4 \left(\frac{\phi \cdot y}{2}\right)^4 + 60\left(\frac{b}{\phi}\right)^3 \left(\frac{\phi \cdot y}{2}\right)^3 + 90\left(\frac{b}{\phi}\right)^2 \left(\frac{\phi \cdot y}{2}\right)^2 + 90\left(\frac{b}{\phi}\right) \left(\frac{\phi \cdot y}{2}\right) + 45 \right] e^{-2\left(\frac{b}{\phi} \frac{\phi \cdot y}{2}\right)} \left(\frac{1}{x}\right)^{\frac{7}{2}}}{24\left(\frac{b}{\phi}\right)^6 \sqrt{\pi}} \dots \\
 & + \frac{\left[ 2\left(\frac{b}{\phi}\right)^8 \left(\frac{\phi \cdot y}{2}\right)^8 + 8\left(\frac{b}{\phi}\right)^7 \left(\frac{\phi \cdot y}{2}\right)^7 + 28\left(\frac{b}{\phi}\right)^6 \left(\frac{\phi \cdot y}{2}\right)^6 + 84\left(\frac{b}{\phi}\right)^5 \left(\frac{\phi \cdot y}{2}\right)^5 + 210\left(\frac{b}{\phi}\right)^4 \left(\frac{\phi \cdot y}{2}\right)^4 + 420\left(\frac{b}{\phi}\right)^3 \left(\frac{\phi \cdot y}{2}\right)^3 + 630\left(\frac{b}{\phi}\right)^2 \left(\frac{\phi \cdot y}{2}\right)^2 + 630\left(\frac{b}{\phi}\right) \left(\frac{\phi \cdot y}{2}\right) + 315 \right] e^{-2\left(\frac{b}{\phi} \frac{\phi \cdot y}{2}\right)} \left(\frac{1}{x}\right)^{\frac{9}{2}}}{48\left(\frac{b}{\phi}\right)^8 \sqrt{\pi}} \dots \\
 & + \frac{\frac{11}{\phi} \left(\frac{1}{x}\right)^{\frac{11}{2}}}{\phi} \left[ -e^{-2\left(\frac{b}{\phi} \frac{\phi \cdot y}{2}\right)} \frac{\left(\frac{\phi \cdot y}{2}\right)^{10}}{120 \frac{b}{\phi} \sqrt{\pi}} + \frac{\left[ \frac{\frac{\phi \cdot y}{2}}{\left(\frac{b}{\phi}\right)^2} - \frac{1}{2\left(\frac{b}{\phi}\right)^3} \right] e^{-2\left(\frac{b}{\phi} \frac{\phi \cdot y}{2}\right)} \left(\frac{\phi \cdot y}{2}\right)^8}{24 \sqrt{\pi}} \dots \right. \\
 & + \frac{\left[ \frac{\left(\frac{\phi \cdot y}{2}\right)^2}{\left(\frac{b}{\phi}\right)^3} + \frac{\frac{\phi \cdot y}{2}}{2\left(\frac{b}{\phi}\right)^4} + \frac{\frac{\phi \cdot y}{2} + \frac{3}{4\left(\frac{b}{\phi}\right)^4}}{\frac{b}{\phi}} \right] e^{-2\left(\frac{b}{\phi} \frac{\phi \cdot y}{2}\right)} \left(\frac{\phi \cdot y}{2}\right)^6}{(6\sqrt{\pi})} \dots \\
 & + \frac{\left[ \frac{\left(\frac{\phi \cdot y}{2}\right)^3}{\left(\frac{b}{\phi}\right)^4} + \frac{-\left(\frac{\phi \cdot y}{2}\right)^2}{2\left(\frac{b}{\phi}\right)^5} - \frac{\left[ \frac{\frac{\phi \cdot y}{2}}{\left(\frac{b}{\phi}\right)^3} + \frac{3}{4\left(\frac{b}{\phi}\right)^4} \right] \frac{\phi \cdot y}{2} - \frac{-3\left(\frac{\phi \cdot y}{2}\right)^2}{2} - \frac{3\frac{\phi \cdot y}{2} - 15}{8\left(\frac{b}{\phi}\right)^6}}{\frac{b}{\phi}} \right] e^{-2\left(\frac{b}{\phi} \frac{\phi \cdot y}{2}\right)} \left(\frac{\phi \cdot y}{2}\right)^4}{\dots} \dots \\
 & + \frac{-1}{\sqrt{\pi}} e^{-2\left(\frac{b}{\phi} \frac{\phi \cdot y}{2}\right)} \left(\frac{\phi \cdot y}{2}\right)^2 \left[ \frac{\left(\frac{\phi \cdot y}{2}\right)^4}{\left(\frac{b}{\phi}\right)^5} + \frac{\left(\frac{\phi \cdot y}{2}\right)^3}{2\left(\frac{b}{\phi}\right)^6} + \frac{\left[ \frac{\frac{\phi \cdot y}{2}}{\left(\frac{b}{\phi}\right)^3} + \frac{3}{4\left(\frac{b}{\phi}\right)^4} \right] \left(\frac{\phi \cdot y}{2}\right)^2}{\left(\frac{b}{\phi}\right)^3} \dots \right. \\
 & + \frac{\left[ \frac{-3\left(\frac{\phi \cdot y}{2}\right)^2}{2\left(\frac{b}{\phi}\right)^4} - \frac{3\frac{\phi \cdot y}{2}}{\left(\frac{b}{\phi}\right)^5} - \frac{15}{8\left(\frac{b}{\phi}\right)^6} \right] \frac{\phi \cdot y}{2} + \frac{2\left(\frac{\phi \cdot y}{2}\right)^3}{\left(\frac{b}{\phi}\right)^5} + \frac{15\left(\frac{\phi \cdot y}{2}\right)^2}{\left(\frac{b}{\phi}\right)^6} + \frac{45\frac{\phi \cdot y}{2}}{4\left(\frac{b}{\phi}\right)^7} + \frac{105}{16\left(\frac{b}{\phi}\right)^8}}{\left(\frac{b}{\phi}\right)^2} + \frac{\left(\frac{b}{\phi}\right)^1}{\left(\frac{b}{\phi}\right)^1} \dots \\
 & + \frac{1}{\sqrt{\pi}} e^{-2\left(\frac{b}{\phi} \frac{\phi \cdot y}{2}\right)} \left[ \frac{\left(\frac{\phi \cdot y}{2}\right)^5}{\left(\frac{b}{\phi}\right)^6} + \frac{\left(\frac{\phi \cdot y}{2}\right)^4}{2\left(\frac{b}{\phi}\right)^7} + \frac{\left[ \frac{\frac{\phi \cdot y}{2}}{\left(\frac{b}{\phi}\right)^3} + \frac{3}{4\left(\frac{b}{\phi}\right)^4} \right] \left(\frac{\phi \cdot y}{2}\right)^3}{\left(\frac{b}{\phi}\right)^4} + \frac{\left[ \frac{-3\left(\frac{\phi \cdot y}{2}\right)^2}{2\left(\frac{b}{\phi}\right)^4} + \frac{-3\frac{\phi \cdot y}{2}}{\left(\frac{b}{\phi}\right)^5} - \frac{15}{8\left(\frac{b}{\phi}\right)^6} \right] \left(\frac{\phi \cdot y}{2}\right)^2}{\left(\frac{b}{\phi}\right)^3} \dots \right. \\
 & + \frac{\left[ \frac{2\left(\frac{\phi \cdot y}{2}\right)^3}{\left(\frac{b}{\phi}\right)^5} + \frac{15\left(\frac{\phi \cdot y}{2}\right)^2}{\left(\frac{b}{\phi}\right)^6} + \frac{45\frac{\phi \cdot y}{2}}{4\left(\frac{b}{\phi}\right)^7} + \frac{105}{16\left(\frac{b}{\phi}\right)^8} \right] \left(\frac{\phi \cdot y}{2}\right)^1}{\left(\frac{b}{\phi}\right)^2} + \frac{\left(\frac{b}{\phi}\right)^2}{\left(\frac{b}{\phi}\right)^2} \dots \\
 & + \frac{-5\left(\frac{\phi \cdot y}{2}\right)^4}{2\left(\frac{b}{\phi}\right)^6} + \frac{-15\left(\frac{\phi \cdot y}{2}\right)^3}{\left(\frac{b}{\phi}\right)^7} + \frac{-315\left(\frac{\phi \cdot y}{2}\right)^2}{8\left(\frac{b}{\phi}\right)^8} + \frac{-105\frac{\phi \cdot y}{2} - 945}{2\left(\frac{b}{\phi}\right)^9} - \frac{945}{32\left(\frac{b}{\phi}\right)^{10}}}{\left(\frac{b}{\phi}\right)^1} \dots
 \end{aligned}$$

**Appendix 2- Summarized equivalent series for  $e^{\frac{1}{\phi}} \left( 1 + \operatorname{erf} \left( \frac{-b}{\phi} \sqrt{x} + \frac{\phi y}{2\sqrt{x}} \right) \right)$  :**

$$\begin{aligned}
 & \frac{1}{\frac{b}{\phi}} \left[ \frac{e^{\frac{2\frac{\phi y}{\phi} \frac{b}{\phi} \sqrt{\frac{1}{x}}}}{\sqrt{\pi}} \dots \right. \\
 & \left. - \frac{2\left(\frac{b}{\phi}\right)^2 \left(\frac{\phi y}{2}\right)^2 - 2\frac{b}{\phi} \frac{\phi y}{2} + 1}{2\left(\frac{b}{\phi}\right)^2 \sqrt{\pi}} e^{2\left(\frac{b}{\phi} \frac{\phi y}{2}\right)} \left(\frac{1}{x}\right)^{\frac{3}{2}} \dots \right. \\
 & \left. + \frac{2\left(\frac{b}{\phi}\right)^4 \left(\frac{\phi y}{2}\right)^4 - 4\left(\frac{b}{\phi}\right)^3 \left(\frac{\phi y}{2}\right)^3 + 6\left(\frac{b}{\phi}\right)^2 \left(\frac{\phi y}{2}\right)^2 - 6\left(\frac{b}{\phi}\right) \left(\frac{\phi y}{2}\right) + 3}{4\left(\frac{b}{\phi}\right)^4 \sqrt{\pi}} e^{2\left(\frac{b}{\phi} \frac{\phi y}{2}\right)} \left(\frac{1}{x}\right)^{\frac{5}{2}} \dots \right. \\
 & \left. - \frac{4\left(\frac{b}{\phi}\right)^6 \left(\frac{\phi y}{2}\right)^6 - 12\left(\frac{b}{\phi}\right)^5 \left(\frac{\phi y}{2}\right)^5 + 30\left(\frac{b}{\phi}\right)^4 \left(\frac{\phi y}{2}\right)^4 - 60\left(\frac{b}{\phi}\right)^3 \left(\frac{\phi y}{2}\right)^3 + 90\left(\frac{b}{\phi}\right)^2 \left(\frac{\phi y}{2}\right)^2 - 90\left(\frac{b}{\phi}\right) \left(\frac{\phi y}{2}\right) + 45}{24\left(\frac{b}{\phi}\right)^6 \sqrt{\pi}} e^{2\left(\frac{b}{\phi} \frac{\phi y}{2}\right)} \left(\frac{1}{x}\right)^{\frac{7}{2}} \dots \right. \\
 & \left. + \frac{1 \left[ 2\left(\frac{b}{\phi}\right)^8 \left(\frac{\phi y}{2}\right)^8 - 8\left(\frac{b}{\phi}\right)^7 \left(\frac{\phi y}{2}\right)^7 + 28\left(\frac{b}{\phi}\right)^6 \left(\frac{\phi y}{2}\right)^6 - 84\left(\frac{b}{\phi}\right)^5 \left(\frac{\phi y}{2}\right)^5 + 210\left(\frac{b}{\phi}\right)^4 \left(\frac{\phi y}{2}\right)^4 - 420\left(\frac{b}{\phi}\right)^3 \left(\frac{\phi y}{2}\right)^3 + 630\left(\frac{b}{\phi}\right)^2 \left(\frac{\phi y}{2}\right)^2 - 630\left(\frac{b}{\phi}\right) \left(\frac{\phi y}{2}\right) + 315 \right]}{48\left(\frac{b}{\phi}\right)^8 \sqrt{\pi}} e^{2\left(\frac{b}{\phi} \frac{\phi y}{2}\right)} \left(\frac{1}{x}\right)^{\frac{9}{2}} \dots \right. \\
 & \left. + \frac{\frac{11}{2} \left(\frac{b}{\phi}\right) \left(\frac{1}{x}\right)^{\frac{11}{2}}}{\dots} \left[ -e^{2\left(\frac{b}{\phi} \frac{\phi y}{2}\right)} \frac{\left(\frac{\phi y}{2}\right)^{10}}{120 \frac{b}{\phi} \sqrt{\pi}} + \frac{\left[ \frac{\frac{\phi y}{2}}{\left(\frac{b}{\phi}\right)^2} - \frac{1}{2\left(\frac{b}{\phi}\right)^3} \right] e^{2\left(\frac{b}{\phi} \frac{\phi y}{2}\right)} \left(\frac{\phi y}{2}\right)^8}{24 \sqrt{\pi}} \dots \right. \\
 & \left. + \frac{\left[ \frac{\left(\frac{\phi y}{2}\right)^2}{\left(\frac{b}{\phi}\right)^3} - \frac{\frac{\phi y}{2}}{2\left(\frac{b}{\phi}\right)^4} + \frac{\frac{-\phi y}{2} + 3}{4\left(\frac{b}{\phi}\right)^4} \right] e^{2\left(\frac{b}{\phi} \frac{\phi y}{2}\right)} \left(\frac{\phi y}{2}\right)^6}{(6\sqrt{\pi})} \dots \right. \\
 & \left. + \frac{\left[ \frac{\left(\frac{\phi y}{2}\right)^3}{\left(\frac{b}{\phi}\right)^4} + \frac{-\left(\frac{\phi y}{2}\right)^2}{2\left(\frac{b}{\phi}\right)^5} + \frac{\left[ \frac{-\phi y}{2} + 3 \right] \frac{\phi y}{2}}{\left(\frac{b}{\phi}\right)^2} + \frac{-3\left(\frac{\phi y}{2}\right)^2 + \frac{3\phi y}{2} - 15}{8\left(\frac{b}{\phi}\right)^6} \right] e^{-2\left(\frac{b}{\phi} \frac{\phi y}{2}\right)} \left(\frac{\phi y}{2}\right)^4}{\frac{b}{\phi}} \dots \right. \\
 & \left. + \frac{-1}{\sqrt{\pi}} e^{2\left(\frac{b}{\phi} \frac{\phi y}{2}\right)} \left(\frac{\phi y}{2}\right)^2 \left[ \frac{\left(\frac{\phi y}{2}\right)^4}{\left(\frac{b}{\phi}\right)^5} - \frac{\left(\frac{\phi y}{2}\right)^3}{2\left(\frac{b}{\phi}\right)^6} + \frac{\left[ \frac{-\phi y}{2} + 3 \right] \left(\frac{\phi y}{2}\right)^2}{4\left(\frac{b}{\phi}\right)^4} \dots \right. \right. \\
 & \left. \left. + \frac{\left[ \frac{-3\left(\frac{\phi y}{2}\right)^2}{2\left(\frac{b}{\phi}\right)^4} + \frac{3\frac{\phi y}{2} - 15}{8\left(\frac{b}{\phi}\right)^6} \right] \frac{\phi y}{2}}{\left(\frac{b}{\phi}\right)^2} + \frac{-2\left(\frac{\phi y}{2}\right)^3}{\left(\frac{b}{\phi}\right)^5} + \frac{15\left(\frac{\phi y}{2}\right)^2}{\left(\frac{b}{\phi}\right)^6} - \frac{45\frac{\phi y}{2}}{4\left(\frac{b}{\phi}\right)^7} + \frac{105}{16\left(\frac{b}{\phi}\right)^8} \right]}{\left(\frac{b}{\phi}\right)^2} + \frac{\left(\frac{b}{\phi}\right)^1}{\left(\frac{b}{\phi}\right)^1} \dots \right. \\
 & \left. + \frac{1}{\sqrt{\pi}} e^{2\left(\frac{b}{\phi} \frac{\phi y}{2}\right)} \left[ \frac{\left(\frac{\phi y}{2}\right)^5}{\left(\frac{b}{\phi}\right)^6} - \frac{\left(\frac{\phi y}{2}\right)^4}{2\left(\frac{b}{\phi}\right)^7} + \frac{\left[ \frac{-\phi y}{2} + 3 \right] \left(\frac{\phi y}{2}\right)^3}{4\left(\frac{b}{\phi}\right)^4} + \frac{\left[ \frac{-3\left(\frac{\phi y}{2}\right)^2}{2\left(\frac{b}{\phi}\right)^4} + \frac{3\frac{\phi y}{2} - 15}{8\left(\frac{b}{\phi}\right)^6} \right] \left(\frac{\phi y}{2}\right)^2}{\left(\frac{b}{\phi}\right)^3} \dots \right. \right. \\
 & \left. \left. + \frac{\left[ \frac{-2\left(\frac{\phi y}{2}\right)^3}{\left(\frac{b}{\phi}\right)^5} + \frac{15\left(\frac{\phi y}{2}\right)^2}{\left(\frac{b}{\phi}\right)^6} - \frac{45\frac{\phi y}{2}}{4\left(\frac{b}{\phi}\right)^7} + \frac{105}{16\left(\frac{b}{\phi}\right)^8} \right] \left(\frac{\phi y}{2}\right)^1}{\left(\frac{b}{\phi}\right)^2} \dots \right. \right. \\
 & \left. \left. + \frac{-5\left(\frac{\phi y}{2}\right)^4}{2\left(\frac{b}{\phi}\right)^6} + \frac{15\left(\frac{\phi y}{2}\right)^3}{\left(\frac{b}{\phi}\right)^7} + \frac{-315\left(\frac{\phi y}{2}\right)^2}{8\left(\frac{b}{\phi}\right)^8} + \frac{105\frac{\phi y}{2}}{2\left(\frac{b}{\phi}\right)^9} - \frac{945}{32\left(\frac{b}{\phi}\right)^{10}} \right]}{\left(\frac{b}{\phi}\right)} \dots \right. \\
 & \left. + \frac{\dots}{\left(\frac{b}{\phi}\right)} \dots \right]
 \end{aligned}$$

### Appendix 3- Choosing $N_x$ , $N_y$ , $\Delta x$ and $\Delta y$

The following procedure was followed to generate a large enough discretization ( $N_x$  and  $N_y$ ) to minimize numerical dispersion in the solution of the low permeability. A programming loop was defined in Mathcad to generate a matrix of contaminant concentrations at a desired time,  $\Delta x$  and vertical transect of the low permeability layer ( $x$ ). If the matrix reaches zero concentration in the border of the media,  $N_y$  is reported. Next, this  $N_y$  is used for calculating error in mass in a desired vertical transect of the media for  $\Delta y_1$  and  $\Delta y_2$  as follows:

$$M_1(x, \Delta y_1, t) = \Delta y_1 \cdot n' \cdot \sum_{j=0}^{N_y} (R' \cdot c_o \cdot c_{silt}(x, j \cdot \Delta y_1, t))$$

$$M_2(x, \Delta y_2, t) = \Delta y_2 \cdot n' \cdot \sum_{j=0}^{N_y} (R' \cdot c_o \cdot c_{silt}(x, j \cdot \Delta y_2, t))$$

$$\text{Error} = \frac{M_1(x, \Delta y_1, t) - M_2(x, \Delta y_2, t)}{M_2(x, \Delta y_2, t)} \cdot 100$$

A proper  $\Delta y$  would be the one which yields an error less than 0.1%. A Same procedure is followed for the horizontal transect of the media to calculate  $N_x$  and  $\Delta x$ . The resulting values were a grid spacing as tight as  $\Delta x=0.1$  m and  $\Delta y=0.001$  m and  $N_x=11000$  and  $N_y= 5000$ .

# Chapter 3

## CONCEPTUAL MODEL AND LABORATORY STUDIES ADDRESSING EFFECTS OF ALKALINE PERSULFATE FLUSHING ON CONTAMINANTS STORED IN LOW PERMEABILITY ZONES<sup>2</sup>

### SYNOPSIS

**Keywords:** Low permeability zones, dilute plumes, remediation

After more than three decades of investments, management of historical subsurface releases of chlorinated solvents remains a major technical challenge. Most recently it has been recognized that contaminants stored in low permeability layers in source zones and plumes can sustain dilute groundwater plumes long after sources in transmissive zones are depleted. Unfortunately, this scenario implies the potential need for multiple decades of plume management and monitoring at thousands of sites. This research presents a conceptual model and laboratory-scale sand tank experiment that addresses storage, release, and treatment of contaminants in low permeability zones. A two-dimensional sand tank with low permeability interbedded clay layers is flushed with water spiked with 100 mg/L fluorescein and 67 mg/L bromide for 92 days. During this period, contaminants are attenuated by the clay layers. Subsequently, the tank is flushed with water without fluorescein and bromide for 38 days. This illustrates how the release of contaminant stored in low permeability zones effects downgradient water quality.

---

<sup>2</sup> A. Bolhari, T. Sale and J. Zimbron, Department of Civil and Environmental Engineering, Colorado State University, Fort Collins, Colorado.

Next, contaminants in the tanks are treated by flushing the tank with an alkaline persulfate solution (40,000 mg/L at pH 11) for eight days. This drives depletion of fluorescein in both the transmissive sand and low permeability clay layers. Lastly, the tank is flushed with water with no additives for 69 days to evaluate post-treatment rebound of contaminant levels in the tank effluent. Effluent concentrations of fluorescein and bromide are presented as a function of time. In addition, photographic images and a spectrometer equipped with a fiber optic cable are used to evaluate the distribution of fluorescein within the tank through each phase of the experiment. Results indicate that flushing the tank with an alkaline persulfate solution was effective in depleting fluorescein in both the transmissive and low permeability zones. Extrapolation of this result to field-scale applications is constrained by potential secondary water quality effects of the alkaline persulfate treatment, soil oxidant demands in natural porous media, challenges of delivering a high-density solution to a desired target, and uncertainties regarding treatment of less reactive contaminants. A primary value of this paper is advancing a dataset that can be used to test models that capture concurrent transport and reaction of reactants and contaminants, in a domain governed by advection in transmissive zones and diffusion in low permeability zones.

### **3.1 Introduction**

After more than three decades of attention, managing subsurface releases of chlorinated solvents remains a major technical challenge (USEPA 2003, NRC 2005, and Sale et al. 2008a). Following Sale et al. (2008a), prevailing thinking has evolved from simply managing chlorinated solvents in groundwater in transmissive zones to a far more

complex perspective of managing chlorinated solvents as non-aqueous, aqueous, sorbed, and vapor phases, in transmissive and low permeability zones, occurring in source zones and plumes. A primary constraint to achieving health based cleanup levels at many sites has been a failure to holistically consider all of the compartments that need to be addressed (Chapman and Parker 2005; and Sale et al. 2008a).

The problem is introduced by considering the evolution of a chlorinated solvent release. Most chlorinated solvent releases begin as a subsurface discharge in the form of a Dense Nonaqueous Phase Liquid (DNAPL). Initially, DNAPL moves through transmissive zones and becomes perched above low permeability capillary barriers (Feenstra et al. 1996). With time, DNAPL constituents partition into aqueous and vapor phases in transmissive zones. Aqueous phase chlorinated solvents move through transmissive zones via advection. Furthermore, dissolved phase contaminants migrate into low permeability zones by diffusion and/or slow advection. Ultimately, through natural processes and/or remediation, sources in the transmissive zones are depleted. This reduces aqueous concentrations in transmissive zones and drives the release of contaminants from low permeability zones via back diffusion and/or slow advection (Liu and Ball 2002; Chapman and Parker 200; Liu et al. 2007; Parker et al. 2008; and Sale et al. 2008b). Contaminants move out of low permeability zones more slowly than they move into them (Feenstra et al. 1996). A primary implication of slow release is the potential for dilute plumes to be sustained for decades or even centuries after their original source has been depleted (Chapman and Parker 2005; Parker et al. 2008; and Sale et al. 2008b). Initially, low permeability layers provide a sink for contaminants. At late time, low permeability zones can provide a source of contaminants. Contaminant

sorption and degradation within low permeability zones are key factors governing the significance of contaminants in low permeability zones (Parker et al. 1996 and Sale et al. 2008b). In particular, instances where contaminants are naturally degraded in low permeability zones can lead to scenarios where the potential for contaminant release from low permeability zones is dramatically reduced (Sale et al. 2008b).

Historically, Foster and Crease (1974) observed slow transport of nitrate through a fractured chalk. In Foster (1975) it is noted that diffusion might be playing a key role; he further suggested that extensive investigation of diffusion during fracture flow should be considered. A rich body of related literature include: Freeze and Cherry (1979), Rao et al. (1980), Sudicky (1983), Sudicky et al. (1985), Goltz and Roberts (1987), Wilson (1997), Carrera et al.(1998), Liu and Ball (2002), Chapman and Parker (2005), Liu et al. (2007), Parker et al. (2008), and Sale et al. (2008b). Researchers have also recognized the impact of contaminants stored in low permeability zones on timing and magnitude of the downgradient water quality improvements associated with upgradient reductions in contaminant loading (Wilson 1997; Liu and Ball 2002; Chapman and Parker 2005; Parker et al. 2008; and Sale et al. 2008b). The importance of contaminants in low permeability zones is reflected by a 2009 commitment of \$4 million for related research by the US Department of Defense through the Strategic Environmental Research and Development Program.

An emerging question is: What can be done about contaminants in low permeability zones? In response, Figure 15 presents a conceptual model for treatment of contaminants in low permeability zones. Following Freeze and McWhorter 1997, the scenario considered is a monitoring well in a heterogeneous sandy aquifer downgradient

of a source zone (e.g., a pool of chlorinated solvent DNAPL). It is assumed that no reactive attenuation of the contaminants is occurring. The graph presents the aqueous phase concentration of the contaminant in the well as a function of time. The following text describes each of the phases in more detail.

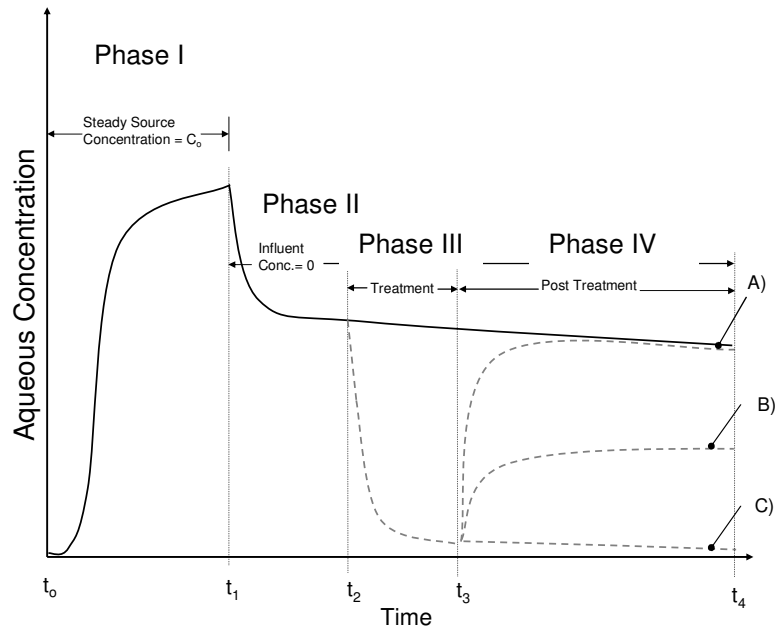


**Figure 15 - Anticipated water quality responses in a downgradient well to technologies addressing contaminants in low permeability zones.**

Phase I (Contaminant Loading) - Following the release at time  $t_0$ , contaminant concentration increases at the well (located downgradient of the source) through time  $t_1$ . During this phase, concentrations at the well approach the source concentration ( $C_0$ ) as the rate of contaminant attenuation by low permeability zones declines. At  $t_1$ , the effect of removing the upgradient source is observed at the downgradient well.

Phase II (Contaminant release without treatment) - During the period  $t_1$  to  $t_2$ , concentrations of chlorinated solvents at the well decrease as the effect of eliminating the contaminant at the source propagates downgradient. In the absence of an upgradient

source, aqueous phase concentrations at the well are sustained by ever-declining rates of contaminant release from low permeability zones via diffusion and slow advection.

Phase III (Treatment) - During the period  $t_2$  to  $t_3$ , a relatively short-duration treatment is employed. Contamination in the transmissive portion of the aquifer is removed via displacement and or reaction with the treatment agent.

Phase IV (Post-treatment) – Time  $t_3$  to  $t_4$  reflects conditions after treatment. Depending on the treatment effectiveness in the low permeability zones, three possible outcomes are anticipated: A) Concentrations at the well return to levels that would have been observed in the absence of treatment. This would be attributed to a treatment that had no effect on contaminant release from low permeability zones. B) Concentrations at the well are reduced to levels below what would have been observed in the absence of treatment but above risk-based numerical standards. This outcome would be attributed to a partial reduction in the rates of contaminant release from low permeability zones. C) Concentrations at the well are reduced to levels below what would have been observed in the absence of treatment and below risk-based numerical standards. This is the optimal outcome reflecting sufficient depletion of contaminants in low permeability zones.

The hypothesis of this research is that flushing an alkaline activated persulfate solution through transmissive zones can deplete contaminants in low permeability zones sufficiently to achieve Type C behavior as illustrated in Figure 15. Results provide a basis for evaluating governing processes and the effectiveness of treating contaminants stored in low permeability via flushing transmissive zones with an alkaline persulfate solution, under ideal conditions. Furthermore, results provide a data set that can be used to test models that capture concurrent transport and reaction of reactants and

contaminants in a domain governed by advection in transmissive zones and diffusion in low permeability zones.

### 3.2 Material and Methods

The tank used for the study is composed of a metal frame, two 2-cm thick panes of glass, and a Plexiglas<sup>TM</sup> spacer used to maintain a fixed gap between the panes of glass. The tank has a horizontal length of 1.07 m, a vertical height of 0.84 m, and a thickness of 0.029 m (Figure 16). The sides and bottom of the tank are sealed by rubber o-ring gaskets set in the Plexiglas<sup>TM</sup> spacer and held in the metal frame by 26 bolts. The tank was filled with layers of medium-grained quartz sand (transmissive zone) and a 9:1 mixture of kaolin and bentonite (low permeability zone). The kaolin provided a white background, enhancing the visualization of a fluorescein tracer.

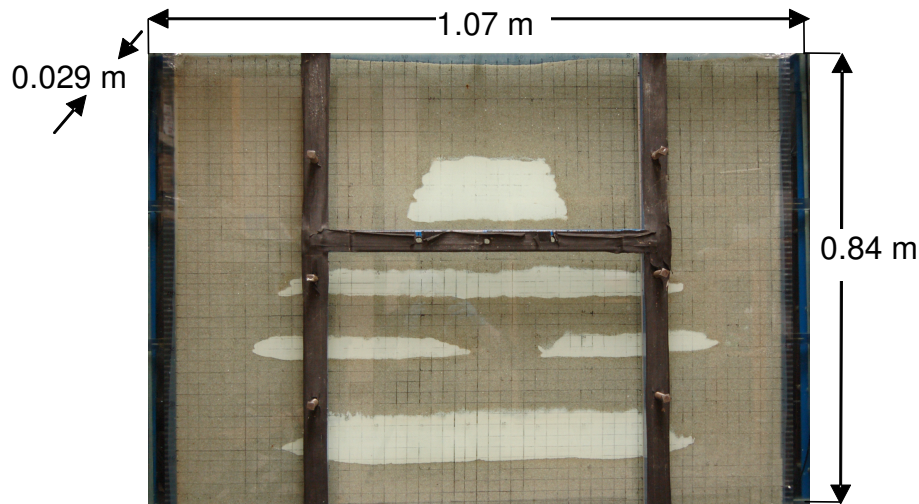


**Figure 16- Dimensions of the sand tank embedded with clay layers**

The bentonite was added to reduce the hydraulic conductivity of the clay layers. The tanks were loaded by a) raining in dry sand ensuring terminal velocity before the sand reached its final position, b) tapping the tank until sand settlement ceased, c)

saturation of the sand with de-aired water, and d) delivering the hydrated clay mixture using a caulk gun. This process was repeated until all layers were placed in the tank. Images of the tank are presented in the results section of this paper. Subsequently, the tank was flushed with de-aired water for 20 days to deplete dissolved gases trapped in the sand during loading. Table 2 presents the physical properties of the emplaced media.

**Table 2- Physical properties of porous media**

Media	Source	Grain size distribution	Composition	Porosity	Hydraulic conductivity (cm/sec)
Sand	UNIMIN® “Industrial quartz”, 4095	40-60 mesh	quartz	0.30	$9 \times 10^{-3}$
Clay	Thiele kaolin/ Wyoming NATURALGEL®	- 200 mesh	9 parts kaolin/ 1 part bentonite	0.58	$< 4 \times 10^{-7}$

Solutions were delivered to the tanks via a 2-cm wide head tank on the left-hand side using an ISMATEC™ peristaltic pump equipped with Viton® hose. Pump flow rates were set at 1.5 mL/min for the entire experiment, resulting in an average flow rate of 30 cm/day in the sand. Solutions were removed from the tank via a 2-cm wide head tank on the right-hand side of the tank at a rate equal to the inflow using a fixed head siphon. Figure 17 presents a timeline for the experiment.

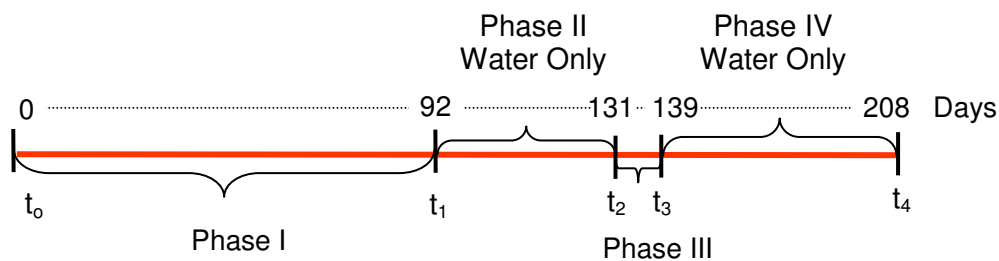


**Figure 17- Experiment timeline**

The following describes each phase of the experiment in more detail:

Phase I (Contaminant Loading) – De-aired tap water (~ 80 mg/L total dissolved solids) with 100 mg/L fluorescein ( $C_{20}H_{10}O_5Na_2$ ) and 67 mg/L bromide ( $Br^-$ ) was flushed through the tank for 92 days. Although the molecular weight of fluorescein is two and half times that of chlorinated solvents, it provides a means of visually observing the transport process. Also, fluorescein can be easily detected over a large range of concentrations (Sabatini and Austin 1991). Bromide is employed as a non-reactive tracer. The aqueous phase diffusion coefficient for bromide ( $2.08 \times 10^{-9} \text{ m}^2/\text{s}$ ) is approximately half that of fluorescein (Nelson et al. 2003). Both tracers have the practical advantage of low toxicity. According to Sabatini and Austin (1991), fluorescein can decay via photochemical processes. Reflecting this, all phases of the experiment were conducted in a dark room, with the exception of brief periods of lighting during sampling.

Phase II (Contaminant release without treatment) – De-aired tap water without fluorescein and bromide was flushed through the tank for 38 days. Lower concentrations in the transmissive sand drives release of the fluorescein and bromide (via diffusion) that had accumulated in the low permeability zones during Phase I.

Phase III (Treatment) – De-aired tap water with sodium hydroxide (pH 11) and 40,000 mg/L sodium persulfate was flushed through the tank for 8 days. Sodium persulfate is a chemical oxidant that has been widely used in subsurface remediation efforts. The high pH was employed to activate the persulfate. The concentration and pH of persulfate were resolved through batch flask studies in which pH and sodium persulfate were adjusted until rapid and irreversible treatment of fluorescein was

achieved. Treatment was defined as the disappearance of the fluorescein's characteristic green color. This was measured quantitatively using an Ocean Optics™ temperature compensated USB 2000 spectrometer equipped with a 410 nm light source and a 300-1000 nm detector. Under a 410 nm excitation, fluorescein emits light with a peak at 517 nm.

Phase IV (Post-treatment) – Following treatment with the alkaline persulfate solution, the tank was flushed with water only for an additional 69 days. This provided a basis for evaluating the effect of the treatment on contaminant release from low permeability zones. In post-treatment, the fluorescein peak was absent in spectrometer readings. Given the fact that pH can affect fluorescence (Sabatini and Austin 1991), all solutions with positive treatment were returned to a neutral pH to verify that disappearance of the fluorescein peak was due to fluorescein degradation, and not to pH effects.

Influent and effluent water samples were collected daily during dynamic phases of the experiment. Samples were collected at a minimum of three times per week during other phases of the experiments. Samples were collected using inline 20 mL glass sample bottles. Samples were sealed with crimp caps and Teflon™ lined septa and stored in a dark refrigerator at 4°C.

Concentrations of fluorescein in water samples were measured using an Ocean Optics™ temperature-compensating USB 2000 spectrometer, connected to an Ocean Optics™ 1 cm CUV cuvette holder through fiber optic cables, and plastic disposable cuvettes (Ocean Optics, Inc. CVD-UV1S, 1.5-3.0 mL, 220-900 nm). Calibrations were performed using standards ranging from 0.01 to 10 mg/L. Given the fact that pH can

affect fluorescence (Sabatini and Austin 1991), all solutions with positive treatment were returned to pH 7 to verify that elimination of the peak at 517 nm was not due to pH effects. Samples were analyzed for bromide using a METROM™ 681 ion chromatograph. Calibrations were performed using standards ranging from 0.1 to 70 mg/L (as bromide).

Photographs of the tank were taken with a Nikon D50 SLR digital camera throughout the 208 days of the experiment. The photographing process employed four 1 m long ultraviolet (UV) light bulbs set up at the sides, base, and top of the experiment. The no-flash and timer functions on the Nikon camera were used. Unfortunately, non-uniform lighting of the tank face made it infeasible to accurately transform photographic images into point estimates of fluorescein concentrations. As an alternative, an Ocean Optics™ USB 4000 spectrometer equipped with a two-fiber optic cable was used to obtain point estimates of the fluorescein concentrations in the sand clay layers via *ex situ* measurement through the glass. The approach involved placing the end of the dual fiber cable on the glass face of the sand tank. One of the fibers provided incident light at 410 nm. This drove an emission of light from the fluorescein in water at the face of the glass. The second fiber conveyed the initiated light back to the spectrometer. A calibration curve was developed by taking readings through the open plastic caps of inverted 20 mL glass vials glued to a piece of glass identical to the glass in the sand tanks. The concentration range for calibration standards was from 0.01 to 100 mg/L. Separate sets of standards were developed for sand and clay. Measurement of water concentrations, in the water-soil standards, at the end of the experiment, indicated no significant sorption of fluorescein to the sediments or losses due to photochemical degradation. Figure 18

presents a photograph of the soil water fluorescein standards mounted on glass. A challenge in measuring *in situ* fluorescein concentrations through the glass was reflection of the incident light back to the spectrometer.

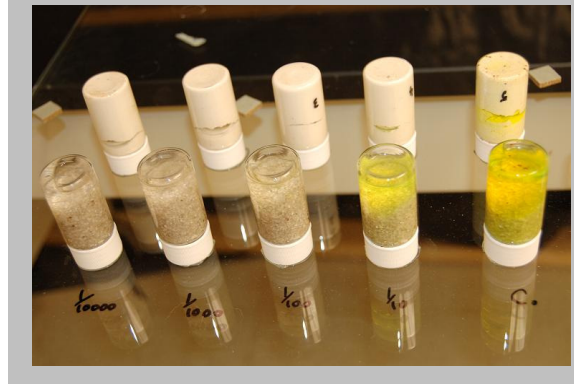


**Figure 18- Soil-water calibration standards.**

For measurements in the white kaolin-bentonite clay, the reflected light created a peak at about 410 nm that covered the fluorescein peak maximum signal at 519 nm. This problem was overcome by using a wavelength of 597 nm, on the flank of the fluorescein peak, as the basis for estimating concentration fluorescence in the sand and clay standards. With this procedure, the fluorescein detection limit in both the sand and clay layers was 1 mg/L.

### **3.3 Results and discussion**

The following presents experimental results including photographic images, plots of fluorescein and bromide tank effluent concentrations as a function of time, and spectrometer-based measurement of fluorescein concentrations in the sand and clay layers at the end of each phase of the experiment.

### 3.3.1 Photographic Images

Figure 19 presents images of the sand tank at key points during the 208 day study. The visible light image at the top presents the tank at  $t_0$  (immediately prior to delivery of the fluorescein and bromide – day 0). Black lines on the face of the tank provide a 2-cm grid that was employed in measuring point concentration using the spectrometer and fiber optic cables.

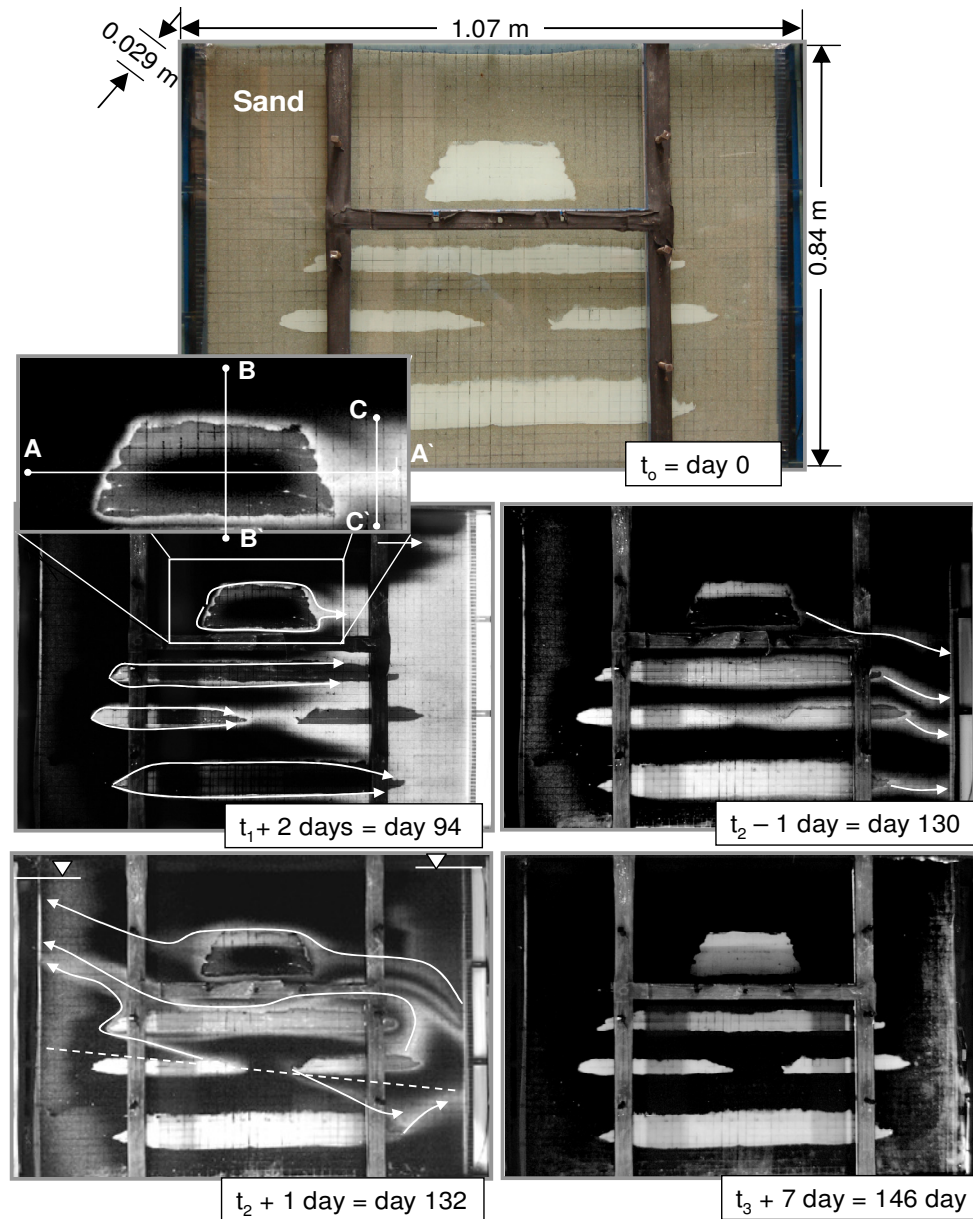


**Figure 19- Images of the sand tanks at critical times in the experiment**

The middle left hand image in Figure 19 presents the tank at  $t_1+2$  days (2 days after initiating the water only flushing, 94 days after the beginning of the experiment). At this time, lower solute concentrations in the transmissive sand is initiating release of the fluorescein (and bromide) stored in the low permeability clay layers. The telescoped portion of the image illustrates the distribution of fluorescein in the upper clay layer.

This image and all subsequent images in Figure 4 have been modified using Adobe Photoshop to highlight the distribution of fluorescein. White lines with an arrow trace flow patterns in the tank based on the observed tracer trails. Throughout the experiment, tracer trails indicated minimal mixing due to hydrodynamic dispersion.

The middle right hand image in Figure 19 presents the tank at  $t_2-1$  day (1 day before delivery of the alkaline persulfate solution, 130 days after the beginning of the experiment). At this time, slow release from the clay layers was sustaining narrow plumes of fluorescein (and bromide) that flowed to the right hand effluent head tank. In this image, highlighting the faint fluorescein trails in the transmissive sand results in loss of the apparent fluorescein concentrations in the clay layers.

The lower left hand image (Figure 19) presents the tank at  $t_2+1$  day (1 day after initiating the alkaline persulfate flood, 132 days from experiment startup). At this time, the high density of the alkaline persulfate solution ( $\sim 1.04 \text{ gm/cm}^3$ ) led to an unanticipated flow pattern. The solutions, delivered at the top of the left hand head tank fell through the water column in the head tank and formed a layer of high density solution at the base of the tank. This water formed a wedge of high density water (analogous to saltwater intrusion) that flowed across the base of the tank. Water was withdrawn from the tank via a hose at the bottom of the head tank on the right hand side. With this, the high density solution was recovered at a rate similar to its arrival at the base of the right hand head tank. Concurrently, the difference in average fluid densities on the left and right hand sides of the tank caused water to flow in the opposite direction (right to left) across the top of the tanks. This could be seen through the tracer trails from the upper clays and right hand head tank that lead all of the way back to the left hand head tank. This also

resulted in a higher water surface on the right hand side of the tank. This problem was corrected on  $t_2+2$  days (133 days from experiment startup) by moving the discharge line on the right hand side of the tank to the top of the water column. This depleted the wedge of low density water in the tank and led to full saturation of the tank with the alkaline persulfate solution by  $t_2+3$  days (day 134). These observations point to the pragmatic challenges of delivering solutions with high density to subsurface remediation targets.

Lastly, the lower right hand image (Figure 19) presents the tank at  $t_3+7$  days (7 days after ending the alkaline persulfate flood and returning to flushing with water only). At this time and through the remainder of the experiment there were no visual indications of fluorescein in clay or sand layers.

### **3.3.2 Effluent Water Quality Data**

Normalized concentrations are determined by dividing the daily effluent concentrations by the average influent concentrations for the period  $t_0$  to  $t_1$ . The 99% confidence intervals, based on the calibration data, are  $\pm 5\%$  for fluorescein and  $\pm 1\%$  for bromide. Figure 20 presents normalized effluent concentrations of fluorescein and bromide over the duration of the experiment. Over the first ten days, normalized effluent concentrations ( $C/C_0$ ) gradually rise to near 1. Over the next 81 days, normalized concentrations are slightly less than 1. Normalized effluent concentrations less than 1 reflect ongoing attenuation of fluorescein and bromide by the clay layers.

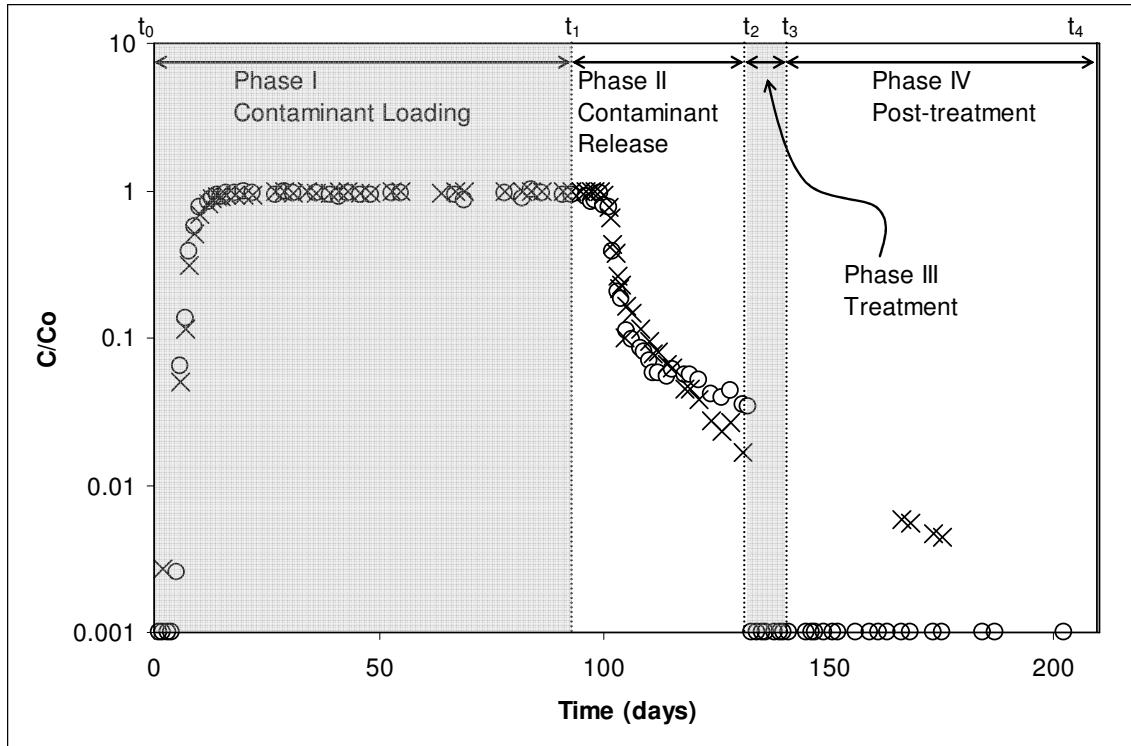


**Figure 20- Normalized fluorescein and bromide effluent concentrations versus time (o fluorescein, x bromide)**

During Phase II, contaminant release, the normalized effluent concentrations decay by  $1\frac{1}{2}$  orders of magnitude. The difference in the Phase II fluorescein and bromide concentrations may be due to the factor of 2 difference in diffusion coefficients for the compounds. As seen in the photographic images sustained fluorescein effluent concentrations in this period is due to slow releases of fluorescein stored in the clay layers.

After introduction of the alkaline persulfate solution at  $t_2$ , concentrations of fluorescein drop below method detection limits for the remainder of the 208 day experiment. As introduced in Figure 15, this is a Type C behavior. This is attributed to depletion of sufficient contaminant mass in the clay layers to preclude consequential long-term releases from the low clay layers. This is consistent with post-treatment visual observations of fluorescein.

In contrast, bromide, a species that would not be depleted by the alkaline persulfate treatment, illustrates Type A behavior (see Figure 15). Unfortunately, accurate measurement of bromide during and immediately after the alkaline persulfate flood was not possible due to the high total dissolved solids and strong oxidizing conditions. Four measurements of bromide were obtained during Phase IV, Post-treatment (from day 160 to day 170). These lie on the decay curve that was observed prior to the alkaline persulfate treatment. After this time effluent bromide concentrations were below method detection limits.

### **3.3.3 Fiber Optic Spectrometer Data**

Throughout the experiment, point measurements of fluorescein concentrations were made along transects in the sand and clay layers using a spectrometer and a fiber optic cable. This included a horizontal transect through the upper clay (A-A'), a vertical transect through the upper clay (B-B'), and a vertical transect 6 cm downgradient of the upper clay (C-C'). These transects are shown in the expanded image in Figure 19.

Figure 21 plots concentration as a function of position along each transect at the end of each experimental phase. At the end of the first phase (loading) the concentrations in the sand are on the order of 56 to 105 mg/L. Lower concentrations are observed in the sand layer near the clay boundary due to diffusion of fluorescein into the clay. Concentrations are also reduced along the C-C' downgradient transect, reflecting the fact that the clay acts as a contaminant sink during this first loading phase. Concentrations in the clay range from 1 (detection limit) to 22 mg/L. Reflecting inward diffusion from the

sand, concentrations are greatest at the clay-sand boundary and lowest in the center of the clay.

At the end of the Phase II (contaminant release), concentrations in the sand are near zero everywhere except at the clay-sand contact and along transect C-C` (downgradient from the clay). Fluorescein concentrations in the sand reflect on going release from the clay via diffusion and slow advection. Within the clay layer, concentrations are greatest 2 cm into the clay and, again, are lowest in the center of the clay. Through Phase II, concentrations in the middle of the clay rise by 8 mg/L due to ongoing inward diffusion. Fluorescein concentrations in the clay reflect ongoing releases from the clay via diffusion at the clay-sand contact and concurrent inward diffusion toward the interior of the clay. Critically, diffusion, a process that occurs over small distances, is a primary governing process. This is consistent with observations presented in Feenstra et al. 1996; Liu and Glass, 2002; Chapman and Parker, 2005; Parker et al. 2008; and Sale et al. 2008b.

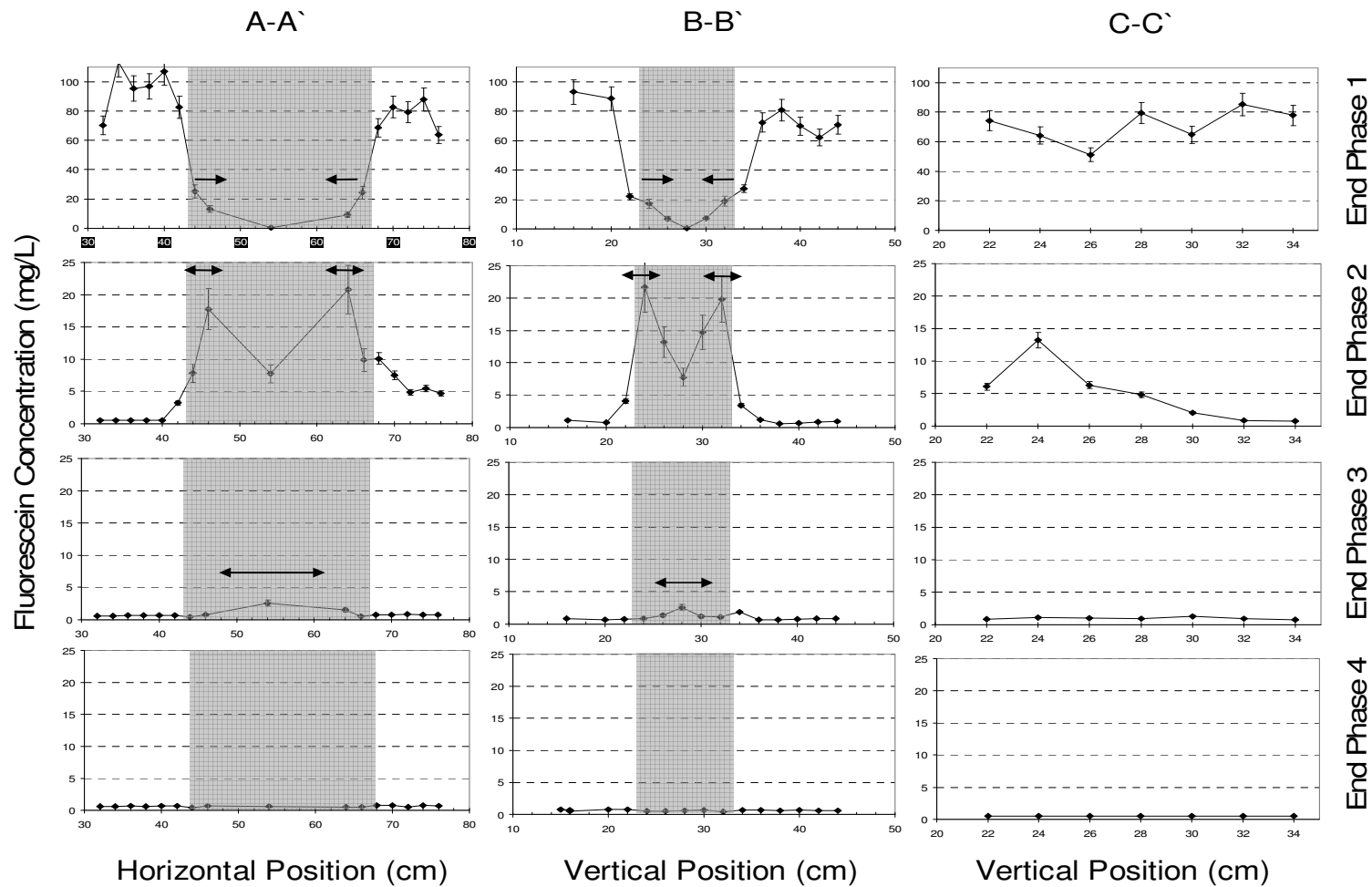


**Figure 21- Profiles of fluorescein concentration through the upper clay and adjacent sand layer. The point 0,0 is at the lower left hand corner of the tank. Horizontal position increasing to the right and vertical position increase upward. Transect A-A` lies along a line with a vertical position of 59 cm. Transect B-B` lies along a line with a horizontal position of 51cm. Transect C-C` lies along a line with a (vertical position of 71 cm. Gray shading indicates the position of the clay. Arrows indicate directions of diffusion-driven fluorescein transport in the clay.**

At the end of the Phase III (alkaline persulfate flushing), fluorescein is absent in the sand. As indicated by the downgradient (C-C`) transect through the sand, the clay is no longer releasing fluorescein at detectable levels. Fluorescein concentrations are lower than pre-treatment levels everywhere within the clay layer, with a maximum at the center of the clay. Observed conditions in the clay at this time reflect concurrent transport and reaction of fluorescein and persulfate in a domain where transport is governed by diffusion.

At the end of the last phase of the experiment (post-treatment flushing) fluorescein is almost completely absent. Most critically, treatment in the clay continued after the alkaline persulfate flushing ended, preventing a rebound of fluorescein concentrations. Results from all four lower clay layers in the tank are consistent with the trends observed in the upper clay.

### **3.3.4 Additional Considerations**

Collectively, the photographic effluent water quality data, and fiber optic spectrometer data indicate an ideal Type C response to treatment of fluorescein stored in the low permeability clay layers. Nevertheless, these favorable results need to be balanced by pragmatic considerations. First, the porous media used in the experiment is atypical in two ways: It lacks the levels of soil oxidant demand that are common in natural media and the porosity of the clay (0.65) is larger than typical values. Both these attributes are likely to result in more favorable treatment than is probable under field conditions. Secondly, the high total dissolved solids (40,000 mg/L) and pH (11) of the

treatment system may create secondary water quality issues of equal or greater concern to that of the targeted contaminant. Thirdly, advective delivery of high-density solutions to targets may be difficult, as illustrated by the complex flow fields observed in Figure 19. Fourthly, fluorescein, and its apparent treatment via reduction in the peak emitted about 519 nm, may not be a valid surrogate for treatment of other contaminants of concern such as tetrachloroethene or trichloroethene. Lastly, the two-dimensional 1-meter scale of the study may not provide a rigorous analog to field applications.

### **3.4 Conclusions**

This paper explores the concepts that a) contaminants stored in low permeability zones can provide persistent releases to groundwater in transmissive zones and b) resolving what can be done to manage contaminants in low permeability zones is an emerging question of importance. These concepts are supported through a two-dimensional sand tank study involving collection of photographic images, tank effluent data, and point measurements of contaminant concentrations in sand and clay layers through time. Results from the experiment suggest that an alkaline persulfate flood is a viable means (at a laboratory scale) of depleting fluorescein in low permeability zones. Specifically, results indicate that a Type C response to treatment, in which fluorescein concentrations in low permeability layers are depleted sufficiently to preclude consequential releases from low permeability zones. Promising results are balanced by concerns that ideal aspects of the study create more favorable results than might be attainable under common field conditions and concerns that water quality impacts of the high TDS, high pH solution could be unacceptable at many field sites.

As described by Chapman and Parker 2005, Parker et al. 2008, and Sale et al. 2008b; advection in transmissive zones and diffusion in low permeability zones are key process governing storage and release of contaminants in low permeability zones. Progressing to treatment, key processes are a) advection of the reactants to the contact between the transmissive and low permeability zones and b) diffusion controlled transport and reaction of contaminants in low permeability zones.

Building on this work, current research is exploring the use of high-resolution numerical modeling techniques to address transport and reaction of contaminants and reactants in systems where advection and diffusion are primary transport processes. In addition to demonstrating governing processes, a primary value of this paper is the advancement of data sets that can be used to test models that can explore solutions for contaminants in low permeability zones.

## **Acknowledgments**

Primary financial support for this work was provided by DuPont. Complementary financial support was provided by the University Consortium for Field-Focused Groundwater Contamination Research and GE. Students and staff at Colorado State University contributing to this effort include Mitch Olson, Nicholas Mahler, and Patrick Clem.

## REFERENCES

- Carrera, J., Sanchez-Villa, X., Benet, I., Medina, A., Galarza G., Guimera, I., 1998. On matrix diffusion: solutions methods and qualitative effects, *Hydrogeology Journal* 6 (1), 178–190.
- Chapman, S.W. and B.L. Parker, 2005. Plume Persistence Due to Aquitard Back Diffusion Following Dense Nonaqueous Phase Liquid Removal or Isolation, *Water Resource Research* 41 (12), W12411.
- Feenstra, S., Cherry, J.A., Parker, B.L., 1996. Conceptual Models for the Behavior of Dense Nonaqueous Phase Liquids (DNAPLs) in the Subsurface, Chapter 2 in Dense Chlorinated Solvents and Other DNAPLs in Groundwater, J.F Pankow and J.A. Cherry, Editors. Waterloo Press, pp. 53-88.
- Foster, S. S. D., Crease, R. I., 1974. Nitrate pollution of chalk groundwater in east Yorkshire – A hydrogeological appraisal, *Journal of Institution of Water Engineers and Scientists* 28, 178-194.
- Foster, S. S. D., 1975. The chalk groundwater tritium anomaly—a possible explanation, *Journal of Hydrology* 25, 159–165.
- Freeze, R.A., Cherry, J.A., 1979. Groundwater. Prentice Hall, Englewood Cliffs, NJ, pp. 410-413..
- Freeze, R. A., McWhorter, D. B., 1997. A framework for assessing risk reduction due to DNAPL mass removal from low permeability soils. *Journal of Ground Water*, 35, 1, 111-123.
- Goltz, M.N., Roberts, P.V., 1987. Using the method of moments to analyze three-dimensional diffusion-limited solute transport from temporal and spatial perspectives. *Water Resour. Res.* 23, 1575–1585.
- Liu, G., Ball, W. P., 2002. Back diffusion of chlorinated solvent contamination from a natural aquitard to a remediated aquifer under well-controlled field conditions: predictions and measurements, *Journal of Ground Water* 40, 175–184.
- Liu, G., Zheng, C., Gorelick, S., 2007. Evaluation of the applicability of the dual-domain mass transfer model in porous media containing connected high-conductivity channels, *Water Resource Research* 43, p. W12407.
- National Research Council (NRC), 2005. Contaminants in the Subsurface: Source Zone Assessment and Remediation. National Academies Press, Washington, D.C.

- Nelson, N. T., Hu, Q., and Brusseau, M. L., 2003. Characterizing the contribution of diffusive mass transfer to solute transport in sedimentary aquifer systems at laboratory and field scales. *Journal of Hydrology* 276, 275-286.
- Parker, B.L., J.A. Cherry, and R.W. Gillham, 1996. The Effects of Molecular Diffusion on DNAPL Behavior in Fractured Porous Media, Chapter 12 in Dense Chlorinated Solvents and Other DNAPLs in Groundwater, J.F Pankow and J.A. Cherry, Editors. Waterloo Press, pp. 53-88.
- Parker, B.L., S.W. Chapman, and M.A. Guilbeault 2008, Plume persistence caused by back diffusion from thin clay layers in a sandy aquifer followed by TCE source-zone hydraulic isolation, *Journal of Contaminant Hydrology*, 120, 86-104.
- Rao, P.S.C., Rolston, D.E., Jessup, R.E., Davidson, J.M., 1980. Solute transport in aggregated porous media: theoretical and experimental evaluation, *Journal of Soil Science of America* 44, pp. 1139–1146.
- Sabatini, D.A., Austin, T.A., 1991. Characteristics of rhodamine WT and fluorescein as adsorbing groundwater tracers. *Ground Wat.* 29, 341–349.
- Sale, T., C. Newell, H. Stroo, R. Hinchee, P. Johnson, 2008a, Frequently Asked Questions Regarding Management of Chlorinated Solvent in Soils and Groundwater, Developed for the Environmental Security Testing and Certification Program (ER-0530).
- Sale, T. C., Zimbron, J., Dandy, D., 2008b. Effects of reduced contaminant loading on downgradient water quality in an idealized two-layer granular porous media, *Journal of Contaminant Hydrology* 102, 72-85.
- Sudicky, E.A., 1983. A convection–diffusion theory of contaminant transport for stratified porous media, Ph.D. dissertation, 203 pp., University of Waterloo, Waterloo, Canada, 6 May.
- Sudicky, E.A., Gillham, R.W., Frind, E.O., 1985. Experimental investigation of solute transport in stratified porous media 1. The nonreactive case, *Water Resources Research* 21, 1035–1041.
- U.S. Environmental Protection Agency (EPA), 2003. The DNAPL Remediation Challenge: Is There a Case for Source Depletion? EPA/600/R-03/143.
- Wilson, J.L., 1997. Removal of aqueous phase dissolved contamination: non-chemically enhanced pump and treat. In: C.H. Ward et al. Editors, *Subsurface Remediation Handbook*, Ann Arbor Press, Chelsea, MI, pp. 271–285.

## Chapter 4

# POTENTIAL OF THREE INNOVATIVE APPROACHES FOR TREATING TRICHLOROETHENE IN LOW PERMEABILITY ZONES

### SYNOPSIS

This research explores the potential of three innovative treatment approaches for *in situ* treatment of trichloroethene (TCE) in low permeability zones. Options considered include: carbon sequestration, sonication, and calcium polysulfide (CPS). Delivery of carbon in sand columns resulted in clogging the influent pores precluding effective delivery. Furthermore, no evidence was developed to support our hypothesis that carbon could poise a redox condition that would drive reductive dechlorination of TCE. Initial sonication studies involving TCE solutions indicated that chloride level could be increased with sonication. Furthermore, an increasing trend in chloride concentration was observed with greater periods of sonication. Unfortunately, the sonication results were not reproducible and it seems that part of the losses of TCE may have been due to heating. Results obtained from laboratory experiments show that CPS imposed a redox condition of -500 mV (Ag-AgCl) and drove partial reduction of TCE. Overall, considering deliverability, effectiveness and cost, CPS appears to be the most promising option.

## 4.1 Introduction

Aquifers are composed of media that exhibit a wide range of capacities to transmit fluids. This is generally referred to as heterogeneity. Portions of aquifers with large permeability values typically contain mobile water. In contrast, water is largely immobile in portions of aquifers with lower permeability (Payne et al. 2008). Releases of Dense Non-aqueous Phase Liquids (DNAPLs) or dissolved phase constituents move preferentially along pathways with the greatest permeability. Initially, little or no contamination is present in the low permeability zones (e.g., clay layers). However, with extended time, dissolved phase contaminants migrate into low permeability zones via diffusion and/or slow advection (Sale et al. 2007; Liu et al. 2007; Sale et al. 2008). Contaminants in low flow zones are stored in both dissolved and sorbed phases (Freeze and Cherry 1979 and Parker et al. 1994).

Ultimately, through natural processes and/or remediation, contaminants in the transmissive zones are depleted. This reduces aqueous concentrations in transmissive zones and drives the release of contaminants from low permeability zones via back diffusion and slow advection (e.g., Sudicky et al. 1986 and Parker et al. 1994).

Contaminant storage-release in low permeability zones is a hysteretic process (Feenstra et al. 1996). Contaminants move out of low permeability zones far more slowly than they move into them. A primary implication of slow release is the potential for dilute plumes to be sustained by releases from low permeability zones for decades or even centuries after their original source has been depleted (Chapman and Parker 2005 and Sale et al. 2008).

The impacts of low permeability zones on water quality have been studied at a laboratory scale (Rao et al. 1980; Tang et al. 1981; Sudicky et al. 1985; Sale et al. 2007; and Doner 2008), at a field scale (Chapman and Parker 2005; Sale et al. 2007; and Chapman and Parker 2008), and through modeling studies (Tang et al. 1981; Sudicky et al. 1985; Liu and Ball 2002; Chapman and Parker 2005; Sale et al. 2007; Liu et al. 2007; and Sale et al. 2008).

At a field-scale, common treatment technologies have limitations. The following are some of the examples:

- Pump and Treat – Slow rates of contaminant depletion lead to an extended period of operation and high costs.
- *In Situ* Chemical Oxidation – Costs (for chemicals, delivery, and monitoring) per unit volume and the volume of material treated can be prohibitively large.
- *In Situ* Biological Treatment – Again, costs (for chemicals, delivery, and monitoring) per unit volume and the volume of material treated can become prohibitively large. Furthermore, this process has the potential to be exceedingly slow.
- Multiple Permeable Reactive Barriers (PRBs) – Limited research suggests that a prohibitively large number of PRBs would need to be installed to deplete contaminant stored in plumes in a significant period of time.

Due to limited performance and high cost of these technologies, consideration of alternative approaches is warranted.

The objective of this research is to explore the potential of three innovative approaches for managing contaminants stored in low permeability zones. These include

carbon sequestration, sonication, and emplacement of reactive metal sulfides via calcium polysulfide. For each approach, mechanisms of operation, potential performance are evaluated. The approaches and our hypotheses for each are:

- Carbon sequestration- Our hypothesis is that solid phase carbon placed in transmissive zone can adsorb contaminants and create a redox poise that favors reductive dechlorination and enhance back diffusion of contaminants from low permeability zones.
- Sonication- Our hypothesis is that sonication could reduce aqueous concentration in transmissive and low permeability zones (through high frequency pressure waves) and/or provide preferential displacement of contaminants out of low permeability zones.
- Calcium polysulfide- Our hypothesis is that aquifers can be flushed with sulfide-iron solutions (from calcium polysulfide, CPS) that can lead to precipitation of reactive sulfide on the solid media in transmissive zones. Reactive iron sulfides in transmissive zones deplete aqueous and sorbed phase contaminants in transmissive zones via reductive dechlorination and consequently enhance back diffusion of contaminants from low permeability zones.

For each of the above the following presents an overview of the technology, proof of concept, laboratory studies, and results.

## 4.2 Carbon sequestration

### 4.2.1 Overview

The vision of carbon sequestration is to initially inject a slurry of water and carbon at a sufficiently large flow rates to advance carbon particles into transmissive zones. Due to density, once the system returns to natural seepage velocity (multiple orders of magnitude lower) carbon particles should settle in the porous media and become immobile. It is also possible that electrostatic effects will provide a mechanism for stabilizing carbon particles under natural gradient conditions. In addition, our hope is that the carbon will poise redox conditions that favor dechlorination of TCE. The overall mechanism of action is envisioned as reduced aqueous concentration in transmissive zones, resulting in: a) Depletion of sorbed contaminants in transmissive zones and b) Enhanced back diffusion of contaminants (dissolved and sorbed phases) from low permeability zones. The potential for long-term persistence of the solid carbon phases is a favorable attribute.

It is important to note that the mechanisms of adsorption are complex. Among many factors, sorption might depend on the type of carbon, time of contact, concentrations of contaminants, and aqueous chemistry (Schwarzenbach et al. 2003). In general, sorption can be an instantaneous equilibrium process, a hysteretic process where desorption occurs far more slowly than sorption, and/or as an irreversible process (Schwarzenbach et al. 1993; Dondelle and Loehr 2002; and Shackelford 1991).

The inspiration for this approach comes from PCB sequestration efforts led by Dr. Dick Luthy at Stanford University (e.g., Luthy and Tomaszewski 2006 and Luthy 2007). An appealing aspect of this approach is that solid-phase carbon can be a low-cost material

with relatively simple chemistry. The following sections review mechanism of action and potential performance of three types of carbon that seem to be appropriate for carbon sequestration from the perspectives of particle size, adsorption capacity, and cost.

#### *4.2.1.1 Carbon Black*

*Description* - Carbon black [C.A.S. NO. 1333-86-4] is nearly pure elemental carbon with most types containing greater than 97% elemental carbon arranged as aciniform (grape-like cluster) particulate in the form of colloidal particles produced by incomplete combustion or thermal decomposition of gaseous or liquid hydrocarbons under controlled conditions (International Carbon Black Association, 2004). Although carbon black is classified by the International Agency for Research on Cancer (IARC) as a Group 2B carcinogen based on sufficient evidence in animals and inadequate evidence in humans, recent evidence indicates that the phenomenon of carcinogenicity in the rat lung is species-specific, resulting from persistent overloading of the rat lung with poorly soluble particles smaller than 1.0 micrometer in diameter. Mortality studies of carbon black manufacturing workers did not show an association between carbon black exposure and elevated lung cancer rates. Despite this, on February 21, 2003, Carbon black (airborne, unbound particles of respirable size) was added to the California Office of Environmental Health Hazard Assessment (OEHHA) list of substances known to cause cancer. Carbon black is not a hazardous substance under the Comprehensive Environmental Response, Compensation and Liability Act (CERCLA, 40 CFR 302) or the Clean Water Act (40 CFR 116). In addition, according to the Resource Conservation and Recovery Act (RCRA, 40 CFR 262) carbon black is not a hazardous waste. Similarly, based on the

Clean Air Act Amendments of 1990 (CAA, 40 CFR Part 63) carbon black would not be considered a hazardous air pollutant.

*Mechanisms* - Carbon black is a form of amorphous carbon that has an extremely high surface area to volume ratio, which makes it favorable for treatment of contaminants via sorption. In addition, it is hypothesized that carbon black could exert a redox poise that would favor reductive dechlorination and/or serve as a substrate for microorganisms that can facilitate reductive dechlorination. A potential example of the latter of the two mechanisms is the production of methane in coal beds.

*Potential Performance* - The fact that water discharges containing carbon black must comply with applicable requirements for solid and oxygen demand could be a limiting parameter for use of carbon black in a treatment project. Carbon black has very low solubility in water and a specific gravity of 1.7 to 1.9. Gravity settling can be effective and the most common technique employed to remove carbon black from wastewater. Under some circumstances, settling may be inhibited because of the small particle size and/or high surface areas that may resist wetting. Various metallic salts, such as ferric or aluminum sulfate and synthetic polymers are effective as flocculating agents to enhance settling.

#### *4.2.1.2 Activated carbon*

*Description* - Activated carbon is produced from carbonaceous source materials like nutshells, wood, and coal through physical or chemical reactivation. Physical reactivation is generally made by using one of or combining the following processes:

- Carbonization: Material with carbon content is pyrolysed at temperatures in the range of 600-900 °C in absence of air (with gases like argon or nitrogen).
- Activation/Oxidation: Raw material or carbonized material is exposed to oxidizing atmospheres (carbon dioxide, oxygen, or steam) usually in the temperature range of 600-1200 °C.

A gram of activated carbon can have a surface area in excess of 500 m<sup>2</sup>, with 1500 m<sup>2</sup> being readily achievable. Traditionally, active carbons are made in particular form as powders or fine granules less than 1.0 mm in size with an average diameter between .15 and .25 mm.

*Mechanisms* - It is predicted that activated carbon will share similar mechanisms of performance with the other carbon types, with the possible variation that it will have the highest capacity to sorb chlorinated solvents. As noted for carbon black, key processes could include sorption, favorable redox poises, and substrate for microbes.

*Potential Performance* - It has been shown by Li et al. (2002) that adsorbent polarity expressed by the sum of the oxygen and nitrogen (O+N) content can provide a good criterion for selecting activated carbon. As the polarity of a carbon (the O+N content) increases the micro-pollutant adsorption capacity decreases. They also suggest an O+N content of less than about 2 to 3 mmol/g to assure that activated carbons are sufficiently hydrophobic to effectively remove organic contaminants from aqueous solution. Aktas and Cecen (2006) suggest that rather than the physical form, the type of carbon activation and the chemical characteristics of the surface play a more important role in the adsorbability of phenol and its reversibility. The primary advantage of using activated carbon is that surface adsorption through Granulated Activated Carbon (GAC)

application is a very simple technology with generally stable operations. In addition, GAC is very well-established way to remove organic compounds. Because of the wide commercial availability of GAC, carbon systems are relatively easy to implement. Carbon systems require no off-gas treatment and the creation of by-products is limited to spent carbon that requires regeneration or disposal (Creek and Davidson 2008).

Some of the limitations of treating organic contaminants with GAC can be as follows:

- Characteristics of the contaminants: adsorbents exhibit a larger adsorptive capacity for TCE than for methyl tertiary butyl ether: MTBE (Li et al. 2002).
- Presence of natural organic background in groundwater: can considerably decrease the adsorption rate and activated carbon capacity for TCE (Wilmanski and Van Breemen 1990).
- Delivery of particulate matter into porous media.

#### *4.2.1.3 Charcoal*

*Description* - Charcoal is generally made from wood that has been burnt or charred while being deprived of oxygen. What remains after combustion is an impure carbon residue. In a recent study, charcoal was prepared and mixed with forest soil and left in the soil in each of three contrasting forest stands in northern Sweden for ten years. A substantial increase in soil microorganisms (bacteria and fungi) was observed when charcoal was mixed into humus. These microbes decompose organic matter (carbon) of the soil and as a result a significant loss of organic matter and carbon in the native soil for

each of the three forest stands was observed. Carbon dioxide (a greenhouse gas) was the end result of much of this soil carbon loss (Wardle et al. 1998).

Pietikainen et al. (2000) suggest that charcoal obtained from burning can support microbial communities, which are small in size but have a higher specific growth rate than those of the humus. Charcoal also increases  $\text{NO}_3\text{-N}$  levels in soil, which is in agreement with earlier studies showing that charcoal has positive effects on nitrification (Nilsson et al. 2008). It was also found that charcoal reduced Substrate Induced Respiration (SIR), which is in contrast with the results of some of the earlier studies that indicated charcoal would promote microbial biomass (Wardle et al. 1998; Pietikainen et al. 2000). Regardless of the carbonization method or the kind of wood used, the surface of charcoals prepared at low temperature was acidic and that of charcoals prepared at high temperature was basic. The charcoal prepared at  $600^\circ\text{C}$  had the largest mean pore size, and also showed the fastest adsorption rate and the highest adsorption capacity. Of the charcoals prepared by air stream (versus nitrogen stream) the charcoal prepared at  $900^\circ\text{C}$  had the highest adsorption capacity. The charcoal prepared at  $1000^\circ\text{C}$  showed a decrease in adsorption capacity because of thermal shrinkage of the pores (Ikuo et al. 1998).

*Mechanisms* - It is predicted that charcoal will share similar mechanisms of performance with other carbon types. The key processes could include sorption, favorable redox poises, and substrate for microbes.

*Potential Performance* - Charcoal is potentially the lowest cost carbon, provides a favorable porous media for surface adsorption of contaminants, and has been shown to facilitate microbial activity. Charcoal is safe to handle and stores well. Charcoal

supplies nutrients, increases bio-available water, builds soil organic matter, enhances nutrient cycling, lowers the bulk density, and acts as a liming agent. The half-life of charcoal based in soil can be in excess of 1,000 years. This means that soil-applied charcoal will make a lasting contribution to soil quality and the carbon in the charcoal will be removed from the atmosphere and sequestered in the soil for millennia. Additionally, charcoal is a porous substance with high water and air holding capacity which makes it suitable habitat for some microbes and plant growth. Other characteristics of charcoal include high alkalinity, neutralization of acidic soil, and improvement of chemical components of soil and selection of microorganisms. Charcoal does not contain organic matter which will lead to exclusion of saprophytes (organisms which obtain nutrients from dead organic matter) and propagation of autotrophic and symbiotic microorganisms, including free living nitrogen fixing bacteria, root nodule bacteria, Frankia and some mycorrhizal fungi. Charcoal also has low mineral content, and therefore has no role as a fertilizer (Ogawa 2008). On the other hand, charcoal can provide a substrate for useful microorganisms (spores of bacteria, root nodule bacteria, mycorrhizal fungi, Frankia etc).

Potential limitations of applying charcoal as a treatment material could include its low mechanical stability, low selectivity and low adsorption speed. As with other forms of carbon, it may be challenging to deliver to porous media.

## 4.2.2 Carbon laboratory studies

Laboratory studies were conducted to explore deliverability of carbon black, activated carbon, and charcoal into porous media. Furthermore, the redox poises imposed by each carbon types were evaluated. Both of these issues are critical and need to be addressed to resolve the feasibility of carbon sequestration.

### 4.2.2.1 Methods

The carbon types used included: activated carbon (Fisher Scientific), carbon black (Columbian Chemicals Company) and charcoal (ACROS ORGANICS). All of these materials were ground into a fine powder and passed through a #200 sieve. To investigate the delivery of carbon types four cylindrical extruded acrylic columns were set up (Figure 22). The columns had the inside diameter of 2” and the inside length of 6”.

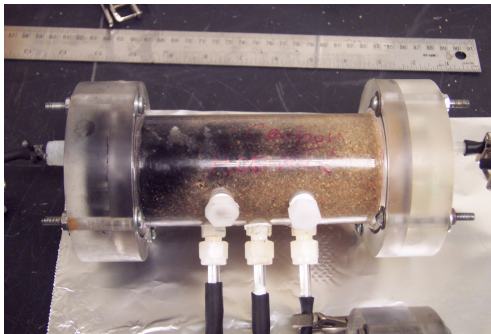


**Figure 22- Acrylic cylindrical columns used for the carbon experiment**

Three of the columns served as carbon tests. A fourth no carbon column provided a control. Each column was packed with medium to coarse quartz-feldspar sand. The porosity and hydraulic conductivity of the materials were 0.345 and 0.035 cm/s, respectively. Deionized water (DIW) with 80 mg/L Na<sub>2</sub>SO<sub>4</sub> (Fisher Scientific) and 20

mg/L Na<sub>2</sub>HPO<sub>4</sub> (Fisher Scientific) flushed through columns (positioned vertically) from the bottom using a four-channel ISMATEC peristaltic pump for a week at seepage velocity of 1 ft/day. After one week visible entrapped gasses were displaced from the columns. Slurries of 4% carbon by weight were prepared in a 500 mL Erlenmeyer flasks with magnetic stir bar, placed on a stir plate for each of carbon types. The slurry was pumped into test columns through glass tubings at a seepage velocity of 20 ft/day. Throughout the test, head loss across the column was measured as a function of time using 1 m manometer tubes.

Carbon content of columns was calculated using suction filtration as follows: Columns were disassembled and their content was emptied onto a No. 80 sieve. Next, the content was washed with DIW to separate the carbon from sand. Next, the carbon-water was pour into a porcelain Buchner funnel (equipped with a pre-weighted 0.45 micron filter paper wetted with DIW) connected to a side-arm flask with a tube leading to a vacuum pump. The liquid was drawn through the perforated plate by vacuum suction leaving carbon particles on top. Next, the filter papers were dried in the oven for 24 hours and weighted.

Carbon-water slurries were prepared to evaluate the potential of the carbon materials to poise favorable redox condition. Also, a saturated TCE stock solution was prepared with nonaqueous TCE in DIW with 80 mg/L Na<sub>2</sub>SO<sub>4</sub> and 20 mg/L Na<sub>2</sub>HPO<sub>4</sub>. Consequently, in an anaerobic chamber 40 mL glass vials were filled with 20 mL of well mixed carbon types topped off with 21 and 21.5 mL of TCE stock solution to minimize the head space (Figure 23, panel b). Two 40-mL glass vials were filled up with the TCE saturated solution only. This provided a no treatment control. Eh and pH values were

measured using Oxidation Reduction Potential (ORP) probe (Thermo Electron Corporation, Orion 4 Star) through five weeks (three weeks before and two weeks after addition of the TCE stock solution). After a week of treatment, the vials were tested for TCE using a Hewlett Packard 5890 gas chromatograph (GC) and chloride using a METROM 681 ion chromatograph (IC).

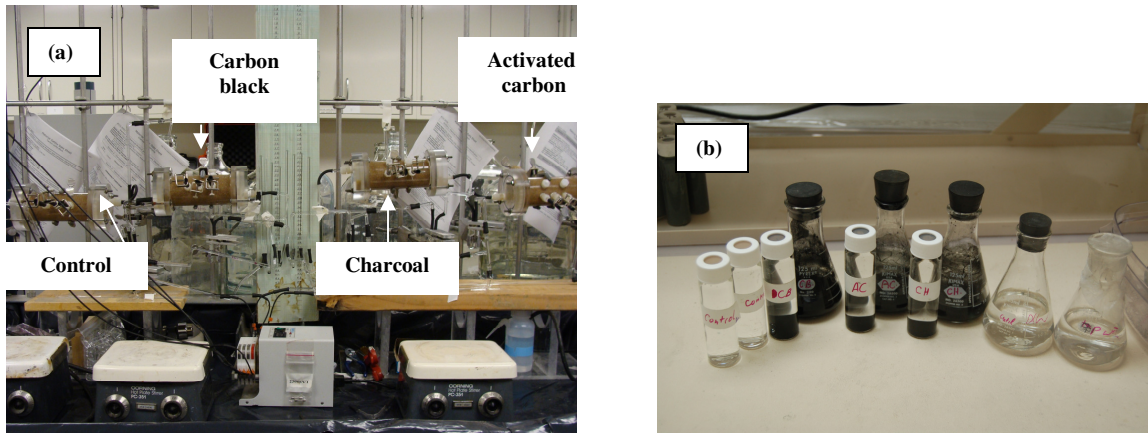


**Figure 23- a) Carbon deliverability column experiment, b) Carbon types redox poise vial study**

#### 4.2.2.2 Results

Delivery of carbon in sand columns was not successful (Figure 24). For all three carbon materials, the influent pores clogged. Pressure climbed quickly and fittings connecting glass tubings failed due to high hydraulic pressure. A similar problem was also observed by Vagharfard (2001) feeding a sand column with activated carbon. Post delivery, the carbon contents of activated carbon, carbon black and charcoal columns were 5.3, 3.8, and 8.4 (gm OC/Kg soil), respectively. It should be noted that the higher amount of carbon in charcoal column may have resulted from inclusion of the carbon that was washed off from the entrance wall of the column.

Activated carbon      Carbon black      Charcoal

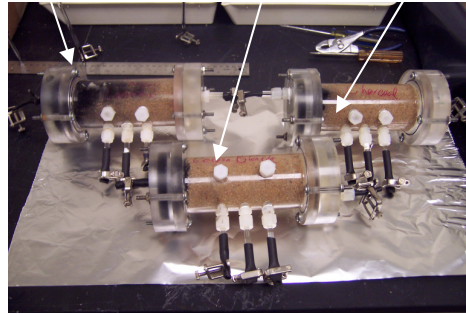


Figure 24- Clogged columns after carbon delivery

No consequential Eh or pH shifts were observed in any of the carbon water slurries in the anaerobic chamber (Figure 25). In general, the ORP probe performed poorly in carbon solutions (e.g. drifting, non-repeatable measurements).

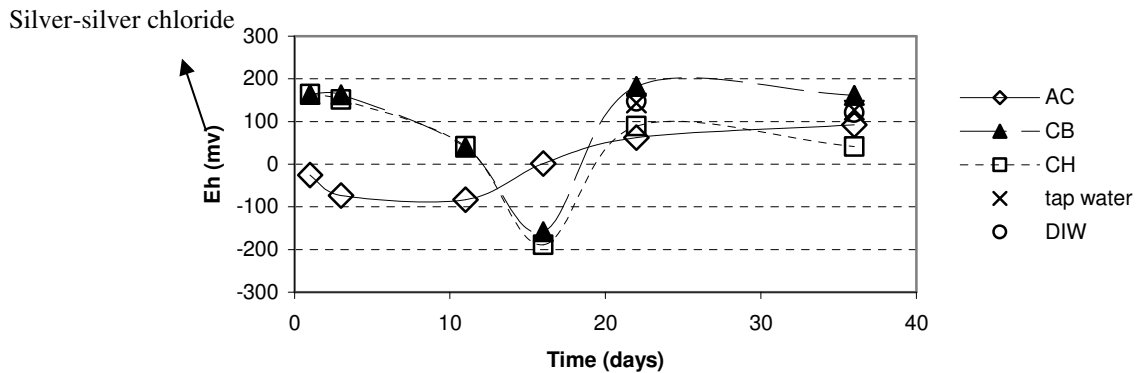
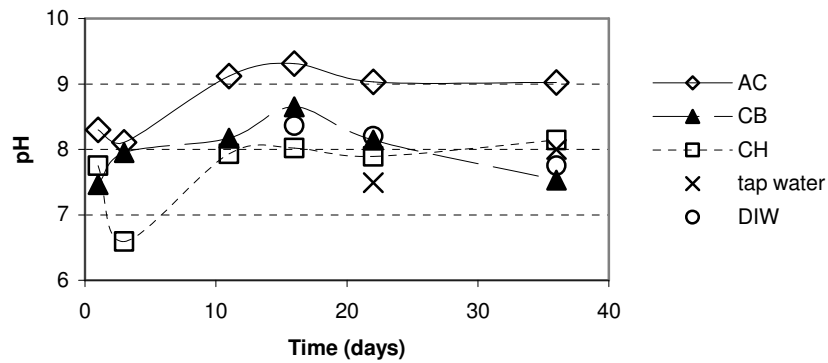


Figure 25- pH and Eh data of carbon types vs. time

Our assumption is that the solutions lacked a measurable redox couple. The IC and GC results show that most of the TCE is sorbed to carbon from the aqueous phase and no significant amount of chloride is produced by carbon types.

### **4.2.3 Summary of carbon sequestration approach**

Carbon black, activated carbon and charcoal, all held promise as options for carbon sequestration. Laboratory studies were performed to investigate deliverability of the carbon types in porous media and also to resolve if they poise redox or not. Delivery of carbon in sand columns resulted in clogging the influent pores that hindered a successful delivery. No Eh or pH shifts were observed in any of the carbon water slurries in the anaerobic chamber, either. Based on these likely flaws, use of carbon sequestration for management of contaminants in low permeability zones seems to have limited feasibility.

## **4.3 Sonication**

### **4.3.1 Overview**

*Description.* Sonication involves ultrasonic compression waves imparting through water. Ultrasound sound has a higher frequency that is not audible to human. The speed of ultrasound does not depend on its frequency but on what material it is traveling through. For instance, ultrasound waves travel faster in dense materials and slower in compressible materials.

The vision of this approach is to induce high frequency pressure waves in water in porous media. The processes would involve emplacing wells in a pattern through a plume and operating sonication tools in the wells for a sufficient time, perhaps several

days. The hope is that effects of sonication could be sweep through a plume (via application of many holes) over a period of a few months. The inspiration for this approach comes from:

- Use of sonication equipment to clean glassware at a laboratory scale
- Commercial efforts to enhance LNAPL (Light Non-Aqueous Phase Liquid) recovery using sonication (Wavefront Energy and Environmental Services Inc.).
- Comments from Dr. Art Corey (CSU faculty emeritus) regarding removal of fine particulate from laboratory core samples using sonication.

At a laboratory-scale, sonication systems are widely used in contaminant extractions from soils and for cleaning glassware. Also, high frequency sonication is widely used to accelerate settlement of concrete in forms.

*Mechanisms.* Relative to our interest, three potential mechanisms have been identified that could drive treatment of TCE. These include:

- **Cavitation** – Compression waves can cause localized formation of gas bubbles. With these gas bubbles localized, temperatures of 4,000 to 5,000 K can be achieved. This can pyrolyze compounds, especially more volatile ones that enter the vapor phase of the bubble. Once a radical is generated via pyrolysis, it can react with oxygen to initiate free radicals such as  $H^{\bullet}$ ,  $OH^{\bullet}$ ,  $HO_2^{\bullet}$ , and  $O^{\bullet}$ . (Maynard 2000). The radicals can either react with each other or diffuse into the surrounding liquid to act as oxidants. The presence of oxygen greatly enhances the formation of radicals since it acts as a scavenger for hydrogen radicals to form  $HO_2^{\bullet}$ , thus inhibiting the recombination of  $H^{\bullet}$  and  $OH^{\bullet}$  (Adewuyi 2001). Beside

radical reactions, pyrolytic decomposition and supercritical water oxidation lead to the destruction of organic compounds (Hoffmann, Hua et al. 1996).

- **Differential compression** – Our hypothesis is that low permeability layers may be more prone to cyclic compression than transmissive zones. With this, sonication might actually drive advective flow of water from low permeability layers to transmissive layers. The analogy here is that low permeability layers may be like a hose in a peristaltic pump.
- **Enhanced reactions and/or desorption** – Energy imparted via sonication may increase collision between molecules and/or diffusion with a net benefit of enhanced rates of reactions and/or diffusion. Little is known about these processes.
- **Microstreaming** – Sonication has two important physical effects in heterogeneous systems, i.e. systems where solid particles are present. First, when a cavitation bubble collapses symmetrically, shock waves are produced which can create microscopic turbulences in nearby films surrounding solid particles (such as sorbed contaminants). This effect is called microstreaming and leads to an increase in mass transfer of the sorbed phase (Elder 1959). Secondly, near a solid surface, the bubble will collapse asymmetrically, forming a microjet perpendicular to the solid surface. This microjet has an estimated velocity of 100 m/s and causes pitting, erosion, and breakup of the adjacent particle and consequently a larger contact area (Adewuyi 2005) (Thompson and Doraiswamy 1999).

*Potential Performance.* Kim and Wang (2003) found out that the rate of contaminant extraction increased considerably with increasing sonication power up to the level where cavitation occurred. A similar cavitation effect on oil flow through sandstone was also reported by Fairbanks and Chen (1971), and by Kim and Wang (2003). They also showed that the effectiveness of sonication is inversely related with  $(D_{10})^2 * i$ , in which  $D_{10}$  is the effective grain size and  $i$  is the hydraulic gradient. Therefore, the effectiveness of sonication in contaminant removal is greater at lower hydraulic gradient (flow rate and discharge velocity). With sonication, the influence of soil density on contaminant removal seems to be less significant than when sonication is not utilized. Also, Reddi and Challa (1994) and Reddi and Wu (2008) presented that ultrasonic waves can increase not only the mobility of NAPL ganglia but the porosity of the soil as well, resulting in a decrease in viscosity and buoyant pressure. Ellen and Lansink (1995) also observed a 30% increase in contaminant (diesel oil) extraction due to acoustic excitation. Another study by Iovenitti et al. (1995) reported a 6% to 26% improvement in contaminant extraction. The efficiency of ultrasonic processes strongly depends on several physicochemical properties and the aqueous medium's solutes. Some of the most important factors are listed in Table 3.

Sonochemistry has the appealing attribute that no chemicals need to be delivered to achieve contaminant destruction. Although strong oxidants such as hydroxyl radicals are produced, the amount generated is relatively small and can be dosed more accurately compared to the application of Fenton's reagent, where hydroxyl radicals are typically applied in vast excess. Oxidation induced by ultrasound is about 10,000 times faster than natural aerobic oxidation (Koskinen, Sellung et al. 1994). Furthermore, sonochemistry is

independent of the target compound concentration, whereas biodegradation, for example, can be inhibited by substrate concentrations that are too low (Adewuyi 2001).

To our knowledge, sonication has not been applied for *in situ* groundwater aqueous phase contaminant remediation yet; however, it has proven to be useful in large scale wastewater cleanup as well as in a pilot plant scale using a 30% slurry of river sand spiked with 1,2,3,4-tetrachloronaphthalene (Collings, Gwan et al. 2007).

**Table 3- Influences of cavitation and aquasonolysis and their respective effects (After confidential Center for Contaminant Hydrology document written for GE).**

Parameter	Effect	Reference
<b>Device-related Parameters</b>		
frequency	increase leads to decrease in bubble size and collapse time; there are different frequency optima for different compounds: for volatile compounds ca. 300-800 kHz, for non-volatile compounds around 200 kHz	[Lifka et al. 2002]
power	increase leads to increase in degradation up to a certain maximum	[Lifka et al. 2002]
mode of operation	pulsed ultrasound allows for after-reactions and can enhance efficacy dramatically; however, if pulses are too short, they will not have any effect	[Casadonte et al. 2005] [Henglein 1987]
<b>Substance- and Environment-related Parameters</b>		
solvent	intensity of cavitation is benefited by using solvents with opposing characteristics such as low vapor pressure but high viscosity and high surface tension	[Thompson & Doriaswamy 1999]
solute volatility	highly volatile compounds enter the bubble interior and are thus predominantly destroyed pyrolytically; compounds of low volatility are mainly attacked by radicals in the bubble interface and surrounding bulk liquid	[Lifka et al. 2002]
ambient temperature	increase leads most often to decrease in degradation rates; however, for volatile compounds an optimal ambient temperature of 60 °C was reported	[Lifka et al. 2002] [Thompson & Doriaswamy 1999]
ambient pressure	increase leads to increase in degradation rates up to a maximum; further increase decrease degradation rates by inhibiting cavitation	[Thompson & Doriaswamy 1999]
dissolved gases	act as nucleation sites and facilitate bubble production; however, the type of gas is important: most efficient are gases with high solubilities, high specific heat ratios, and low thermal conductivities	[Lifka et al. 2002] [Thompson & Doriaswamy 1999]
particle concentration	increase leads to decrease in degradation rates	[Lu & Weavers 2002]
humic acid concentration	increase leads to decrease in degradation rates	[Lu & Weavers 2002]
free radical scavenger concentration	increase leads to decrease in degradation rates	[Lifka et al. 2002] [Zhang et al. 2004]

### 4.3.2 Sonication laboratory studies

The following bench experiment was performed to evaluate if sonication enhances *in situ* degradation of TCE. Topic addressed includes experimental methods, results, and conclusions.

#### 4.3.2.1 Methods

Eighteen 20-mL crimp-cap-top glass vials were filled with deionized water (DIW) saturated with TCE. Triplicate sets of vials were sonicated for 1, 2, 4, 8 and 12 hours. Three vials were not sonicated to serve as control. Tap water was circulated into the tub to limit heatings to 104° F. The sonication bath used was an ANALOG AQUAWAVE™ 9376. Samples were analyzed for TCE using a Hewlett Packard 5890 gas chromatograph (GC) and chloride using a METROM 681 ion chromatograph (IC).

#### 4.3.2.2 Results

Figure 26 presents TCE and chloride concentration in the sonicated vials and the controls. The primary feature of the chloride data is that sonication resulted in minor chloride generation. Unfortunately, the observed chloride levels are small relative to the total chlorine present in TCE. Also, the results of the triplicates have large variations. This could be due to non-uniform sonication energy in the sonication tub or TCE loss due to sonication heating.

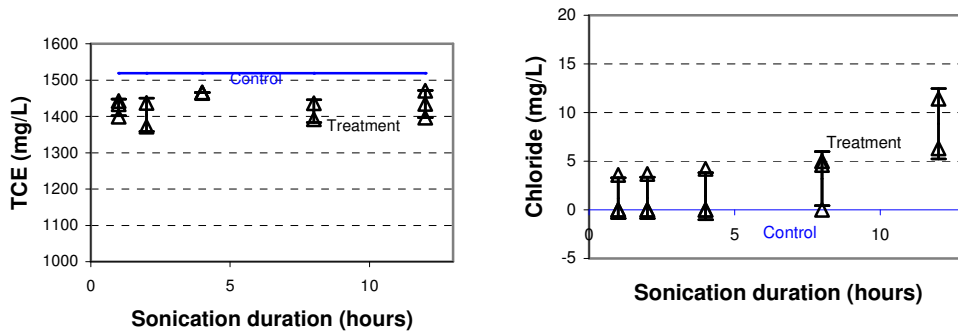


**Figure 26- TCE and chloride concentration from sonication triplicate vials (one standard deviation bars are depicted on the graphs)**

### 4.3.3 Summary for sonication

The vision of sonication was to induce high frequency pressure waves in water in porous media that drive degradation of TCE in transmissive and low permeability zones. A primary appeal of sonication is its potential to address contaminants in low permeability zones. Our primary concern was the feasibility of driving beneficial reactions at significant distances from the sonication source. Initial sonication vial studies involving TCE solutions indicated increase in chloride level with sonication. Unfortunately, the amounts of chloride produced were small and were not reproducible. Part of the TCE losses might have been due to heating from sonication. Overall, the feasibility of driving TCE depletion at consequential distances from a sonication source appears to be low.

## 4.4 Calcium polysulfide (CPS)

### 4.4.1 Overview

A number of researchers including Wilson et al. (2000), Lee and Batchelor (2002) have demonstrated that chlorinated solvents will react abiotically with naturally-occurring iron sulfide minerals. Hassan et al. (1995) and Sivavec et al. (1995) also reported transformation of TCE and PCE in presence of iron sulfide minerals. Key references on this topic include Butler (1999), Weerasooriya and Dharmasena (2001) and Kennedy et al. (2006). The fact that natural iron sulfide species can deplete chlorinated solvents leads to the question of whether it might be possible to flush aquifers with sulfide-iron solutions that would lead to precipitation of reactive sulfide on the solid media in transmissive zones. Precipitates of this nature are commonly observed at petroleum hydrocarbon sites with high background levels of sulfate that are subsequently reduced to sulfide (Sale, 2010, personal communications).

The method envisioned herein for applying the treatment is concurrent injection of solutions of ferrous chloride and calcium polysulfide (CPS). Ferrous chloride ( $\text{FeCl}_2$ ) provides  $\text{Fe}^{+2}$  and is routinely used in water treatment. CPS provides reduced sulfur and is a common soil amendment. Both CPS and  $\text{FeCl}_2$  are inexpensive. The hope is that the mixed solution can easily be emplaced into transmissive zones and that precipitation reactions will not cause adverse plugging of the formation.

Mechanisms of action include:

- Depleting aqueous and sorbed phase contaminants in transmissive zones via reductive dechlorination

- Enhanced back diffusion of contaminants (dissolved and sorbed phases) from low permeability zones

The most appealing aspect of this technology is that it is potentially low cost. Challenges include delivery of the solution without plugging the formation, formation of a reactive precipitate, and the longevity of the treatment. The following sections describe three preliminary laboratory experiments performed to resolve applicability of calcium polysulfide for treating trichloroethylene (TCE).

#### **4.4.2 Calcium polysulfide laboratory studies**

Laboratory studies were conducted to evaluate the redox poise of CPS and its deliverability. Four experiments envisioned to meet those goals are: 1) short term proof of concept, 2) TCE degradation through CPS only, 3) TCE degradation through FeCl<sub>2</sub> activated CPS and 4) Deliverability of CPS. Each of the experiments includes methods and results sections.

##### *4.4.2.1 Short term proof of concept*

In order to apply iron sulfide as a treatment agent for chlorinated solvents in the subsurface, this proof of concept experiment was conducted. This experiment evaluated degradation of TCE through ferrous chloride activated CPS. For simplicity, the experiment was performed in aqueous phase rather than the porous media. The duration of the experiment was one week.

##### *4.4.2.1.1 Methods*

Three 40 mL glass vials were prepared adding 4.5, 9.0 and 13.5 gm/L of ferrous chloride (Fisher Scientific) and 86 gm/L of calcium polysulfide (Bonide Production Inc., 29% calcium polysulfide) in anaerobic chamber. Three iron sulfide controls were also

prepared with 4.5, 9.0 and 13.5 gm/L of ferrous chloride and 86 gm/L of calcium polysulfide in deionized water (DIW) only. Other control vials included TCE saturated solution, DIW and tap water (Figure 27). The pH and Eh of these vials were recorded for a couple of months. Saturated TCE solution (prepared in DIW) was added to the vials when the pH-Eh curves reached a steady line. After a week, vials were analyzed for TCE and chloride concentration using METROM 681 IC and a Hewlett Packard 5890 GC.



**Figure 27- From left to right: two saturated TCE solution controls, three iron sulfide vials, DIW and tap water controls in anaerobic chamber**

#### *4.4.2.1.2 Results*

The pH and Eh of the iron sulfide vials are illustrated in Figure 28. The very low Eh observed (about -500 mV, Ag-AgCl) indicates a reduced environment that could be favorable for reductive dechlorination of TCE.

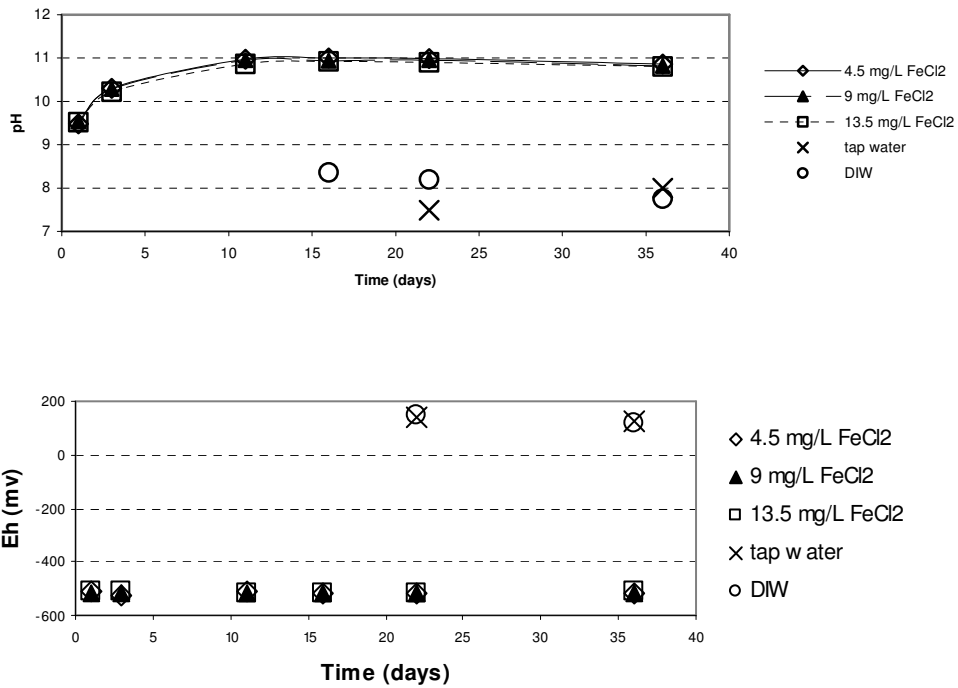


**Figure 28- PH and Eh (silver-silver chloride) of iron sulfide vials in anaerobic chamber**

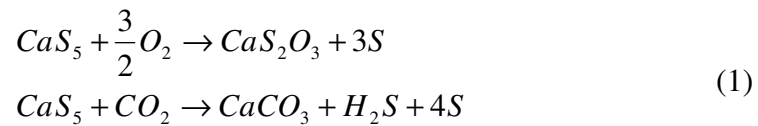
As demonstrated in Table 4 there is an average of 1.7 times more chloride and 0.7 less TCE in test vials, compared to the controls. Based on the results from this experiment, a secondary experiment was proposed considering only calcium polysulfide as the treatment (See section 0).

**Table 4- Chloride and TCE results of the preliminary CPS experiment**

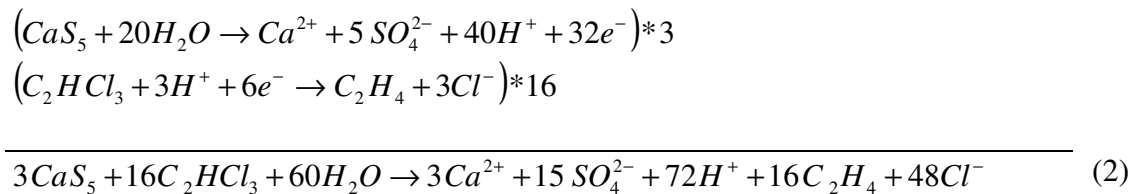
vial name	Chloride (mg/L)		TCE (mg/L)	
	Control	Test	Control	Test
IS-1	826	1635	1950	1492
IS-2	1932	2647	1945	1470
IS-3	2505	4326	1944	1586

#### 4.4.2.2 TCE degradation through CPS only

The objective of this experiment was to examine whether calcium polysulfide alone enhances *in situ* degradation of TCE in transmissive and low permeability zones. Calcium polysulfide has been used for removal of heavy metals from wastewater. Calcium polysulfide solution decomposes slowly in contact with air and produces calcium thiosulfate, hydrogen sulfide and solid sulfur (Yahikozawa et al. 1978 and Wazne et al. 2007). The principal reactions of calcium polysulfide decomposition by carbon dioxide and oxygen can be represented as the following equation:



What we are interested in is the reaction of calcium polysulfide with TCE, which does not necessarily follow the above pathway. Assuming that all the sulfur is oxidized to sulfates, the proposed reaction mechanism is as follows:



Therefore, measurement of reduced TCE, generated chloride, and generated can test our hypothesized reaction.

#### *4.4.2.2.1 Methods*

To find out if the reaction environment is going to be favorable having CPS only, CPS (Bonide Production Inc.) was added to DIW using a burette in 0.05 mL droplets and their relevant pH and Eh were recorded (CPS titration). The pH-Eh data is illustrated in Figure 29.

Based on the achieved pH-Eh graph, dilution factors of 1, 5, 25, 150, 300 and 600 times the stoichiometric amount of CPS required for degrading 20 ppm of TCE (Equation 2) were chosen for the experiment. These dilution factors are relevant to 6, 30, 149, 893, 1787 and 3575 ppm of CPS, respectively. Consequently, a set of 20 mL glass vials were filled with CPS (6, 30, 149, 893, 1787 and 3575 ppm), TCE saturated solution (20 ppm) and topped off with de-aired DIW solution containing 100 mg/L sodium bicarbonate. Each concentration category consisted of 15 vials (triplicates for 5 sampling times) to minimize error. The sampling times were 2 hours, 1 day, 7, 21 and 42 days after the start of the experiment. For each sampling time, 6 control vials were considered too (3 vials as TCE control and 3 vials as CPS control). The TCE control vials contained 20 ppm TCE saturated solution in DIW. The CPS control vials contained 30 ppm CPS (for test vials with 6, 30 and 149 ppm CPS) and 1787 ppm CPS (for test vials with 893, 1787 and 3575 ppm CPS) in DIW. Samples were analyzed for TCE using a Hewlett Packard 5890 gas chromatograph (GC) and chloride using a METROM 681 ion chromatograph (IC).

#### *4.4.2.2.2 Results*

Figure 29 presents the pH-Eh results of CPS titration which indicates that CPS is active in a wide range of concentrations. TCE and chloride results of the vial study are

illustrated in Figure 30. Initial data points (less than 7 days) show variability due to different sampling procedure.

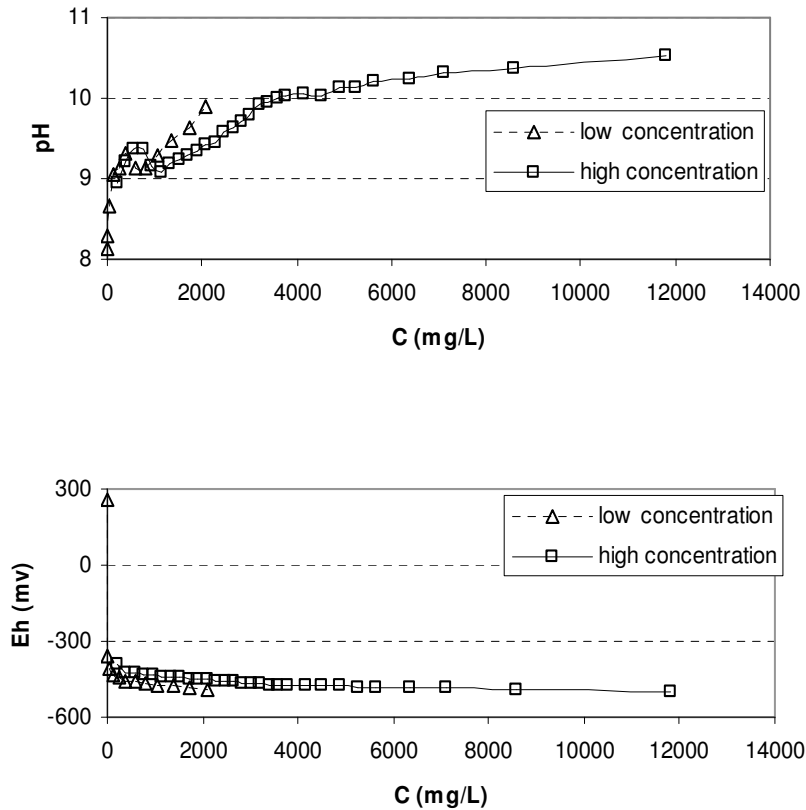


**Figure 29- Titration of calcium polysulfide: pH data Eh data (mV of silver-silver chloride)**

Even the highest CPS concentration vial (Figure 30, panel I) does not achieve significant lower TCE concentration than controls after up to 42 days (same result for all levels of CPS up to 3575 mg/L). Generated chloride in the highest CPS concentration (Figure 30, panel J) is also about 3% of the expected stoichiometric amount (16 mg/L). The bottom-line of Figure 30 is that iron seems to be the key missing ingredient. Therefore, to demonstrate if iron sulfide enhances *in situ* degradation of TCE in transmissive and low permeability zones the following experiment was conducted.

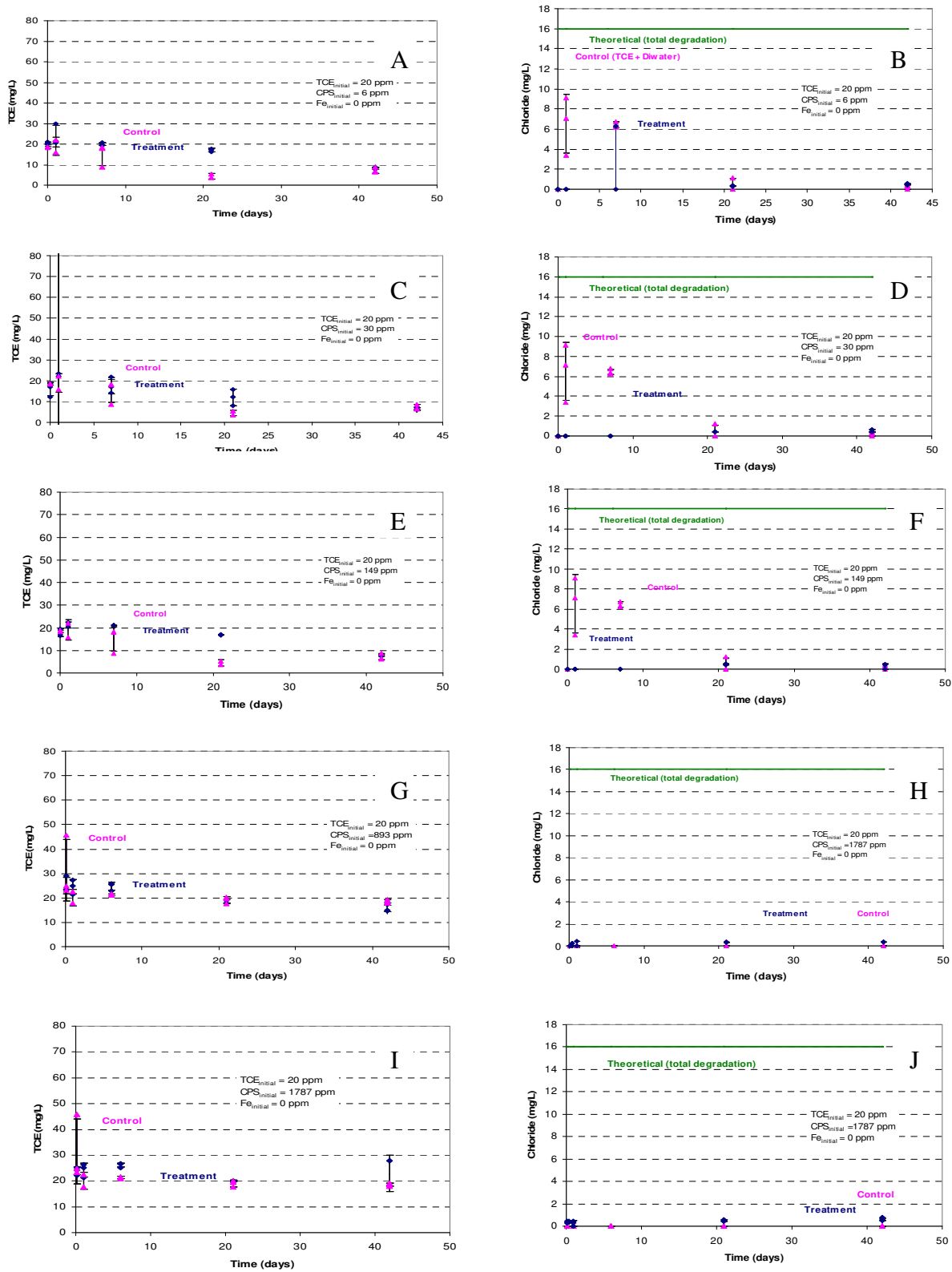
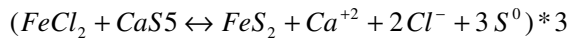
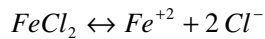
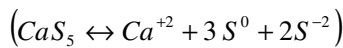


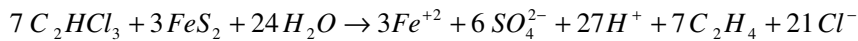
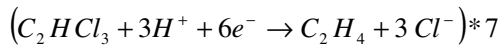
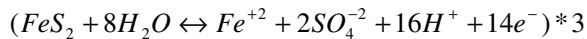
Figure 30- TCE (on left) and chloride (on right) concentration in CPS vials with time.

#### 4.4.2.3 TCE degradation through FeCl<sub>2</sub> activated CPS

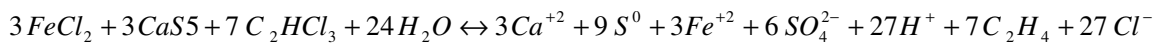
No significant amount of chloride was generated in section 0 experiment (which examined degradation of TCE through CPS only). Therefore, it was concluded that for efficient reaction of CPS with TCE, iron is the key element. Therefore, the objective of this experiment was to investigate the effect of adding iron to the previous experimental setup (section 0). The difference between this experiment and the one in section 0 is that here lower CPS concentrations were utilized. It was hypothesized that the reaction will proceed as follows:



Reduction of TCE :



Adding up the two above equations together we will have :



##### 4.4.2.3.1 Methods

The experiment involved a triplicate set of 20 mL glass vials containing FeCl<sub>2</sub> (Fe<sup>+2</sup>: 44, 248 and 992 ppm), CPS (149, 893 and 3575 ppm) and TCE saturated solution (10 ppm) and topped off with de-aired DIW solution containing 100 mg/L sodium bicarbonate. Each concentration category consisted of 9 vials (triplicates for 3 sampling

times) to minimize error. The sampling times were 1 day, 3 and 7 days after the start of the experiment. For each sampling time, 9 control vials were considered (6 vials as TCE control and 3 vials as CPS control). Three TCE control vials consisted of vials filled with 10 ppm TCE saturated solution in DIW. The other three vials contained 10 ppm TCE saturated solution and 2250 ppm  $\text{FeCl}_2$ . The CPS control vials contained 3575 ppm CPS DIW. The vials were analyzed for TCE using a Hewlett Packard 5890 gas chromatograph (GC) and chloride using a METROM 681 ion chromatograph (IC).

#### *4.4.2.3.2 Results*

As illustrated in Figure 31, at short times CPS-iron seems to achieve ~ 30 -40% TCE degradation (consistent with the results of the experiment in 0). At later times, data is hard to explain. Noise levels and TCE results of all three CPS levels tested (Figure 31: panels A, B and C) were consistent. Chloride levels were not measurable due to high chloride background resulting from  $\text{FeCl}_2$ .

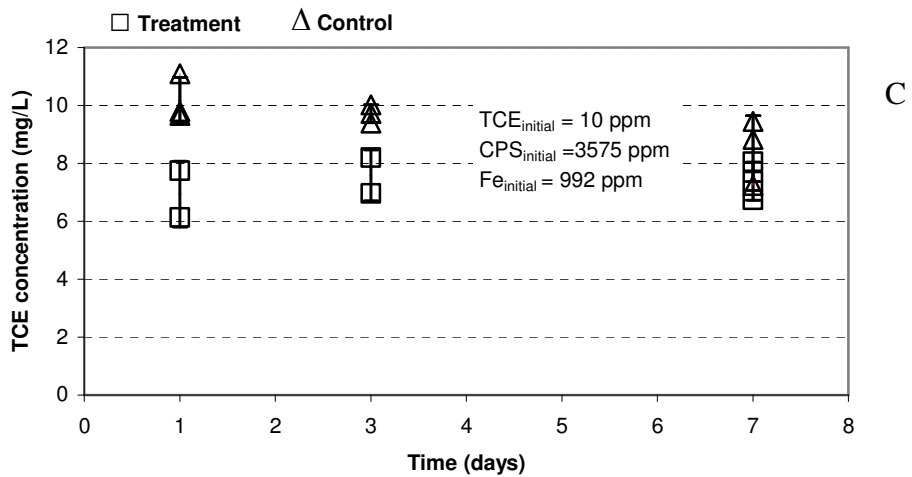
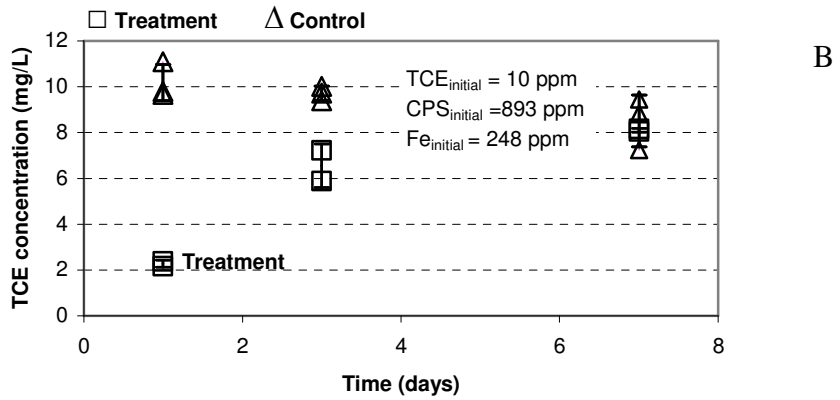
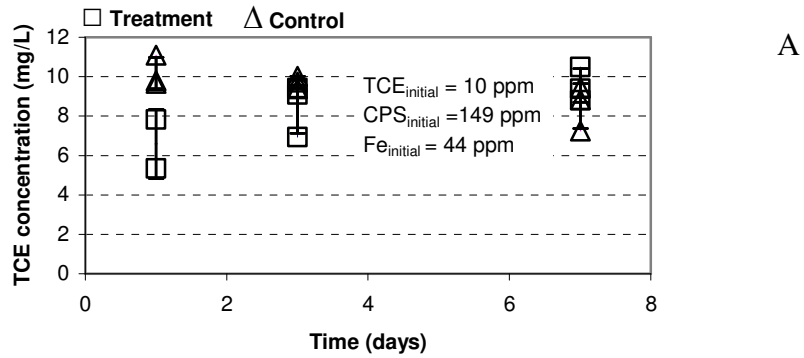


Figure 31- TCE concentration with time: A) CPS (149 ppm) +FeCl<sub>2</sub> (44 ppm), B) CPS (893 ppm) +FeCl<sub>2</sub> (248 ppm) and C) CPS (3575 ppm) +FeCl<sub>2</sub> (992 ppm)

#### 4.4.2.4 Deliverability of CPS

The purpose of this experiment was to investigate whether CPS is deliverable in porous media or not. A column study was conducted as follows, similar to carbon sequestration column study, to resolve this issue.

##### 4.4.2.4.1 Methods

A cylindrical acrylic column (with inside diameter and length of 2” and 6” respectively) was packed with medium to coarse quartz-feldspar sand (Figure 32). The porosity and hydraulic conductivity of the material were 0.345 and 0.035 cm/s, respectively.

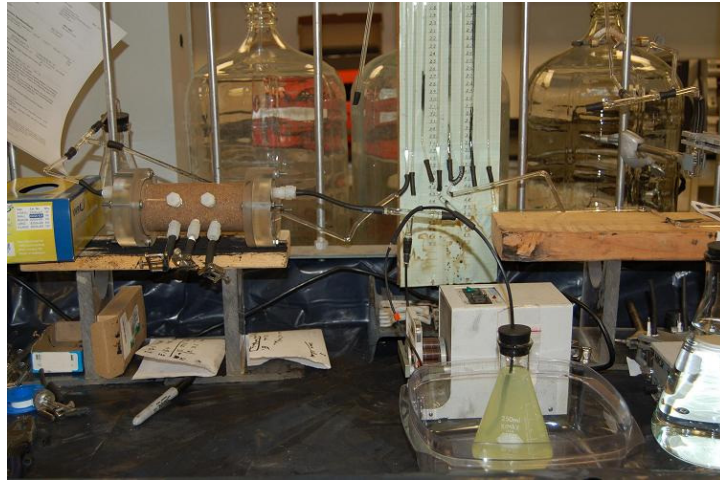


**Figure 32- Deliverability of CPS solution column study**

DIW with 80 mg/L  $\text{Na}_2\text{SO}_4$  (Fisher Scientific) and 20 mg/L  $\text{Na}_2\text{HPO}_4$  (Fisher Scientific) was flushed through the column (positioned vertically) from the bottom using a four-channel ISMATEC peristaltic pump for a week at 1 ft/day (pump speed of 3.2) to fully saturate it. A solution of 76 mg/L CPS was prepared using DIW in a 250 mL Erlenmeyer flasks containing a magnetic stir bar, sitting on a stir plate. The solution was

pumped into the column (positioned horizontally) through viton tubings at a flow rate of 2 ft/day. Throughout the test, head loss across the column was measured as a function of time using 1 m manometer tubes.

#### *4.4.2.4.2 Results*

Delivery of CPS did not cause any clogging. Therefore, CPS is deliverable in porous media.

#### **4.4.3 Summary of CPS approach**

CPS can be used to produce reactive iron sulfides and those iron sulfide minerals can drive treatment of TCE in low permeability zones. Results obtained from laboratory experiments showed reductions in TCE concentrations. Overall, considering effectiveness and deliverability CPS appears to be a promising option.

### **4.5 Conclusion**

In this chapter three innovative alternatives for managing contaminant stored in plumes were evaluated. A review of results of carbon sequestration, sonication and iron sulfides bench experiments were presented. Considering the delivery issues of carbon particle to porous media we decided to put carbon sequestration aside as an option. Considering the difficulties of implementing sonication under the ground, sonication does not appear to be a viable treatment option either. The results of this work imply that high sulfide concentrations might have caused sulfide toxicity to microorganisms resulting in an ineffective treatment. Therefore, path forward may include emplacing sulfate reducing bacteria along with biological electron donors (i.e., vegetable oil, lactate) to

promote competitive electron accepting with chlorinated solvents resulting in precipitating out sulfides.

## REFERENCES

- Adeyuyi, Y.G., 2001. Sonochemistry: Environmental science and engineering applications. *Industrial & Engineering Chemistry Research* 40, 4681-4715.
- Adeyuyi, Y.G., 2005. Sonochemistry in environmental remediation. 2. Heterogeneous sonophotocatalytic oxidation processes for the treatment of pollutants in water. *Environmental Science & Technology* 39, 8557-8570.
- Aktas, O., Cecen, F., 2006. Effect of type of carbon activation on adsorption and its reversibility. *Journal of Chemical Technology and Biotechnology* 81, 94–101.
- Butler, E. C., Hayes, K. F., 1999. Kinetics of the Transformation of Trichloroethylene and Tetrachloroethylene by Iron Sulfide. *Environ. Sci. Technol.* 33, 2021- 2027.
- Chapman, S.W. and B.L. Parker, 2005. Plume Persistence Due to Aquitard Back Diffusion Following Dense Nonaqueous Phase Liquid Removal or Isolation, *Water Resource Research* 41 (12), 4224-4235.
- Collings, A.F., Gwan, P.B., Pintos, A.P.S., 2007. Soil remediation using high-power ultrasonics. *Separation Science and Technology* 42, 1565-1574.
- Dondelle, M. M., Loehr, R. C., 2002. Comparison of Estimated and Experimentally Obtained Soil Water Distribution Coefficients. *Practice Periodical of Hazardous, Toxic, and Radioactive Waste Management* 6 (4), 218-226.
- Doner, L.A., 2008. Tools to resolve water quality benefits of upgradient contaminant flux reduction. MS thesis, Colorado State University, Fort Collins, COLORADO.
- Ellen, T.V., Lansink, C.J.E., 1995. Sandker, J.E., Acoustic soil remediation: introduction of a new concept. *Contaminated Soil* 95, 1193–1194.
- Elder, S. A., 1959. Cavitation Microstreaming. *Journal of the Acoustical Society of America* 31(1): 54-64.
- Fairbanks, H.V., Chen, W.I., 1971. Ultrasonic acceleration of liquid flow through porous media. *Chemical Engineering Progressive Symposium Series* 67, 108–116.
- Feenstra, S., Cherry, J.A., Parker, B.L., 1996. Conceptual Models for the Behavior of Dense Nonaqueous Phase Liquids (DNAPLs) in the Subsurface, Chapter 2 in Dense Chlorinated Solvents and Other DNAPLs in Groundwater, J.F Pankow and J.A. Cherry, Editors. Waterloo Press, pp. 53-88.
- Freeze, R.A., Cherry, J.A., 1979. Groundwater, Prentice Hall, Englewood Cliffs, NJ. pp. 410–413.

- Hassan, S. M., Wolfe, N. L., Cippolone, M. G. Preprints of Papers Presented at the 209th ACS National Meeting, April 2–7, 1995, Anaheim, CA; American Chemical Society: Washington, DC, 1995; Vol. 35, pp 735–737.
- Hoffmann, M.R., Hua, I., Hochemer, R., 1996. Application of ultrasonic irradiation for the degradation of chemical contaminants in water. *Ultrasonics Sonochemistry* 3, S163-S172.
- Ikuo, A., Satoshi, I., Yoshimi, I., Hiroshi, K., Yoshiya, K., 1998. Relationship between Production Method and Adsorption Property of Charcoal. *Tanso* 185, 277-284.
- Iovenitti, J.L., Rynne, T.M., Spencer, Jr., J.W. 1995. Acoustically enhanced remediation of contaminated soil and ground water, in: *Proceedings of Opportunity 95-Environmental Technology through Small Business*, Morgantown, West Virginia.
- Kennedy, L. G., Everett, J. W., Becvar, E., DeFeo, D., 2006. Field-scale demonstration of induced biogeochemical reductive dechlorination at Dover Air Force Base, Dover, Delaware. *Journal of Contaminant Hydrology* 88, 119-136.
- Kim, Y.U., Wang, M.C. 2003. Effect of ultrasound on oil removal from soils. *Ultrasonics* 41, 539–542.
- Koskinen, W.C., Sellung, K.E., Baker, J.M., Barber, B.L., Dowdy, R.H., 1994. Ultrasonic Decomposition of Atrazine and Alachlor in Water. *Journal of Environmental Science and Health Part B-Pesticides Food Contaminants and Agricultural Wastes* 29, 581-590.
- Lee, W., Batchelor, B. 2002. Abiotic Reductive Dechlorination of Chlorinated Ethylenes by Iron-Bearing Soil Minerals. 1. Pyrite and Magnetite. *Environ. Sci. Technol.* 36, 5147-5154.
- Li, L., Quinlivan, P.A., Knappe, D.R.U., 2002. Effects of activated carbon surface chemistry and pore structure on the adsorption of organic contaminants from aqueous solution. *Carbon* 40, 2085–2100.
- Liu, C., Ball, W.P., 2002. Back diffusion of chlorinated solvent contamination from a natural aquitard to a remediated aquifer under well-controlled field conditions: predictions and measurements. *Journal of Ground Water* 40, 175–184.
- Liu, G., Zheng C., Gorelick S., 2007. Evaluation of the applicability of the dual-domain mass transfer model in porous media containing connected high-conductivity channels, *Water Resource Research* 43, W12407, 12 pp.
- Luthy, R., 2007 (Stanford University), Personal communication at DuPont’s 2020 Remediation Meeting, Wilmington, Delaware.

- Luthy, R. G., Tomaszewski, J. E., 2006. Activated Carbon Treatment of Sediments Contaminated with Hydrophobic Organic Compounds, US Patent Application No. 11/512,740, August 29.
- Maynard, B.J. 2000. Sonochemistry. *Chemistry* 17-22.
- Nilsson, M.C., Wardle, D. A., DeLuca, T.H., 2008. Belowground and aboveground consequences of interactions between live plant species mixtures and dead organic substrate mixtures. *Oikos* 117, 439-449.
- Parker, B.L., Gillham, R.W., Cherry, J.A., 1994. Diffusive disappearance of immiscible-phase organic liquids in fractured geologic media. *Journal of Ground Water* 32, 805–820.
- Payne, F.C., Quinnan, J.A., Potter, S.T., 2008. *Remediation Hydraulics*. Boca Raton, Florida: CRC Press.
- Pietikäinen, J., Kiikkilä, O., Fritze, H., 2000. Charcoal as a habitat for microbes and its effect on the microbial community of the underlying humus. *OIKOS* 89, 231–242.
- Rao, P.S.C., Rolston, D.E., Jessup, R.E., Davidson, J.M., 1980. Solute transport in aggregated porous media: theoretical and experimental evaluation. *Journal of Soil Science of America* 44, 1139–1146.
- Reddi, L.N., Challa, S., 1994. Vibratory mobilization of immiscible liquid ganglia in sands. *Journal of Environmental Engineering* 120 (5) 1170–1190.
- Reddi, L.N., Wu, H., 2008. Mechanisms involved in vibratory destabilization of NAPL ganglia in sands. *Journal of Environmental Engineering*. 1996, 122 (12), 1115–1119.
- Sale, T.C., Illangasekare, T., Zimbron, J., Rodriguez, D., Wilkins, B., Marinelli, F., 2007. AFCEE Source Zone Initiative, Report Prepared for the Air Force Center for Environmental Excellence by Colorado State University and Colorado School of Mines.
- Sale, T. C., Zimbron, J., Dandy, D., 2008. Effects of reduced contaminant loading from analog DNAPL sources on downgradient water quality in an idealized two layer system, *Journal of Contaminant Hydrology* 102, 14, 72-85.
- Schwarzenbach, R. P., Gschwend, P. M., Imboden, D. M., 1993. *Environmental Organic Chemistry*, John Wiley & Sons, Inc.: New York, NY, 255-341.
- Schwarzenbach, R. P., Gschwend, P. M., Imboden, D. M., 2003. *Environmental Organic Chemistry*, John Wiley-Interscience, Inc.: New York, NY.

- Shackelford, C. D., Daniel, D. E., 1991. Diffusion in Saturated Soil. II: Results for Compacted Clay. *Journal of Geotechnical Engineering* 117 (3), 485-506.
- Sivavec, T.M., Horney, D.P., Baghel, S.S., 1995. In *Industrial & Engineering Chemistry Division*; Tedder, D. W., Ed.; American Chemical Society: Atlanta, GA, 1995; pp 42–45.
- Sudicky E.A., 1986. A natural gradient experiment on solute transport in a sand aquifer: Spatial variability of hydraulic conductivity and its role in the dispersion process. *Water Resour. Res.* 22, 2069-2082.
- Sudicky, E.A., Gillham, R.W., Frind, E.O., 1985. Experimental investigation of solute transport in stratified porous media 1. The nonreactive case, *Water Resources Research* 21(7), 1035–1041.
- Tang, D.H., Frind, E.O., Sudicky, E.A., 1981. Contaminant transport in fractured porous media: analytical solution for a single fracture. *Water Resources Research* 17, 555–564.
- Thompson, L.H., Doraiswamy, L.K., 1999. Sonochemistry: Science and engineering. *Industrial & Engineering Chemistry Research* 38, 1215-1249.
- Vagharfard, H., 2001. Permeability reduction in porous media due to suspended particles. Doctoral dissertation, Colorado State University, Fort Collins, COLORADO.
- Wardle, D. A., Nilsson, M.C., Zackrisson, O., 1998. Fire-derived charcoal causes loss of forest humus. *Science* 320 (5), p 629.
- <http://esciencenews.com/articles/2008/05/01/limitations.charcoal.effective.carbon.sink>
- Wardle, D.A., Zackrisson, O., Nilsson, M.C., 1998. The charcoal effect in Boreal forest: mechanisms and ecological consequences. *Oecologia* 115, 419-426.
- Wazne, M, Jagupilla, S.C., Moona, D.H., Jagupilla, C.S., Christodoulatos, C., Kimb, M.G., 2007. Assessment of calcium polysulfide for the remediation of hexavalent chromium in chromite ore processing residue (COPR). *Journal of Hazardous Materials* 143 (2007) 620–628.
- Weerasooriya, R., Dharmasena, B., 2001. Pyrite-assisted degradation of trichloroethene (TCE). *Chemosphere* 42, 389-396.
- Wilmanski, K., Van Breemen, A. N., 1990. Competitive Adsorption of Trichloroethylene and Humic Substances from Groundwater on Activated Carbon. *Water Research* 24(6), 773-779.

Wilson, J.T., Cho, J.S., Wilson, B.H., Vardy, J.A. 2000. Natural attenuation of MTBE under methanogenic conditions. US Environmental Protection Agency, Ada, OK.

Yahikozawa, K., Aratani, T., Ito, R., Sudo, T., Yano, T., 1978. Kinetic studies on the lime sulfurated solution (calcium polysulfide) process for removal of heavy metals from wastewater, *Bullet. Chem. Soc. Jpn.* 51 (1978) 613–617.

## **ONLINE REFERENCES**

International Carbon Black Association (ICBA), Carbon black user guide, 2004. [www.carbon-black.org](http://www.carbon-black.org) (accessed May 28, 2008).

ASTM COMMITTEE D24: Keeping the Rubber Industry in the Black, 1998. <http://www.astm.org/COMMIT/CUSTOM1/D24.htm> (accessed May 28, 2008).

Activated carbon particles, 2007. Dennis Kunkel Microscopy, Inc. <http://www.denniskunkel.com/DK/Miscellaneous/23836A.html> (accessed May 28, 2008).

Creek, D., Davidson, J. Granular activated carbon. National Water Research Institute. [www.nwri-usa.org/uploads/TT%20Chapter%204.pdf](http://www.nwri-usa.org/uploads/TT%20Chapter%204.pdf) (accessed May 30, 2008).

Ogawa, M. Charcoal characteristics and uses, 2008. Information on the intentional use of Biochar (charcoal) to improve soils. <http://terrapreta.bioenergylists.org/charcoaluses> (accessed June 10, 2008).

MISONIX, How does a sonicator work? [www.sonicator.com/pdf/Howdoesitwork.pdf](http://www.sonicator.com/pdf/Howdoesitwork.pdf) (accessed June 15, 2008).

## **Chapter 5**

### **SUMMARY OF RESULTS AND RECOMENDATIONS FOR FUTURE WORK**

Over the last decade there has been growing recognition that contaminants stored in low permeability layers in source zones and plumes can sustain dilute groundwater plumes long after sources in transmissive zones are depleted. Unfortunately, this scenario implies the potential need for multiple decades of plume management and monitoring at thousands of sites.

The overarching goal of this research was to resolve feasibility of treating contaminants stored in low permeability zones in sandy aquifers. Three studies were undertaken including:

1. Modeling the evolution of a chlorinated solvent release to evaluate temporal and spatial evolution of contaminant phases (Chapter 2)
2. Laboratory studies demonstrating the use of alkaline sodium persulfate to treat contaminants stored in low permeability zones (Chapter 3)
3. Exploration of three innovative solutions (sequestration, sonication, and calcium polysulfide) for managing contaminat in low permability zones (Chapter 4)

The following presents a summary of each chapter and suggestions for future work of each activity.

## **Chapter 2: Modeling Release Evolution**

*Objective:* The objective of this activity was to elucidate the evolution of subsurface releases of chlorinated solvents using analytical solutions for a two-layer system.

*Method:* This study addressed a two-layer system involving semi-infinite transmissive and low permeability zones using analytical solutions developed in Sale et al. (2008). The study addressed perchloroethene contaminant mass present in transmissive and low permeability zones. All calculations were carried out using Mathcad<sup>TM</sup> 14. An important constraint to using the Sale et al. (2008) Mathcad worksheet is the challenge of applying the solution to plume lengths greater than 100 m in transmissive zone. To overcome the challenge a hybrid approach was developed wherein a series approximation was used for portions of the domain where the Sale et al. (2008) Mathcad worksheet is inaccurate. The hybrid approach also has a limited domain of application. In the end, the manuscript relies on the low permeability zone solution, which can be applied at large domains. Contaminant mass in transmissive zones was estimated as the difference between the mass released from the source and the mass in the low permeability zone.

*Results:* The hypothesis that chlorinated solvent releases can evolve with time has been validated. In particular, through time, the nature of the problem changed from DNAPL in the transmissive layer to that of aqueous and sorbed contaminants in the low permeability layer. Another result of this research is that retardation in the low permeability layer controls contaminant mass stored in the low permeability layer at late time. At the end of the loading with no retardation in the low permeability zone, 32% of

the released contaminant was present in the low permeability layer. Given a retardation factor of 10 in the low permeability zone, 58% of the released contaminant was present in the low permeability layer. Moreover, estimate of PCE distribution in low permeability zone as a function of position suggests that even at late stages much of the contaminant mass in the low permeability zone remains in proximity to the DNAPL source. This suggests that the domain in which contaminant in low permeability zone needs to be treated is a subset of the overall plume.

*Limitations:* The analytical modeling relies on simplified assumptions. Some of the assumptions include a homogeneous, isotropic, 2-D two-layer system with no degradation. Therefore, the results may not be applicable to more complex systems.

*Suggestions for future work:* A similar study could consider more elaborate settings such as a multi-layer system with degradation.

### **Chapter 3: Laboratory Studies Addressing Effects of Alkaline Persulfate Flushing on Contaminants Stored in Low Permeability Zones**

*Objective:* The objective of this activity was to evaluate alkaline persulfate flushing as an option for mitigating contaminant release from low permeability zones.

*Method:* This research presented a conceptual model and laboratory-scale sand tank experiment that addresses storage, release, and treatment of contaminants in low permeability zones. The experiment involved transmissive sand with interbedded low permeability clay layers. Fluorescein and bromide were employed as reactive and conservative contaminants. Data from the experiment include photographic images,

fluorescein and bromide tank effluent concentrations, and spectrometer-based point measurement of fluorescein concentrations in the sand and clay layers.

*Results:* The results from the experiment suggest that an alkaline persulfate flood is a viable means (on a laboratory scale) of depleting fluorescein in low permeability zones. Specifically, results indicate a no-rebound response to treatment, in which fluorescein concentrations in low permeability layers are depleted sufficiently to preclude consequential releases from low permeability zones.

*Limitations:* In spite of promising results of this research they may not be representative of the field-scale. Promising results are balanced firstly by concerns that ideal aspects of the study created more favorable results than might be attainable under common field conditions, and secondly by concerns that water quality impacts of the high TDS, high pH solution could be unacceptable at many field sites. Other constraints could be soil oxidant demands in natural porous media, challenges of delivering a high-density solution to a desired target, and uncertainties regarding treatment of less reactive contaminants.

*Suggestions for future work:* Building on this work, future research could explore the use of high-resolution numerical modeling techniques to address transport of contaminant and reactants in systems where advection, diffusion, retardation and reaction are primary transport processes. Critically, this research provides a data set that can be used to test models addressing concurrent transport of contaminants and reactants.

## **Chapter 4: Potential of Three Innovative Approaches for Treating Trichloroethene in Low Permeability Zone**

*Objective:* The objective of this activity was to explore the potential of three innovative treatment approaches for *in situ* treatment of trichloroethene (TCE) in low permeability zones. Options considered include: carbon sequestration, sonication, and calcium polysulfide (CPS).

*Method:* Column studies were performed to investigate deliverability of three carbon types in porous media and also vial studies were conducted to resolve if conditions favoring reductive dechlorination were imposed. The effectiveness of sonication was evaluated through a series of vial studies involving TCE solutions as the target contaminant. To investigate if CPS forms reactive sulfide precipitants a series of vial studies were undertaken using a range of CPS concentrations. Subsequently, a column study was conducted to examine the deliverability of CPS in porous media.

*Results:* Delivery of carbon in sand columns resulted in clogging the influent pores precluding effective delivery. Furthermore, no evidence was developed to support the research hypothesis that carbon could poise a redox condition that would drive reductive dechlorination of TCE. Initial sonication studies involving TCE solutions indicated that chloride level could be increased with sonication. Considering the difficulties of implementing sonication under the ground, sonication does not appear to be a viable treatment option, either. Results obtained from laboratory experiments show that CPS imposed a redox condition of -500 mV (Ag-AgCl) and drove partial reduction of TCE.

*Suggestions for future work:* The outcome came from this work implies that high sulfide concentrations might have caused sulfide toxicity to microorganisms resulting in an ineffective treatment. Therefore, the path forward may include emplacing sulfate-reducing bacteria along with biological electron donors (i.e., vegetable oil, lactate) to promote competitive electron accepting with chlorinated solvents resulting in precipitating out sulfides.

## **REFERENCE**

Sale, T. C., Zimbron, J., Dandy, D., 2008. Effects of reduced contaminant loading from analog DNAPL sources on downgradient water quality in an idealized two layer system, *Journal of Contaminant Hydrology* 102, 14, 72-85.

## LIST OF ABBREVIATIONS

ATSDR: Agency for Toxic Substances and Disease Registry

CCOHS: Canadian Centre for Occupational Health and Safety

CMR: Chemical Marketing Reporter

CNS: Central Nervous System

CPS: Calcium Polysulfide

DIW: Deionized Water

DNAPLs: Dense Non-Aqueous Phase Liquids

EPA: Environmental Protection Agency

ESTCP: Environmental Security Technology Certification Program

GC: Gas Chromatograph

IC: Ion Chromatograph

ITRC: Interstate Technology Regulatory Council

LNAPL: Light Non-Aqueous Phase Liquid

MCL: Maximum Contaminant Level

MTBE: Methyl Tertiary Butyl Ether

NRC: National Research Council

ORP: Oxidation Reduction Potential

PRBs: Permeable Reactive Barriers

PCE: Tetrachloroethylene (perchloroethylene)

SERDP: Strategic Environmental Research and Development Program

TCE: Trichloroethene